Pathogenesis of Mortalin in Manganese-induced Parkinsonism

Travis J. Cook

A dissertation

submitted in partial fulfillment of the

requirements for the degree of

Doctor of Philosophy

University of Washington

2014

Reading Committee:

David L. Eaton, Co-chair

Jing Zhang, Co-chair

Lucio G. Costa

Program Authorized to Offer Degree:

School of Public Health

Environmental and Occupational Health Sciences

University of Washington

Abstract

Pathogenesis of Mortalin in Manganese-induced Parkinsonism

Travis J. Cook

Co-Chairs of the Supervisory Committee:

Professor David L. Eaton, PhD

Department of Environmental & Occupational Health Sciences

Professor Jing Zhang, MD, PhD

Department of Pathology

Manganese (Mn) is an essential dietary micronutrient for which excessive exposure has long been known to be neurotoxic. Historically, short-term, high-intensity exposure in occupational settings was recognized to cause acute-onset parkinsonism (PS) termed manganism. Although modern day exposures are typically several orders of magnitude lower than those necessary to cause manganism, chronic, low-level exposures are not uncommon among a number of occupations and communities. Recent epidemiologic studies have demonstrated an association between Mn exposure and risk of PS, and in this regard Mn remains a public health concern. The work described here was designed to provide insight toward questions which remain with respect to Mn exposure and its toxic effect on the brain, and includes studies utilizing Mn exposed human populations and *in vitro* model systems to address these objectives. Blood plasma samples obtained from a cohort of welders, whose work is recognized as generating appreciable amounts of

airborne Mn, and post-mortem brain tissue of Mn mine workers were both found to have discernable alterations related to the mitochondrial chaperone protein mortalin. Furthermore, *in vitro* studies demonstrated that reduced astroglial expression of mortalin confers neuronal susceptibility to toxicity elicited by low levels of Mn, possibly via mechanisms of endoplasmic reticulum and oxidative stress mediated by α-synuclein. Taken together, the results of these studies indicate that Mn exposures experienced by modern day populations are sufficient to cause biological alterations in humans that are potentially neurotoxic.

TABLE OF CONTENTS

LIST OF FIGURES

LIST OF TABLES

ACKNOWLEDGEMENTS

This work could not have been accomplished without the invaluable intellectual, technical and personal support of countless individuals over the course of my graduate studies. The conception of the project that would eventually evolve into the dissertation presented here can be credited to the guidance of Dr. Harvey Checkoway, Dr. David L. Eaton and Dr. Jing Zhang. Their willingness to collaborate in a manner that made my research interests a reality cannot be understated. It was Dr. Checkoway who introduced me to the interesting field of research on environmental factors as potential contributors to neurodegenerative conditions. My early work in this area was supported by his UW Superfund Research Center grant (P42ES4696), which included a collaborative project with Dr. Zhang focusing on the development of novel biomarkers of exposure, effect and/or susceptibility in manganese-exposed occupational welders. Dr. Eaton's initial and ongoing support of this arrangement were critical to its success. I also thank Dr. Lucio G. Costa for his participation on my doctoral committee. These studies would not have been even remotely possible without each of their generous contributions.

In my five years working in Dr. Zhang's highly productive lab, I had the good fortune to work with dozens of outstanding scientists. I remember very well feeling quite intimidated just being in the presence of this team during my first lab meeting, but I was immediately impressed with the expertise, unique skills and intense focus that characterized each member. I have had great experiences with at least 50 research scientists, postdoctoral fellows and medical researchers and I am very appreciative of the working relationships I have developed with each and every member of the Zhang Lab over this time. There are several members who especially contributed substantially to the

work described here and my professional development as a scientist. Carmen Ginghina was incredibly helpful in getting me oriented in the laboratory early on, and continued to support my work administratively throughout my tenure. My first opportunity to contribute to the publication of a research article came about in my work with Dr. Xiangmin Lin, and I am very pleased with our ongoing collaborative relationship. Dr. Min Shi and Dr. Tessandra Stewart provided regular intellectual contributions to the direction of this work. The human tissue component of this dissertation was generously supported by the work of Dr. Luis F. Gonzalez-Cuyar, who provided incredible technical expertise and was my greatest resource for every question pertaining to neuropathology I could come up with. I am incredibly grateful for the hard work our many undergraduates put in toward all aspects of the lab, but especially those of Klondy Canales, Pokuan Ho and Allion Salvador whose dedication toward helping me complete this work astounds me to this day. One could not ask for better supporters and I look forward to supporting them in their future career endeavors. Most of all, I thank Dr. Jake G. Hoekstra, who not only closely supported this work both intellectually and technically, but has grown to become one of my very best friends.

The UW Department of Environmental & Occupational Health Sciences has been a wonderful place to call home for the past eight years. I have learned so very much from all of its world-class faculty and outstanding students over this time. I would particularly like to thank Dr. Michael G. Yost for admitting me into this department as a student in the M.S. Industrial Hygiene program, which is really where my subsequent research interests originated. Along the same line, Dr. Christopher D. Simpson provided me with outstanding mentorship both throughout my time in his laboratory as a master's student

which continued as I transitioned into the doctoral program. I am forever thankful to Dr. Thomas M. Burbacher, current director of both the Toxicology graduate program and the UW Superfund Research Program, who provided considerable academic and morale support at times where it was direly needed. The administrative staff in the DEOHS departmental office have been instrumental in helping me through this process. I am in great debt to Rory Murphy, whose thoughtful support, advice and guidance helped me navigate numerous difficulties along the way. Lastly, I thank all of my fellow graduate students who I have had the pleasure of calling not only my colleagues, but also my dear friends throughout my time in this department. I have enjoyed many memorable times both inside and outside of the labs and classrooms which I will reflect upon happily for the rest of my life. I have been fortunate to develop many friendships that I foresee as being lifelong, and a few of those deserve special attention here. Due to our mutual research interests and a number of additional similarities, Dr. Pamela Roque and Dr. Daniella M. Pizzurro of the Costa laboratory provided me with invaluable technical and morale support that kept my work moving forward during difficult times. On my first day on campus in 2006 I was fortunate to meet Dr. Ryan P. Blood who has become an irreplaceable friend, and whose selfless support of me in all aspects of my life in Seattle contributed tremendously to the successful completion of this work. The single most important relationship I developed while at UW is that with Dr. Vanessa E. Galaviz, who captured my heart and inspired me to persevere in my studies no matter the circumstance.

There were numerous centers, cores and training programs that supported my work intellectually, technically and financially. First and foremost, I am greatly appreciative of the generous support Dr. Lianne Sheppard provided me as a pre-doctoral

trainee on her Biostatistics, Bioinformatics and Epidemiologic Training in Environmental Health grant (TSES015459). Further, I would like to thank Dr. Kathleen F. Kerr for serving as both my quantitative mentor in the BEBTEH program and graduate school representative to my committee. Human brain tissue specimens were provided courtesy of both the UW Neuropathology Core, which is supported by the Alzheimer's Disease Research Center (AG05136), the Adult Changes in Thought Study (AG006781), and Morris K Udall Center of Excellence for Parkinson's Disease Research (NS062684) and Dr. Brad Racette at Washington University in St. Louis, MO. The plasma biomarker studies presented here were largely supported with the help of the UW Center for Ecogenetics and Environmental Health (P42ES4696) and their tremendous staff including Dr. Frederico M. Farin and Dr. Theo K. Bammler. I also greatly appreciate the statistical expertise Dr. Susan Searles Nielsen provided in the biomarker study.

Finally, I most greatly owe the successful completion of this work to my entire loving family, who have so patiently waited for its culmination. I particularly thank my father, Douglas, my mother, Mary Kay, and my sister, Bryana, who supported me up and over every hurdle along the way, some of which would have been insurmountable without them. I look forward to making up for my absence while taking on this challenge.

CHAPTER 1: INTRODUCTION

Manganese & Parkinsonism

Parkinsonism (PS) refers to a group of neurological syndromes whose clinical symptoms include bradykinesia, muscle rigidity, postural instability, and resting tremor (Galvan and Wichmann 2008). There are many causes associated with symptoms of PS, the most common being Parkinson disease (PD), with its motor symptoms largely attributable to the death of dopaminergic neurons in the substantia nigra pars compacta (SNpc) and resultant depletion of striatal dopamine. The incidence of PD increases with age, with populations over the age of 65 having an estimated disease prevalence of 3% (Orr et al. 2002). This makes PD the second most common neurodegenerative disease after Alzheimer disease (AD), and symptoms of PS are even more common with a prevalence reported as 15% in populations 65 to 75 years of age and exceeding 50% in people over 85 years of age (Bennett et al. 1996). A small portion of PD cases can be attributed to genetics alone, as both autosomal dominant and recessive mutations causative of rare familial forms of the disease have been identified in several genes to date, including *SNCA*, *LRRK2*, parkin, *PINK1*, and *DJ-1* (Singleton et al. 2013). On the other hand, syndromes which resemble PD but have distinct pathologies leading to symptoms of PS can be attributed solely to exposure to environmental toxicants, as is the case with 1-methyl-4-phenyl-1,2,3,6-tetrahydropyridine (MPTP) (Langston et al. 1983). Overall, a great majority of PD cases are of unknown etiology and are therefore referred to as being idiopathic, though many investigators consider that the evidence to date implies individual genetic makeup combined with exposure to environmental toxicants as the most likely explanation.

Various specific environmental factors, including pesticides and heavy metals, have been inconclusively implicated in the development of symptoms of PS, with possible overlapping mechanisms resulting in the manifestation of idiopathic PD (iPD). A particular environmental agent of interest is manganese (Mn), an essential dietary nutrient of which excessive exposure has been long known to cause symptoms of PS commonly referred to as manganism (Couper 1837). While the association between acute or chronic high-level Mn exposure and PS is well established, it is quite clear that pathologically, manganism is largely different from iPD, given the fact that the pathology associated with high-level Mn exposure is not consistently seen in the SNpc, a pathological hallmark of iPD. However a potential role of lower-level chronic exposure in the development of iPD remains to be established, and indeed more recent investigations have shown evidence demonstrating that PS affecting welders who are exposed to modestly increased levels of Mn may indeed have overlapping pathologies with iPD (Racette et al. 2012). Oxidative stress, mitochondrial dysfunction, and neuroinflammation have been reported upon exposure both *in vitro* and *in vivo*, suggesting possible underlying mechanisms of Mn-induced neurotoxicity (Milatovic et al. 2009).

Manganese Brain Deposition

Passage of Mn through the blood-brain barrier has been found to occur through a variety of mechanisms, including transport via DMT1 (Au et al. 2008), NMDA receptor channel (Itoh et al. 2008), transferrin (Aschner and Gannon 1994), diffusion, and active transport (Rabin et al. 1993). Mn may also enter the brain by crossing the choroid plexus and into the capillary endothelium at higher blood concentrations (Rabin et al. 1993).

Upon entry into the brain, Mn tends to accumulate preferentially within the basal ganglia and particularly the globus pallidus as demonstrated by nonhuman primate studies using T1-weighted magnetic resonance imagining *in vivo* (Dorman et al. 2006, Guilarte et al. 2006). No studies were identified where brain Mn concentrations were reported in humans exposed to the metal. Similarly, data on Mn brain tissue concentrations of PD patients are very limited, with the only identified study of this type reporting no difference in Mn levels within any of the structures of the basal ganglia when compared to controls (Dexter et al. 1991). A study in Japanese accident victims (not known to have a history of Mn exposure occupationally or otherwise) indicated cerebellar brain Mn concentrations of approximately 9-10 μM, presumably a lower-end concentration as the cerebellum does not accumulate Mn to the extent of other brain regions (Suzuki et al. 1975), and the samples were taken from previously healthy subjects who likely did not experience abnormal Mn exposure. One study in nonhuman primates chronically exposed to Mn dioxide reported concentrations of 264 μM within the striatum and 334 μM within the globus pallidus (Suzuki et al. 1975). Intratracheal instillations of 1.22 mg Mn/kg body weight over a 4-week period in rats resulted in a twofold increase of Mn concentrations within the striatum compared to controls (Roels et al. 1997). Intrathecal administration of 250 μg $MnCl_2$ resulted in an increase of Mn concentration from 0.57 to 31.8 μg Mn/g tissue in the rat ventral mesencephalon (Ingersoll et al. 1999). Together these findings illustrate the preferential deposition of Mn to areas of the basal ganglia and globus pallidus in both nonhuman primates and rats to concentrations in the approximate range of 200-350 μM in exposed animals.

Cellular Distribution of CNS Mn

Mn may be taken up by astrocytes via divalent metal transporter 1 (DMT1) and by the neurons via transferrin and other specific transporter systems, such as the dopamine transporter (DAT) (Chen et al. 2006, Erikson and Aschner 2006, Anderson et al. 2007). Astrocytes have been demonstrated to sequester the metal to concentrations 50 to 60-fold greater than similarly exposed neurons (Aschner et al. 1992, Aschner et al. 1999). Once inside the cell, initial experimental evidence suggested that Mn accumulates mainly within the mitochondria (Gavin et al. 1999, Morello et al. 2008); however, recent studies provide evidence of preferential accumulation within the nucleus (Kalia et al. 2008) and Golgi apparatus (Carmona et al. 2010). The critical role of glial cells in Mn-induced neurotoxicity is evidenced in a recent study demonstrating a dependence upon the presence of these cells in order to elicit toxic effects on dopaminergic neurons at low concentrations *in vitro* (1-30 μM) (Zhang et al. 2010).

Mechanisms of Manganese Neurotoxicity

Mechanisms of Mn-related neuronal toxicity have been proposed to include disruption of mitochondrial respiration, generation of oxidative stress, and damage to the dopaminergic, glutamatergic, and GABAergic synapses. The water soluble $MnCl_2$ is most often used in the delivery of Mn to *in vitro* systems. *In vitro* studies aimed at evaluating cellular response to estimated physiologically relevant concentrations of Mn typically use treatment regimens in the range of 1-500 μM (Erikson et al. 2004, Giordano et al. 2009). Mn enters the mitochondria via the calcium uniporter, and once inside primarily binds to the inner mitochondrial membrane or matrix proteins (Gavin et al. 1999). The metal may then interact directly with proteins involved in oxidative

phosphorylation, and has been shown to interfere with ATP synthesis (Gunter et al. 2006) via the inhibition of F_1ATPase (Gavin et al. 1992) and inhibition of complex I at higher concentrations (Chen et al. 2001). While divalent Mn is the predominant ionic species found in the brain tissue (Gunter et al. 2006), trivalent Mn is a more effective complex I inhibitor (Chen et al. 2001) and oxidizer of intracellular substrates, including dopamine (Archibald and Tyree 1987). However, divalent Mn has been hypothesized to become concentrated within the mitochondria, whereupon it may interfere with ATP production by binding Ca^{2+} activated intramitochondrial sites that otherwise would be capable of significantly increasing the rate of ATP generation (Gunter et al. 2006). Mn accumulation in the mitochondria of the rat striatum and accompanying generation of ROS has been demonstrated *in vivo* upon daily intraperitoneal administration of Mn for 6 weeks at a dose of 15 mg/kg (Zhang et al. 2003), following previous findings that Mn exposures of 1750 μmol/kg for 7 days resulted in a significant decrease of glutathione peroxidase activity in the rat striatum (Liccione and Maines 1988).

Role of the Astrocyte in Manganese Neurotoxicity

It is quite clear that Mn has profound effects on astrocytes, typically at much lower concentrations than needed to induce neuronal toxicity. For example, Mn has been demonstrated to suppress ATP-dependent calcium release and subsequent signaling events upon administration of low concentrations (1-10 μM) to rat primary astrocytic cultures, indicating Mn-induced disruption of calcium sequestration (Tjalkens et al. 2006). Astrocytes treated with Mn at concentrations as low as 1 μM produced large increases in mitochondrial calcium accompanied by mitochondrial osmotic swelling, loss of interconnected mitochondrial networks, and depletion of thapsigargin-releasable ER

Ca^{2+} stores. Mn has also been shown to decrease mitochondrial membrane potential while elevating intracellular reactive oxygen species in cultured rat C6 glioma cells, resulting in the enhanced induction of iNOS via the NF-κB pathway (Barhoumi et al. 2004). Decreased membrane potential has furthermore been associated with activation of the astrocytic caspase-3 and ERK pathways in primary rat astrocyte cultures (Yin et al. 2008). Moreover, NMR spectroscopy has demonstrated that Mn decreases ATP/adenosine diphosphate ratios and impairs glucose metabolism and metabolic activity in cultures derived from the globus pallidus upon high doses (50 mg/kg/day) of Mn given to rats *in vivo* (Zwingmann et al. 2007). Similar studies have also shown that Mn is capable of inhibiting glutamine synthesis and release in astrocytes, accompanied by a failure of ability to provide neurons with substrates for energy and neurotransmitter metabolism and a subsequent decrease of neuronal GSH levels and energy metabolism (Zwingmann et al. 2003).

The generation of reactive oxygen species upon Mn treatment has been well documented both *in vitro* and *in vivo*. Primary rat astrocyte cultures treated with Mn at a concentration of 100 μM induced a significant increase of F_2-isoprostanes following 2 hours of treatment (Milatovic et al. 2007), and the same treatment resulted in a significant increase of ROS as indicated by 2',7'-dichlorofluoroscein fluorescein fluorescence, an effect that was reversed by co-treatment with N-acetylcysteine (Chen and Liao 2002). Rats exposed to Mn via inhalation exhibited decreased GSH levels and increased metallothionein levels (Dobson et al. 2003), markers indicative of oxidative stress, a finding that was replicated in nonhuman primates (Erikson et al. 2007).

Dysregulation of excitatory glutamatergic neurotransmission may play a role in Mn-induced neurotoxicity. Glutamate levels were increased in rodents upon exposure to Mn (Lipe et al. 1999, Gwiazda et al. 2002, Reaney et al. 2006). In cultured rat astrocytes, Mn treatment reduced the expression of glutamate transporter (Erikson and Aschner 2002) and astrocytic glutamate uptake (Hazell and Norenberg 1997). This finding has been further extended to rodents (Erikson et al. 2004) and non-human primates (Erikson et al. 2007), accompanied by a simultaneous reduction in glutamine synthetase. Such alterations of glutamate homeostasis have the potential to negatively affect glutamate metabolism and distribution at the synapses, further evidenced by a recently observed reduction in the glial-specific enzyme glutamine synthetase in the globus pallidus of Mn-exposed nonhuman primates (Burton and Guilarte 2009).

Manganese Exposure, Delivered Dose and Toxic Effects

A number of *in vivo* animal studies involving Mn administration have been completed. Gianutsos et al. (Gianutsos et al. 1985) demonstrated elevated brain Mn concentrations following a single subcutaneous injection of $MnCl_2$ at a dose of 11 mg Mn/kg, and persistent Mn accumulation within the brain following repeated injections in CD-1 mice. In C57BL/6 mice, Dodd et al. (Dodd et al. 2005) reported marked Mn accumulation within the striatum accompanied by significant reductions in horizontal movement as assessed by open field grid crossing following subcutaneous injections of $MnCl_2$. A single injection of 100 mg/kg resulted in a doubling of striatal Mn concentration compared to controls, with a 30.9% decrease in horizontal movement. Three injections of 50 mg/kg over a 7-day period resulted in a 4-fold increase in striatal Mn concentration with a 38.9% decrease in horizontal movement, while the same dosing

regimen at 100 mg/kg resulted in striatal concentrations 6 times greater than controls and a 43.2% decrease in horizontal movement. These results implicate the Mn-treated C57BL/6 mouse as a potential model of Mn toxicity, demonstrating deposition within the basal ganglia accompanied by significant, but not severe, motor dysfunction. Ordonez-Librado et al. (Ordoñez-Librado et al. 2008) developed a novel parkinsonian model by administering a mixture of divalent and trivalent Mn to CD-1 male mice via inhalation. Animals were exposed to a 40 mM mixture of $MnCl_2$ and $MnOAc_3$ for 1 hour twice a week over a period of 5 months. Mn-exposed mice were found to be deficient in motor function as assessed by behavioral tests. They also reported an approximate 68% reduction in TH-positive neurons in the SNpc without any reduction in the VTA. After administering intraperitoneal injections of $MnCl_2$ to mice at a dose of 5 mg/kg/day for a period of 30 days, Stanwood et al. (Stanwood et al. 2009) observed a 20% reduction in TH-positive neurons accompanied with a reduction in neurite length in the SNpc, in comparison to saline treated controls. However, dopaminergic neuron death was not exclusively selective, as GAD-positive neurons in the striatum and globus pallidus were also subtly, but significantly, reduced. Adult Wistar rats exposed to either 10 mg/mL or 25 mg/mL $MnCl_2$ in their drinking water were observed to have decreased locomotor activity in comparison to controls, with those in the higher treatment group also demonstrating increased striatal oxidative stress as indicated by lipid peroxidation (Avila et al. 2008). Interestingly, repeated high doses of the organic gasoline additive methylcyclo-pentadienyl Mn tricarbonyl (MMT) administered to rats over a period of 5 months did not result in dopaminergic neuronal loss, as had been previously observed

upon similar administration to mice, even though brain Mn concentrations were elevated upon treatment (Yong et al. 1986).

Rodent models of Mn-induced neurodegeneration most often involve either subcutaneous or intraperitoneal injections of $MnCl_2$ (Gianutsos et al. 1985, Baek et al. 2003, Baek et al. 2004, Saito et al. 2005, Stanwood et al. 2009), although parkinsonian features have also been reported after exposure via ingestion (Avila et al. 2008) and inhalation (Ordoñez-Librado et al. 2008). Experiments using administration of Mn by injection have used dosing regimens ranging from single high-dose exposures (100 mg/kg) (Dodd et al. 2005), to multiple lower-dose exposures. In lower-dose experiments, Stanwood et al. (Stanwood et al. 2009) observed a reduction in TH-positive neurons in the SNpc following $MnCl_2$ injections of 5 mg/kg/day for 30 days, and Baek et al. (Baek et al. 2004) observed alterations in the expression levels of some genes in the SN and the striatum following $MnCl_2$ injections of 2 mg/kg/day for 3 weeks.

Mortalin: A Protein Critical to Health & Disease

Mortalin, most commonly recognized as a mitochondrial heat shock protein, was initially identified 20 years ago in studies which sought to identify unique proteins that differentiated mortal and immortal cells (Wadhwa et al. 1993). While the protein is an established mitochondrial chaperone, it has also been associated with the cytosol, endoplasmic reticulum (ER), Golgi apparatus, nucleus, and even the extracellular space (Ran et al. 2000, Ma et al. 2006). In addition to its localization to multiple cellular organelles, mortalin has been found to be multifunctional as it participates in the import, folding and degradation of mitochondrial proteins (Deocaris et al. 2008), and also interacts with a wide variety of proteins outside of the mitochondrion, including those

involved with metabolism, the immune system, the ER, growth factors, centrosomes, and p53 (Baselar et al. 2012).

Mortalin & Parkinson Disease

The importance of mortalin has been recognized not only in its basic biological functions, but also in a variety of diseases ranging from cancer to neurodegeneration. The role of mortalin in PD was first described by Jin and colleagues, who by using a proteomic approach found the protein to be decreased in the mitochondrial fraction of brain tissue isolated from the SNpc of PD patients as compared to similar tissue isolated from age-matched controls (Jin et al. 2006). This finding was confirmed in an *in vitro* dopaminergic neuronal cellular model of PD in which it was found that MES cells treated with rotenone expressed less mortalin than those treated with vehicle control (Jin et al. 2006). Furthermore, cells manipulated to inhibit the expression of mortalin were found to be more sensitive to rotenone-induced toxicity than their uncompromised counterparts (Jin et al. 2006). A follow-up study, also utilizing the MES cell line, found by co-immunoprecipitation that the protein interacts directly with α-synuclein and DJ-1 (Jin et al. 2007). A final related study by Shi and colleagues found that expression levels of the protein were decreased as a function of disease severity (Shi et al. 2008). Taken together, these studies strongly implicate that the level of expression of the mortalin protein is decreased in the brain tissue of PD patients. Additionally, the demonstration that mortalin levels in dopaminergic neurons decreased upon exposure to rotenone, a toxicant commonly employed in PD model systems, provides some plausibility to the hypothesis that the expression levels of mortalin in target tissues are modulated by environmental insults from neurotoxic xenobiotics such as Mn.

Mutations in the *HSPA9* gene which encodes the mortalin protein have been implicated to contribute to PD etiology in some cases. A screening of mortalin mutations in a population in Spain consisting of 330 PD patients and 250 healthy controls revealed the four most common polymorphisms of the gene did not modulate risk of PD development, but two PD patients were found to each carry a more rare missense mutation in exons (identified as R126W & P509S) and one was found with an intron insertion of 17 base pairs, raising the possibility that these three variants contribute to disease risk (De Mena et al. 2009). A subsequent screening of gene mutations in a German population revealed an additional PD-associated mutation (A476T) in a single patient, and the group further characterized the functional aspects of the three PD-associated amino acid substitutions identified in the two populations using an *in vitro* system (Burbulla et al. 2010). Interestingly, cells in which mutated forms of mortalin were overexpressed exhibited elevated generation of reactive oxygen species in response to cell stress, elevated mitochondrial membrane potential, and altered mitochondrial morphology as compared to those overexpressing the wild type form of mortalin (Burbulla et al. 2010), linking the variants with phenotypes that would be expected to contribute to PD development. However, these mutations appear to be quite rare as no additional carriers of these variants were identified in an expanded screening of the German population (1,008 PD patients & 1,342 matched controls) (Burbulla et al. 2010).

Experimentally, mortalin expression has been found to be consistently decreased under several other conditions relevant to PD. Mortalin was found to be decreased in a two-dimensional electrophoresis (2-DE) profiling study of rat brain mitochondria treated with dopamine quinone (Van Laar et al. 2008), an oxidized and reactive form of the

neurotransmitter critical to PD motor symptomatology. Utilizing a similar experimental design following overexpression of α-synuclein, a known risk factor for PD in humans, Pennington et al. (Pennington et al. 2010) identified decreased mitochondrial mortalin levels in SH-SY5Y cells in a 2-DE profiling study and confirmed the observation by traditional one-dimensional Western blotting. In another 2-DE study, mortalin was found to be decreased in the striatal tissue of rats treated *in vivo* with 6-hydroxydopamine (6-OHDA) (Chiasserini et al. 2011), a toxicant commonly used to mimic PD in rodents. In exploring the physiologic consequence of mortalin inhibition, the group demonstrated depolarization of striatal neurons and depressed corticostriatal field potentials which were potentiated with treatment of the complex I inhibitor rotenone (Chiasserini et al. 2011). In a separate mechanistic study, susceptibility of HeLa cells transfected with mortalin siRNA to the toxic effects of H_2O_2 treatment was found to be reversed by overexpression of parkin (Yang et al. 2011), a key mitochondrial protein demonstrated to be of importance in PD in that loss of function confers disease susceptibility. Direct interaction of mortalin with parkin was observed upon treatment with carbonyl cyanide 3-m-chlorophenylhydrazone (Yang et al. 2011), and it has also been demonstrated that mortalin interacts directly with the antioxidant DJ-1 (Jin et al. 2007), another important protein in PD as its impaired function elevates disease risk. The interaction between mortalin and DJ-1 has been reported to be augmented under conditions of oxidative stress (Li et al. 2005). The studies described above provide evidence that mortalin is responsive to exogenous toxicants and interacts with several proteins known to be important in the pathogenesis of PD, presenting as a possible link between PD-related genes and environmental toxicants.

References

Anderson, J. G., P. T. Cooney, and K. M. Erikson. 2007. Inhibition of DAT function attenuates manganese accumulation in the globus pallidus. Environ Toxicol Pharmacol **23**:179-184.

Archibald, F. S., and C. Tyree. 1987. Manganese poisoning and the attack of trivalent manganese upon catecholamines. Arch Biochem Biophys **256**:638-650.

Aschner, M., and M. Gannon. 1994. Manganese (Mn) transport across the rat blood-brain barrier: saturable and transferrin-dependent transport mechanisms. Brain Res Bull **33**:345-349.

Aschner, M., M. Gannon, and H. K. Kimelberg. 1992. Manganese uptake and efflux in cultured rat astrocytes. J Neurochem **58**:730-735.

Aschner, M., K. E. Vrana, and W. Zheng. 1999. Manganese uptake and distribution in the central nervous system (CNS). Neurotoxicology **20**:173-180.

Au, C., A. Benedetto, and M. Aschner. 2008. Manganese transport in eukaryotes: the role of DMT1. Neurotoxicology **29**:569-576.

Avila, D. S., P. Gubert, R. Fachinetto, C. Wagner, M. Aschner, J. B. Rocha, and F. A. Soares. 2008. Involvement of striatal lipid peroxidation and inhibition of calcium influx into brain slices in neurobehavioral alterations in a rat model of short-term oral exposure to manganese. Neurotoxicology **29**:1062-1068.

Baek, S. Y., J. H. Cho, E. S. Kim, H. J. Kim, S. Yoon, B. S. Kim, J. B. Kim, C. R. Lee, C. Yoo, J. H. Lee, H. Lee, J. Park, J. W. Kim, and Y. Kim. 2004. CDNA array analysis of gene expression profiles in brain of mice exposed to manganese. Ind Health **42**:315-320.

Baek, S. Y., M. J. Lee, H. S. Jung, H. J. Kim, C. R. Lee, C. Yoo, J. H. Lee, H. Lee, C. S. Yoon, Y. H. Kim, J. Park, J. W. Kim, B. S. Jeon, and Y. Kim. 2003. Effect of manganese exposure on MPTP neurotoxicities. Neurotoxicology **24**:657-665.

Barhoumi, R., J. Faske, X. Liu, and R. B. Tjalkens. 2004. Manganese potentiates lipopolysaccharide-induced expression of NOS2 in C6 glioma cells through mitochondrial-dependent activation of nuclear factor kappaB. Brain Res Mol Brain Res **122**:167-179.

Baselar, W., T. Croston, and J. Hollander. 2012. Functional characteristics of mortalin. Pages 55-80 *in* S. C. Kaul and R. Wadwha, editors. Mortalin Biology: Life, Stress and Death. Springer Science+Business Media B.V., Springer Dordrecht Heidelberg London New York.

Bennett, D. A., L. A. Beckett, A. M. Murray, K. M. Shannon, C. G. Goetz, D. M. Pilgrim, and D. A. Evans. 1996. Prevalence of parkinsonian signs and associated mortality in a community population of older people. N Engl J Med **334**:71-76.

Burbulla, L. F., C. Schelling, H. Kato, D. Rapaport, D. Woitalla, C. Schiesling, C. Schulte, M. Sharma, T. Illig, P. Bauer, S. Jung, A. Nordheim, L. Schöls, O. Riess, and R. Krüger. 2010. Dissecting the role of the mitochondrial chaperone mortalin in Parkinson's disease: functional impact of disease-related variants on mitochondrial homeostasis. Hum Mol Genet **19**:4437-4452.

Burton, N. C., and T. R. Guilarte. 2009. Manganese neurotoxicity: lessons learned from longitudinal studies in nonhuman primates. Environ Health Perspect **117**:325-332.

Carmona, A., G. Devès, S. Roudeau, P. Cloetens, S. Bohic, and R. Ortega. 2010. Manganese accumulates within golgi apparatus in dopaminergic cells as revealed by synchrotron X-ray fluorescence nanoimaging. ACS Chem Neurosci **1**:194-203.

Chen, C. J., and S. L. Liao. 2002. Oxidative stress involves in astrocytic alterations induced by manganese. Exp Neurol **175**:216-225.

Chen, J. Y., G. C. Tsao, Q. Zhao, and W. Zheng. 2001. Differential cytotoxicity of Mn(II) and Mn(III): special reference to mitochondrial [Fe-S] containing enzymes. Toxicol Appl Pharmacol **175**:160-168.

Chen, M. K., J. S. Lee, J. L. McGlothan, E. Furukawa, R. J. Adams, M. Alexander, D. F. Wong, and T. R. Guilarte. 2006. Acute manganese administration alters dopamine transporter levels in the non-human primate striatum. Neurotoxicology **27**:229-236.

Chiasserini, D., A. Tozzi, A. de Iure, M. Tantucci, F. Susta, P. L. Orvietani, K. Koya, L. Binaglia, and P. Calabresi. 2011. Mortalin inhibition in experimental Parkinson's disease. Mov Disord **26**:1639-1647.

Couper, J. 1837. On the effects of black oxide of manganese when inhaled into the lungs. British Annals of Medicine, Pharmacy, Vital Statistics, and General Science **1**:2.

De Mena, L., E. Coto, E. Sánchez-Ferrero, R. Ribacoba, L. M. Guisasola, C. Salvador, M. Blázquez, and V. Alvarez. 2009. Mutational screening of the mortalin gene (HSPA9) in Parkinson's disease. J Neural Transm **116**:1289-1293.

Deocaris, C. C., S. C. Kaul, and R. Wadhwa. 2008. From proliferative to neurological role of an hsp70 stress chaperone, mortalin. Biogerontology **9**:391-403.

Dexter, D. T., A. Carayon, F. Javoy-Agid, Y. Agid, F. R. Wells, S. E. Daniel, A. J. Lees, P. Jenner, and C. D. Marsden. 1991. Alterations in the levels of iron, ferritin and other trace metals in Parkinson's disease and other neurodegenerative diseases affecting the basal ganglia. Brain **114 (Pt 4)**:1953-1975.

Dobson, A. W., S. Weber, D. C. Dorman, L. K. Lash, K. M. Erikson, and M. Aschner. 2003. Oxidative stress is induced in the rat brain following repeated inhalation exposure to manganese sulfate. Biol Trace Elem Res **93**:113-126.

Dodd, C. A., D. L. Ward, and B. G. Klein. 2005. Basal Ganglia accumulation and motor assessment following manganese chloride exposure in the C57BL/6 mouse. Int J Toxicol **24**:389-397.

Dorman, D. C., M. F. Struve, B. A. Wong, J. A. Dye, and I. D. Robertson. 2006. Correlation of brain magnetic resonance imaging changes with pallidal manganese concentrations in rhesus monkeys following subchronic manganese inhalation. Toxicol Sci **92**:219-227.

Erikson, K., and M. Aschner. 2002. Manganese causes differential regulation of glutamate transporter (GLAST) taurine transporter and metallothionein in cultured rat astrocytes. Neurotoxicology **23**:595-602.

Erikson, K. M., and M. Aschner. 2006. Increased manganese uptake by primary astrocyte cultures with altered iron status is mediated primarily by divalent metal transporter. Neurotoxicology **27**:125-130.

Erikson, K. M., A. W. Dobson, D. C. Dorman, and M. Aschner. 2004. Manganese exposure and induced oxidative stress in the rat brain. Sci Total Environ **334-335**:409-416.

Erikson, K. M., D. C. Dorman, L. H. Lash, and M. Aschner. 2007. Manganese inhalation by rhesus monkeys is associated with brain regional changes in biomarkers of neurotoxicity. Toxicol Sci **97**:459-466.

Galvan, A., and T. Wichmann. 2008. Pathophysiology of parkinsonism. Clin Neurophysiol **119**:1459-1474.

Gavin, C. E., K. K. Gunter, and T. E. Gunter. 1992. Mn2+ sequestration by mitochondria and inhibition of oxidative phosphorylation. Toxicol Appl Pharmacol **115**:1-5.

Gavin, C. E., K. K. Gunter, and T. E. Gunter. 1999. Manganese and calcium transport in mitochondria: implications for manganese toxicity. Neurotoxicology **20**:445-453.

Gianutsos, G., M. D. Seltzer, R. Saymeh, M. L. Wu, and R. G. Michel. 1985. Brain manganese accumulation following systemic administration of different forms. Arch Toxicol **57**:272-275.

Giordano, G., D. Pizzurro, K. VanDeMark, M. Guizzetti, and L. G. Costa. 2009. Manganese inhibits the ability of astrocytes to promote neuronal differentiation. Toxicol Appl Pharmacol **240**:226-235.

Guilarte, T. R., J. L. McGlothan, M. Degaonkar, M. K. Chen, P. B. Barker, T. Syversen, and J. S. Schneider. 2006. Evidence for cortical dysfunction and widespread manganese accumulation in the nonhuman primate brain following chronic manganese exposure: a 1H-MRS and MRI study. Toxicol Sci **94**:351-358.

Gunter, T. E., C. E. Gavin, M. Aschner, and K. K. Gunter. 2006. Speciation of manganese in cells and mitochondria: a search for the proximal cause of manganese neurotoxicity. Neurotoxicology **27**:765-776.

Gwiazda, R. H., D. Lee, J. Sheridan, and D. R. Smith. 2002. Low cumulative manganese exposure affects striatal GABA but not dopamine. Neurotoxicology **23**:69-76.

Hazell, A. S., and M. D. Norenberg. 1997. Manganese decreases glutamate uptake in cultured astrocytes. Neurochem Res **22**:1443-1447.

Ingersoll, R. T., E. B. Montgomery, and H. V. Aposhian. 1999. Central nervous system toxicity of manganese. II: Cocaine or reserpine inhibit manganese concentration in the rat brain. Neurotoxicology **20**:467-476.

Itoh, K., M. Sakata, M. Watanabe, Y. Aikawa, and H. Fujii. 2008. The entry of manganese ions into the brain is accelerated by the activation of N-methyl-D-aspartate receptors. Neuroscience **154**:732-740.

Jin, J., C. Hulette, Y. Wang, T. Zhang, C. Pan, R. Wadhwa, and J. Zhang. 2006. Proteomic identification of a stress protein, mortalin/mthsp70/GRP75: relevance to Parkinson disease. Mol Cell Proteomics **5**:1193-1204.

Jin, J., G. J. Li, J. Davis, D. Zhu, Y. Wang, C. Pan, and J. Zhang. 2007. Identification of novel proteins associated with both alpha-synuclein and DJ-1. Mol Cell Proteomics **6**:845-859.

Kalia, K., W. Jiang, and W. Zheng. 2008. Manganese accumulates primarily in nuclei of cultured brain cells. Neurotoxicology **29**:466-470.
Langston, J. W., P. Ballard, J. W. Tetrud, and I. Irwin. 1983. Chronic Parkinsonism in humans due to a product of meperidine-analog synthesis. Science **219**:979-980.
Li, H. M., T. Niki, T. Taira, S. M. Iguchi-Ariga, and H. Ariga. 2005. Association of DJ-1 with chaperones and enhanced association and colocalization with mitochondrial Hsp70 by oxidative stress. Free Radic Res **39**:1091-1099.
Liccione, J. J., and M. D. Maines. 1988. Selective vulnerability of glutathione metabolism and cellular defense mechanisms in rat striatum to manganese. J Pharmacol Exp Ther **247**:156-161.
Lipe, G. W., H. Duhart, G. D. Newport, W. Slikker, and S. F. Ali. 1999. Effect of manganese on the concentration of amino acids in different regions of the rat brain. J Environ Sci Health B **34**:119-132.
Ma, Z., H. Izumi, M. Kanai, Y. Kabuyama, N. G. Ahn, and K. Fukasawa. 2006. Mortalin controls centrosome duplication via modulating centrosomal localization of p53. Oncogene **25**:5377-5390.
Milatovic, D., Z. Yin, R. C. Gupta, M. Sidoryk, J. Albrecht, J. L. Aschner, and M. Aschner. 2007. Manganese induces oxidative impairment in cultured rat astrocytes. Toxicol Sci **98**:198-205.
Milatovic, D., S. Zaja-Milatovic, R. C. Gupta, Y. Yu, and M. Aschner. 2009. Oxidative damage and neurodegeneration in manganese-induced neurotoxicity. Toxicol Appl Pharmacol **240**:219-225.
Morello, M., A. Canini, P. Mattioli, R. P. Sorge, A. Alimonti, B. Bocca, G. Forte, A. Martorana, G. Bernardi, and G. Sancesario. 2008. Sub-cellular localization of manganese in the basal ganglia of normal and manganese-treated rats An electron spectroscopy imaging and electron energy-loss spectroscopy study. Neurotoxicology **29**:60-72.
Ordoñez-Librado, J. L., A. L. Gutierrez-Valdez, L. Colín-Barenque, V. Anaya-Martínez, P. Díaz-Bech, and M. R. Avila-Costa. 2008. Inhalation of divalent and trivalent manganese mixture induces a Parkinson's disease model: immunocytochemical and behavioral evidences. Neuroscience **155**:7-16.
Orr, C. F., D. B. Rowe, and G. M. Halliday. 2002. An inflammatory review of Parkinson's disease. Prog Neurobiol **68**:325-340.
Pennington, K., J. Peng, C. C. Hung, R. E. Banks, and P. A. Robinson. 2010. Differential effects of wild-type and A53T mutant isoform of alpha-synuclein on the mitochondrial proteome of differentiated SH-SY5Y cells. J Proteome Res **9**:2390-2401.
Rabin, O., L. Hegedus, J. M. Bourre, and Q. R. Smith. 1993. Rapid brain uptake of manganese(II) across the blood-brain barrier. J Neurochem **61**:509-517.
Racette, B. A., S. R. Criswell, J. I. Lundin, A. Hobson, N. Seixas, P. T. Kotzbauer, B. A. Evanoff, J. S. Perlmutter, J. Zhang, L. Sheppard, and H. Checkoway. 2012. Increased risk of parkinsonism associated with welding exposure. Neurotoxicology **33**:1356-1361.
Ran, Q., R. Wadhwa, R. Kawai, S. C. Kaul, R. N. Sifers, R. J. Bick, J. R. Smith, and O. M. Pereira-Smith. 2000. Extramitochondrial localization of

mortalin/mthsp70/PBP74/GRP75. Biochem Biophys Res Commun **275**:174-179.
Reaney, S. H., G. Bench, and D. R. Smith. 2006. Brain accumulation and toxicity of Mn(II) and Mn(III) exposures. Toxicol Sci **93**:114-124.
Roels, H., G. Meiers, M. Delos, I. Ortega, R. Lauwerys, J. P. Buchet, and D. Lison. 1997. Influence of the route of administration and the chemical form (MnCl2, MnO2) on the absorption and cerebral distribution of manganese in rats. Arch Toxicol **71**:223-230.
Saito, A., C. M. Maier, P. Narasimhan, T. Nishi, Y. S. Song, F. Yu, J. Liu, Y. S. Lee, C. Nito, H. Kamada, R. L. Dodd, L. B. Hsieh, B. Hassid, E. E. Kim, M. González, and P. H. Chan. 2005. Oxidative stress and neuronal death/survival signaling in cerebral ischemia. Mol Neurobiol **31**:105-116.
Shi, M., J. Jin, Y. Wang, R. P. Beyer, E. Kitsou, R. L. Albin, M. Gearing, C. Pan, and J. Zhang. 2008. Mortalin: a protein associated with progression of Parkinson disease? J Neuropathol Exp Neurol **67**:117-124.
Singleton, A. B., M. J. Farrer, and V. Bonifati. 2013. The genetics of Parkinson's disease: progress and therapeutic implications. Mov Disord **28**:14-23.
Stanwood, G. D., D. B. Leitch, V. Savchenko, J. Wu, V. A. Fitsanakis, D. J. Anderson, J. N. Stankowski, M. Aschner, and B. McLaughlin. 2009. Manganese exposure is cytotoxic and alters dopaminergic and GABAergic neurons within the basal ganglia. J Neurochem **110**:378-389.
Suzuki, Y., T. Mouri, K. Nishiyama, and N. Fujii. 1975. Study of subacute toxicity of manganese dioxide in monkeys. Tokushima J Exp Med **22**:5-10.
Tjalkens, R. B., M. J. Zoran, B. Mohl, and R. Barhoumi. 2006. Manganese suppresses ATP-dependent intercellular calcium waves in astrocyte networks through alteration of mitochondrial and endoplasmic reticulum calcium dynamics. Brain Res **1113**:210-219.
Van Laar, V. S., A. A. Dukes, M. Cascio, and T. G. Hastings. 2008. Proteomic analysis of rat brain mitochondria following exposure to dopamine quinone: implications for Parkinson disease. Neurobiol Dis **29**:477-489.
Wadhwa, R., S. C. Kaul, Y. Ikawa, and Y. Sugimoto. 1993. Identification of a novel member of mouse hsp70 family. Its association with cellular mortal phenotype. J Biol Chem **268**:6615-6621.
Yang, H., X. Zhou, X. Liu, L. Yang, Q. Chen, D. Zhao, J. Zuo, and W. Liu. 2011. Mitochondrial dysfunction induced by knockdown of mortalin is rescued by Parkin. Biochem Biophys Res Commun **410**:114-120.
Yin, Z., J. Aschner, A. dos Santos, and M. Aschner. 2008. Mitochondrial-dependent manganese neurotoxicity in rat primary astrocyte cultures. Brain Res **1203**:1-11.
Yong, V. W., T. L. Perry, W. J. Godolphin, K. A. Jones, R. M. Clavier, M. Ito, and J. G. Foulks. 1986. Chronic organic manganese administration in the rat does not damage dopaminergic nigrostriatal neurons. Neurotoxicology **7**:19-24.
Zhang, P., K. M. Lokuta, D. E. Turner, and B. Liu. 2010. Synergistic dopaminergic neurotoxicity of manganese and lipopolysaccharide: differential involvement of microglia and astroglia. J Neurochem **112**:434-443.

Zhang, S., Z. Zhou, and J. Fu. 2003. Effect of manganese chloride exposure on liver and brain mitochondria function in rats. Environ Res **93**:149-157.
Zwingmann, C., D. Leibfritz, and A. S. Hazell. 2003. Energy metabolism in astrocytes and neurons treated with manganese: relation among cell-specific energy failure, glucose metabolism, and intercellular trafficking using multinuclear NMR-spectroscopic analysis. J Cereb Blood Flow Metab **23**:756-771.
Zwingmann, C., D. Leibfritz, and A. S. Hazell. 2007. Nmr spectroscopic analysis of regional brain energy metabolism in manganese neurotoxicity. Glia **55**:1610-1617.

CHAPTER 2: HYPOTHESIS & SPECIFIC AIMS

Very little is known about the roles of mortalin in neurotoxicity induced by environmental toxicants, including Mn. Since Mn preferentially accumulates within astrocytes, it is of interest to determine its influence on astroglial mortalin expression levels and the subsequent implications in the pathogenesis of PD and/or PS. Therefore, I hypothesize that mortalin and Mn interact within astrocytes via a pathway involving α-synuclein, to contribute to neurodegeneration that is ultimately responsible for clinical PS. Further, if this were to occur, I hypothesize that autoantibodies of mortalin and/or the protein itself will serve as a surrogate biomarker for Mn-induced parkinsonism via mechanisms involving mortalin, thereby, correlating with Mn exposure, disease severity, and/or progression. To fully test these hypotheses, three Specific Aims were designed:

Specific Aim 1: To characterize the potential of blood plasma levels of mortalin protein and autoantibodies to mortalin as novel peripheral biomarkers of PS in a well-characterized cohort of shipyard welders utilizing Luminex-based technology.

Hypothesis: Circulating plasma mortalin protein levels are decreased in individuals experiencing symptoms of PS, relative to asymptomatic individuals; circulating plasma mortalin autoantibodies are increased in individuals experiencing symptoms of PS.

Specific Aim 2: To determine if mortalin protein levels in the post-mortem midbrain and/or corpus striatum are affected by Mn exposure in a cohort comprised of Mn and non-Mn miners using a cell-specific quantitative immunofluorescent staining approach. As a disease control, mortalin protein levels will also be evaluated in the post-mortem

midbrain and corpus striatum tissue specimens obtained from iPD patients and age-matched controls.

Hypothesis: Mortalin protein levels are decreased in the post-mortem midbrain and/or corpus striatum of iPD patients and Mn-exposed miners as compared to age-matched controls (to iPD) and non-Mn miners, respectively, in astroglial cells.

Specific Aim 3: To characterize the influence of astroglial mortalin on neuronal health in the presence or absence of Mn exposure in an *in vitro* co-culture system, and to further investigate potential mechanisms by which astroglial α-synuclein influences the interaction between Mn and mortalin.

Hypothesis: Mortalin expression has been demonstrated to be decreased in the SNpc of human PD subjects. Preliminary data indicate both the presence of mortalin in mouse astrocytes, and that the protein is responsive to Mn treatment. Additionally, we as well as others have demonstrated that Mn has a more profound effect on astrocytes than neurons, and therefore, I hypothesize that the alteration of astroglial mortalin expression levels likely precedes neuronal degeneration. It is expected that knockdown of mortalin gene expression will increase neuronal susceptibility to Mn treatment, whereas overexpression of mortalin will be neuroprotective. As to the potential mechanisms underlying this process, our preliminary data indicate astroglial mortalin expression levels may be modulated by α-synuclein and suggest SNCA KO astrocytes are more resistant to Mn toxicity than their WT counterparts. Consequently, I further hypothesize that astrocytes lacking α-synuclein are more resistant to Mn treatment than their WT counterparts due in part to an enhanced ability to upregulate mortalin.

CHAPTER 3: PLASMA MORTALIN AUTOANTIBODY AND PARKINSONISM

Abstract

Background: Parkinson's disease (PD) is a progressive movement disorder whose classical outward clinical signs are referred to as parkinsonism (PS). PD is the most common cause of PS, but several other conditions present similar clinical signs, including occupational exposure to manganese (Mn) such as in welding or mining. Additionally, few objective measures are available to monitor PS progression.

Objective: To identify novel biomarkers of PS by evaluating autoantibodies in the blood plasma of PS subjects thereby assisting clinical diagnosis of PS and monitoring disease progression.

Methods: We performed a blood plasma profiling study of 9,480 autoantibodies in clinical subjects classified as healthy controls (N=30) and PD (N=75) at various stages. Initial studies were carried out in small pooled samples, followed by developing a robust assay to measure autoantibody against mortalin, a protein strongly implicated in PD pathogenesis, in individual subjects (211 PD patients, 138 controls). We also applied this assay to welders with PS (N=59) and neurologically normal welders (N=95).

Results: Profiling results revealed elevated autoantibodies in the plasma of PD patients compared to controls, and overall increasing autoantibody levels in late-stage PD patients compared to earlier stages of PD. Follow-up analyses with autoantibodies to mortalin in individual samples confirmed the positive association between this autoantibody and PD severity while accounting for age at exam. When the marker was applied to a cohort of

actively working welders with considerably less severe PS, mortalin autoantibody levels were found to be slightly higher in subjects with the most severe signs and symptoms.

Conclusions: Plasma levels of autoantibodies against the mortalin protein are positively associated with PD severity in clinical PD samples, and slightly elevated in actively working welders exhibiting signs of PS. If validated in independent cohorts with samples collected longitudinally, the finding suggests that plasma autoantibodies against mortalin could be potentially used as biomarker of PS severity/progression.

Introduction

Parkinson disease (PD) is a progressive movement disorder typically characterized by tremor, bradykinesia, rigidity, and postural instability. Although PD is the most common cause of this cluster of symptoms in elderly adults, termed collectively as degenerative parkinsonism (PS), many other atypical parkinsonisms exist, including corticobasal degeneration, multiple system atrophy, dementia with Lewy bodies, and progressive supranuclear palsy (Stamelou and Hoeglinger 2013). Another category of atypical PS results from exposure to neurotoxic environmental agents such as carbon monoxide, pesticides, and heavy metals (Lee and Marsden 1994, Caudle et al. 2012, Allen and Levy 2013). A particular metal of interest is manganese (Mn), which has long been known to be causative of acute onset PS, termed manganism, upon high intensity inhalation exposures for even short periods of time (Couper 1837). Recent studies found that chronic occupational exposure to welding fumes containing Mn was associated with an increased prevalence of PS (Racette et al. 2005, Racette et al. 2012), suggesting that even moderate exposures to Mn are capable of inducing clinically significant PS, and possibly increase risk of developing idiopathic PD (iPD) (Racette 2013).

In order to aid clinicians in both early and differential diagnosis of neurodegenerative disorders, including parkinsonisms, biomarkers that reliably reflect disease status are of critical importance. Beyond this basic criterion, ideal biomarkers would also be able to objectively assess disease severity to facilitate tracking disease progression, and be accessible using relatively non-invasive biological sampling methods. To date, little has been done to search for Mn-toxicity related molecular biomarkers of PS, although several candidate biomarkers have been proposed for iPD (Wang et al. 2013). The best-performing biomarkers for iPD to date have been described in the cerebrospinal fluid (CSF). However, CSF collection is relatively invasive and the performance of CSF biomarkers for clinical applications has not yet been utilized (Magdalinou et al. 2014). In response, considerable effort has been spent in an attempt to develop biomarkers in more readily collected blood samples (Chahine et al. 2014). Nonetheless, reports to date have suffered from considerable inconsistency, and therefore reliable biomarkers of iPD and/or PS in these sample media are yet to be identified.

To identify potentially novel biomarkers, in this investigation we focused on autoantibodies, which have been proposed to be of pathological importance in PD, particularly in relation to neuroinflammation, a long-standing underlying mechanistic hypothesis of PD initiation and/or progression (Archelos and Hartung 2000, Monahan et al. 2008, Neff et al. 2008, Gold et al. 2012). More recently, specific autoantibody panels have been reported to be potentially useful in the diagnosis of neurodegenerative disorders, including both PD and Alzheimer disease (AD) (Papachroni et al. 2007, Wilhelm et al. 2007, Double et al. 2009, Nagele et al. 2011, Benkler et al. 2012, Han et al. 2012, Besong-Agbo et al. 2013, Papuc et al. 2014). Here we conducted an initial

profiling study of autoantibodies in pooled samples of human plasma collected from controls, subjects diagnosed with PD at different stages, and those with AD as a disease control. One potential promising candidate marker is autoantibodies against mortalin, a protein associated with PD pathogenesis by multiple investigations (Jin et al. 2006, Jin et al. 2007, Shi et al. 2008, Burbulla et al. 2010). To this end, we developed a robust technique to assess this putative biomarker in individual samples, allowing us to evaluate its potential association with PD. To evaluate the relevance of this autoantibody to other forms of PS, the autoantibody was also determined in welders with and without PS.

Materials & Methods

Participants

This study was approved by the Institutional Review Boards of all participating institutions, and all subjects provided written informed consent, prior to any study procedures. Blood plasma samples were obtained from two sample groups, one of clinical patients and the other of occupational welders, as described previously (Lin et al. 2012, Racette et al. 2012). Briefly, clinical specimens were obtained from the Veterans Affairs Puget Sound Health Care System in Seattle, Washington (Lin et al. 2012). Subject evaluations were performed by a neurologist and included a structured interview, neurological examination, laboratory tests, and neuropsychological assessments. All PD subjects (N=211) met UK PD Society Brain Bank clinical diagnostic criteria (Gibb and Lees 1988). Control subjects (N=138) were community volunteers who had no history of neurological disease, and no evidence of cognitive or functional decline. Further inclusion criteria for cases and controls included a Mini Mental State Exam Score >27 and a paragraph recall score >6. For AD subjects (N=28), probable diagnosis was made

using NINDS-ADRDA criteria (McKhann et al. 1984), applied in the University of Washington Alzheimer's Disease Research Center Clinical Core at a consensus conference. We also included welders with PS (N=59) and welders without PS (N=95) and an intermediate group of welders (N=125), classified by a movement disorders specialist as described below. All were currently working or retired from one of three worksites from the Midwestern U.S., two shipyards and one heavy equipment manufacturing facility (Racette et al. 2012).

Neurological Examination & Sample Collection

All PD patients and all welders underwent a standardized neurological exam by a movement disorder specialist including the Unified Parkinson Disease Rating Scale Motor Part III (UPDRSIII) (Fahn and Elton 1987). PD patients underwent the exam in the on-state (i.e. being medicated to manage their symptoms) and the resulting score was used to approximate disease severity and to categorize them as early-stage PD (UPDRSIII <15, N=70), middle-stage PD (UPDRSIII 15-30, N=78), or late-stage PD (UPDRSIII >30, N=63) as described previously (Lin et al. 2012). Subjects from the welder sample group were classified as normal (UPDRSIII <6), having an intermediate score (UPDRSIII ≥6 and <15), or PS (UPDRSIII ≥15) as described previously (Racette et al. 2012). Blood samples were concurrently collected at the time of clinical examination as described previously (Shi et al. 2010). All blood samples from the clinical sample group were collected in EDTA tubes in the morning following overnight fasting, and plasma was processed and frozen at -80^{o}C within 90 minutes of collection. Blood samples from the welders sample group were collected in EDTA tubes in the morning or afternoon, typically following the work shift without fasting. Processing was conducted

in the field and shipped on dry ice over night to University of Washington. Upon receipt at the University of Washington, all plasma samples were treated with 10% protease inhibiting cocktail (PIC; P2714, Sigma-Aldrich, St. Louis, MO, USA) by volume and aliquoted into single-usage volumes to avoid multiple freeze-thaw cycles prior to long-term storage at -80^{o}C.

Autoantibody Profiling of Pooled Plasma Samples

As part of our search for novel peripheral biomarkers of PS, we conducted a comprehensive profiling study of autoantibodies in human plasma collected from a subset of the clinical sample. This subset consisted of three small pools per study group comprised of 5 to 10 subjects, depending on the availability of individual samples while matching by age. The study groups included: 1) healthy controls (N=10 in each pool, N=30 total); 2) AD (N=5 in each pool, N=15 total); 3) early-stage PD (N=5 in each pool, N=15 total); 4) middle-stage PD (N=10 in each pool, N=30 total); 5) late-stage PD (N=10 in each pool, N=30 total) (**Table 1**). These pooled samples were screened for the presence of plasma autoantibodies for 9,480 proteins using a ProtoArray® Human Protein Microarray (PAH052520; Life Technologies, Carlsbad, CA, USA) platform according to the manufacturer's "immune response biomarker profiling-probing procedure" protocol. Briefly, arrays were placed in the bottom of a 4-chamber incubation tray and incubated with blocking buffer for 1 hour at 4^{o}C while shaking at 50rpm. After washing, plasma samples (diluted 1:500 in wash buffer) were added to each chamber and incubated at 4^{o}C for 90 minutes. The arrays were washed 5 times with wash buffer, then Alexa Fluor® 647 goat anti-human IgG antibody (diluted 1:2000 in washing buffer) was added to the chambers and incubated at 4^{o}C for 90 minutes. The arrays were washed 5

times with wash buffer, allowed to dry and scanned using a GenePix 4000B Microarray Scanner (Molecular Devices, Sunnyvale, CA, USA) with GenePix Pro7 software (Molecular Devices) according to manufacturer's protocol.

Bioinformatics Analysis

The profiling data were analyzed using ProtoArray® Prospector v5.2 software (Life Technologies). Single array analysis in Prospector was performed using the immune response profiling application tool, and the group characterization command was executed for sample group. To compare samples, the two-group comparison command was executed using either the control or early-stage PD samples as the reference group, and the resulting data were ranked according to p-value. Differentially regulated candidates with $p < 0.05$ and a fold change ≥ 1.5 as compared to the reference group were selected for further bioinformatics analysis. Only those that were up-regulated met these criteria (no down-regulated candidates were identified). The Gene Ontology (GO) terms of proteins that appear to be targeted by autoantibodies in PD were analyzed using the online DAVID 6.7 bioinformatics resource (http://david.abcc.ncifcrf.gov/), with Bonferroni corrected p-value <0.05, which is a powerful enrichment tool that can be used to collapse lists of proteins into a smaller set of pathways or processes (Huang da et al. 2009).

In order to assess which classes of cellular and molecular processes have autoantibodies targeted against them among late-stage PD patients in the clinical cohort, heatmaps were generated using the R statistical software (Team 2014), and the heatmap.2 function of the gplots package. Plots were generated comparing late-stage PD patients to (1) healthy controls and (2) early-stage PD patients. Prior to clustering, the mean control

value (by autoantibody) was subtracted from each observation. This aids interpretation of the heatmap, as the cells can be interpreted as increases or decreases from the average control value. Rows were ordered based on a hierarchical clustering, using complete linkage and 1-correlation as a distance measure.

Mortalin Autoantibody Assay Development & Optimization

In order to measure mortalin autoantibodies in individual plasma samples quickly and reliably, we developed a sandwich-type Luminex-based assay similar to what has been described previously (Hong et al. 2010) with slight modifications. Briefly, purified recombinant human full-length mortalin protein (ab79145, Abcam plc, Cambridge, MA, USA) was filtered 3 times using 30K Amicon Ultra centrifugal filters (Millipore, Billerica, MA, USA) with 0.1M 2-(N-morpholino)ethanesulfonic acid (MES) buffer (pH = 6.0). Following this desalting/buffer exchange step, the purified protein was conjugated to activated polystyrene microspheres (Lumninex Corporation, Austin, TX, USA) according to the manufacturer's instructions to act as an analyte capturing system. The mortalin protein coupled beads were then incubated with 100μL of 1:10 diluted plasma [diluted with 0.1% w/v bovine serum albumin (BSA) dissolved in phosphate buffered saline (PBS; pH = 7.4)] in a 96-well MultiScreen filter plate (Millipore) shaking at 600rpm for 30 minutes at room temperature. The beads were washed in the filter plate 10 times with radioimmunoprecipitation assay buffer (150mM NaCl, 1% IGEPAL CA-630, 1% sodium deoxycholate, 0.1% SDS, 5mM Tris pH = 8.0) using a vacuum manifold, and incubated with the detection antibody (100μL biotinylated protein G (Pierce Biotechnology, Rockford, IL, USA) at a concentration of 1ng/mL) for 30 minutes at room temperature while shaking at a speed of 600rpm. The beads were then washed three

times with washing buffer (0.1% Tween-20 & 0.1% Triton X-100 in PBS, pH = 7.4), and incubated with 100μL streptavidin-R-phycoerythrin (ProZyme, Inc., Hayward, CA, USA) diluted to a concentration of 1ng/mL at room temperature for 30 minutes while shaking at a speed of 600rpm. The beads were then washed once again four times with washing buffer, resuspended in 100μL washing buffer, and read on a LiquiChip Luminex 200^{TM} instrument (Luminex Corporation). A standard curve was created in parallel by measuring serially diluted purified rabbit anti-human mortalin antibody (Sigma-Aldrich) to allow for quantification of autoantibody levels. Each plate analyzed included at least 4 replicate measurements (of an identical pooled reference plasma sample) that were used to correct for plate-to-plate assay variability.

Assay performance was determined in several ways. First, to test the assay specificity, mortalin antibodies were depleted from human plasma by immunoprecipitation using increasing capture amounts of recombinant human mortalin protein (0, 1.25, 2.5, and 5μg). Mortalin antibody depleted samples were then analyzed using the developed Luminex method, revealing a consistently decreasing analyte signal with increasing amounts of pre-depletion capturing protein (**Figure 1**). Second, the assay accuracy was determined by spiking mortalin antibody standard into human plasma samples; the average recovery rate was 94.3% using this assay. Finally, the average signal/background ratio of a pooled reference sample of control plasma was 66.2 and the limit of detection was 0.16 ng/mL as determined using the mortalin antibody standard.

Statistical Analysis

To further assess the relation between iPD/PS and mortalin autoantibodies, using an enhanced sample size and individual rather than pooled specimens, we conducted

additional analysis among this clinical cohort (using the 138 PD patients and 211 controls described above), and then repeated these analyses among the occupational cohort (using the 59 welders with PS and the 95 welders without PS described above). Group means of mortalin autoantibody levels were plotted using Graphpad Prism software (version 5, GraphPad Software, Inc., La Jolla, CA, USA). Asterisks denote data points representing groups significantly different statistically from healthy controls or normal welders (*$p<0.05$; **$p<0.01$). Differences among groups were assessed statistically by building a regression model with mortalin autoantibody concentration (natural logarithm transformed for normality) as the dependent variable, and group (dummy variable for each group within the respective cohort), age (continuous), and gender as independent variables (i.e. ANCOVA) using Stata software (version 11, StataCorp LP, College Station, TX, USA). Among subjects with iPD (clinical sample group) or PS (occupational sample group) we likewise examined the relation between mortalin autoantibodies and disease severity, as assessed by UPDRSIII score modeled continuously. We stratified all analyses by sample (clinical, occupational) because preliminary results demonstrated that mortalin levels were generally higher in the clinical and occupational groups, which could relate to known differences in the two samples beyond age and sex (e.g. activity level, geographic region, and blood collection procedures including time of day and fasting status).

Results

Subject Demographics

Welding subjects were generally younger and had a higher proportion of males than the clinical groups (**Tables 2 and 3**). The mean UPDRSIII scores were higher in the clinical PD groups as compared to the welder groups, with mean UPDRSIII of welders with PS slightly lower than those of the on-state mid-stage PD cases.

Autoantibody Profiling of Blood Plasma Samples

A total of 12 autoantibodies were discovered to be higher in patients diagnosed with PD (all PD patient groups combined) as compared to age-matched clinical controls (**Figure 2A and Table 4**). When we investigated the relation between severity and autoantibodies among the iPD patients, autoantibodies to 109 different proteins were at least doubled in pooled samples of iPD subjects with UPDRSIII scores ≥30 as compared to those with scores ≤15 (**Figure 2B**). GO analysis demonstrated these autoantibodies were relevant to several common biological processes, including those involved in regulation of apoptosis (11 candidates) or more specifically its positive regulation (9 candidates), and phosphorylation (14 candidates) or its regulation (8 candidates) (**Figure 3A**). Autoantibodies against proteins involved in phosphorylation processes were also the most identified candidates when comparing PD subjects with UPDRSIII scores ranging from 15-30 as compared to those with scores ≤ 15. The most common classes of molecular processes identified for this comparison (UPDRSIII 15-30 vs. UPDRSIII ≤ 15) included nucleotide binding (involving purines or ribonucleotides), ATP binding, and protein kinase activity (**Figure 3B**).

Plasma Mortalin Autoantibody Level and iPD

Of the candidate autoantibodies identified as potential biomarkers of PD severity, those against mortalin (*HSPA9*) were of significant interest, as decreased levels of this protein in the brain tissue have been associated with both iPD diagnosis (Jin et al. 2006) and progression (Shi et al. 2008) and rare gene variants have been reported to confer risk to developing PD (De Mena et al. 2009). Using a high-throughput Luminex assay to quantify plasma mortalin autoantibody levels in individual samples as described above, plasma mortalin autoantibody levels were measured in the expanded set of iPD and control subjects (originating from the same sample population the pooled sample subsets were derived from and described above), as well as subjects diagnosed with AD to ascertain neurodegenerative disease specificity. Using ANCOVA analysis, we found that subjects with more severe PD (UPDRSIII >30) had significantly greater plasma mortalin autoantibody levels when compared to healthy controls ($r=0.396$; $p<0.001$), patients with AD ($r=0.479$; $p=0.003$) and iPD subjects at earlier stages of the disease (UPDRSIII <15; $r=0.409$; $p=0.001$) (**Figure 4A**). Accordingly, there was also a positive association between plasma mortalin autoantibody levels and disease severity as assessed clinically by UPDRSIII score ($r=0.011$; $p=0.002$) (**Figure 4B**), confirming the profiling results.

Plasma Mortalin Autoantibody Level and Mn-induced PS

We next assessed whether mortalin autoantibodies are associated with signs of PS in a subset of plasma samples obtained from a Mn-exposed cohort of shipyard welders. The cohort is well-characterized and has a high prevalence of PS (15.6%) (Racette et al, 2012). In the subsample included here, the median UPDRSIII score was 19, with one welder in the UPDRSIII >30 category (UPDRSIII = 31). Nonetheless, mortalin

autoantibody levels were slightly greater in welders exhibiting signs of PS as compared to normal welders (**Figure 5A**). However, this possible association was strongly influenced by one subject with particularly high mortalin levels (confirmed in repeat laboratory analysis). Accordingly, no association was observed between natural logarithm transformed mortalin autoantibody level and UPDRSIII score as a continuous measure among all welders (**Figure 5B**) or among the subset of welders with PS. Furthermore, there was no discernible relationship between plasma mortalin autoantibody levels and cumulative welding exposure (data not shown).

Discussion

Our study is unique in two important aspects. First, we performed an extensive profiling investigation of blood plasma autoantibodies in PD patients tiered as a function of disease severity, with AD patients as a disease control. The other major advance was the observation of a positive association of one of the profiling candidates, antibodies against mortalin, with PS severity in individual plasma samples collected from PD patients. Although this autoantibody was not identified in the profiling study to differentiate between PD and controls, nor was it associated with PS severity in an active worker population with generally less severe PS than the present clinical sample, this potential biomarker for severity may prove useful in clinical samples as its levels were found to be significantly elevated in PD patients with advanced disease conditions.

Two observations of the profiling study are worth further discussion. First, autoantibody profiles were increased in PD subjects compared to controls: Although only twelve autoantibodies were identified as differentiating PD patients from controls,

all were higher in iPD subjects than in controls. Similarly, the autoantibodies associated with PD severity among PD patients also demonstrated positive associations. Second, there were unique autoantibodies in each disease profiled (AD and PD), and interestingly those related to phosphorylation and apoptosis were commonly found to be elevated in PD patients with more severe signs of the disease as compared to those with milder forms. Post-translational modification of proteins has been implicated as an important process in PD pathogenesis, particularly in the case of α-synuclein, as it has been reported that 90% of its aggregates within Lewy bodies are phosphorylated at Ser129 (Sato et al. 2013). Further, many of the antibodies discovered are those against proteins that are involved in CNS development or proposed to play a role in a variety of neurodegenerative disorders, including a sizable proportion to proteins that have been proposed to play a role in PD pathogenesis. This observation suggests that the mechanism of autoimmunity may be of importance in the progressive nature of these disorders in general.

A considerably higher number of elevated autoantibodies were identified when comparing later-stage PD patients to early stage PD subjects rather than control subjects. A possible explanation for this counterintuitive observation is that PD subjects are generally well-characterized clinically, whereas the control subjects are less so. Therefore, it is possible that the control subjects may have underlying health issues that are not neurologically related, and less commonly observed among the PD cases. Indeed, it was noted that one of the three profiling samples pooled from the plasma of controls produced a considerably higher signal for most detected autoantibodies as compared to the other two control pools. It is also possible that our early-stage PD cases were more

comparable to the late-stage cases than were the controls with regard to factors known to typically differ between PD cases and controls, such as race, ethnicity and notably tobacco smoking.

We focused on autoantibodies against mortalin because of its purported role in PD (Jin et al. 2006, Jin et al. 2007, Shi et al. 2008, De Mena et al. 2009, Burbulla et al. 2010). The role of mortalin in PD was first described by Jin and colleagues, who by using a proteomic approach found the protein to be decreased in the mitochondrial fraction of brain tissue isolated from PD patients as compared to brain isolated from age-matched controls (Jin et al. 2006). A similar study by Shi and colleagues found brain tissue levels of mortalin protein decreased as a function of disease severity (Shi et al. 2008). A subsequent *in vivo* investigation found mortalin levels to be lower in brain tissue of rats treated with 6-hydroxydopamine (Chiasserini et al. 2011), a toxicant commonly used to mimic PD in rodents. Additionally, various *in vitro* studies have reported decreased mortalin in response to treatment with rotenone (Jin et al. 2006) or dopamine quinone (Van Laar et al. 2008), and also in cells overexpressing α-synuclein (Pennington et al. 2010), a known risk factor for PD in humans in that triplication of the *SNCA* gene is causative of familial forms of the disease (Singleton et al. 2003). Taken together, these studies provide evidence that mortalin is not only implicated in the pathogenesis of PD, but it is also responsive to exogenous toxicants that produce parkinsonian conditions.

Interestingly, although mortalin autoantibody levels were indistinguishable in healthy controls vs. patients in the earliest stages of iPD, there was a trend toward higher mortalin autoantibody levels in patients at more advanced stages of iPD, and a statistically significant difference between mortalin autoantibody levels in early-stage PD

vs. late-stage PD. The relationship between PD severity and mortalin autoantibody level was further supported by partial regression analysis, which revealed a significant positive association between these variables after adjusting for age and gender. These data suggest that although plasma mortalin autoantibody levels are likely not useful as diagnostic biomarkers, the positive association with disease severity is suggestive that they may be useful as a means of tracking disease progression. Future longitudinal studies are needed to evaluate this possibility directly. These findings may also be indicative of underlying neuropathological or neuroprotective processes associated with the progression of PD. Autoantibodies to mortalin could be higher in more advanced disease stages either causally, therefore contributing at least in part to the well-established decline of the protein in iPD brain, or alternatively acting protectively in response to mortalin protein being released from apoptotic neurons. Further mechanistic investigations will be needed to assess this possibility.

The other major component of this study was the inclusion of a sample of occupational welders. Welders have been described to have a significantly increased prevalence of PS as compared to the general population (Racette et al. 2012). A common component of welding fumes is Mn, which has been established as a neurotoxicant under acute, high-exposure scenarios for nearly two centuries (Couper 1837), and more recently to be associated with modest exposure (Racette et al. 2005, Hobson et al. 2011, Racette et al. 2012, Roels et al. 2012, Chang et al. 2013). For these reasons, we applied the methodology described above for iPD patients to a cohort of occupational welders whose neurological health has been studied in detail (Racette et al. 2012). While we found a tendency of plasma mortalin autoantibodies to be higher in welders exhibiting signs of

PS, the results were not statistically significant. It should be emphasized that welders defined as having PS generally had milder signs than those with iPD, and only a single welder had a UPDRSIII score >30, whereas 63 iPD subjects exceeded this score. In other words, the changes in mortalin autoantibody in welders could become more apparent if more advanced cases are included or when the sample size is expanded.

There are several notable limitations to this study. With regard to the profiling characterization of plasma samples, we did not have sufficient clinical information to exclude control subjects who may have an underlying autoimmune disorder (e.g., lupus erythmatosus, rheumatoid arthritis, etc.). Insofar as our PD cases did not have these conditions, inclusion of even a single control subject with one of these conditions using our pooled sample profiling approach would likely impair our ability to observe associations, given that those observed were uniformly positive. This may limit the ability of this study to provide insight toward the significance of autoantibodies in the initiation of iPD. The characterization of PS severity by UPDRSIII score was chosen as an index common to both iPD and welder subjects, however a caveat is that iPD subjects were evaluated while being treated medically and undergoing drug therapy for their condition (i.e. in the on-state), whereas welders were not. UPDRSIII scores of iPD patients undergoing treatment in a clinical setting may be influenced by several factors, including differential benefit from medication, physician differences in treatment, subject expectations, and non-motor signs that contribute to disability. Finally, we did not have sufficient data to adjust for smoking status or race/ethnicity in either group.

In conclusion, we found plasma levels of autoantibodies against the mortalin protein to be positively associated with PD severity in a clinical sample, and an upward

trend was observed between mortalin among normal welders and welders exhibiting signs of PS. Although this finding indicates that mortalin autoantibodies may reflect PS severity, further longitudinal studies are needed in order to confirm this observation, and to further evaluate the capability of mortalin autoantibodies to reflect disease progression.

References

Allen, M. T., and L. S. Levy. 2013. Parkinson's disease and pesticide exposure--a new assessment. Crit Rev Toxicol **43**:515-534.

Archelos, J. J., and H. P. Hartung. 2000. Pathogenetic role of autoantibodies in neurological diseases. Trends Neurosci **23**:317-327.

Benkler, M., N. Agmon-Levin, S. Hassin-Baer, O. S. Cohen, O. D. Ortega-Hernandez, A. Levy, S. D. Moscavitch, M. Szyper-Kravitz, M. Damianovich, M. Blank, J. Chapman, and Y. Shoenfeld. 2012. Immunology, autoimmunity, and autoantibodies in Parkinson's disease. Clin Rev Allergy Immunol **42**:164-171.

Besong-Agbo, D., E. Wolf, F. Jessen, M. Oechsner, E. Hametner, W. Poewe, M. Reindl, W. H. Oertel, C. Noelker, M. Bacher, and R. Dodel. 2013. Naturally occurring α-synuclein autoantibody levels are lower in patients with Parkinson disease. Neurology **80**:169-175.

Burbulla, L. F., C. Schelling, H. Kato, D. Rapaport, D. Woitalla, C. Schiesling, C. Schulte, M. Sharma, T. Illig, P. Bauer, S. Jung, A. Nordheim, L. Schöls, O. Riess, and R. Krüger. 2010. Dissecting the role of the mitochondrial chaperone mortalin in Parkinson's disease: functional impact of disease-related variants on mitochondrial homeostasis. Hum Mol Genet **19**:4437-4452.

Caudle, W. M., T. S. Guillot, C. R. Lazo, and G. W. Miller. 2012. Industrial toxicants and Parkinson's disease. Neurotoxicology **33**:178-188.

Chahine, L. M., M. B. Stern, and A. Chen-Plotkin. 2014. Blood-based biomarkers for Parkinson's disease. Parkinsonism Relat Disord **20 Suppl 1**:S99-103.

Chang, Y., S. U. Jin, Y. Kim, K. M. Shin, H. J. Lee, S. H. Kim, J. H. Ahn, S. J. Park, K. S. Jeong, Y. C. Weon, and H. Lee. 2013. Decreased brain volumes in manganese-exposed welders. Neurotoxicology **37**:182-189.

Chiasserini, D., A. Tozzi, A. de Iure, M. Tantucci, F. Susta, P. L. Orvietani, K. Koya, L. Binaglia, and P. Calabresi. 2011. Mortalin inhibition in experimental Parkinson's disease. Mov Disord **26**:1639-1647.

Couper, J. 1837. On the effects of black oxide of manganese when inhaled into the lungs. British Annals of Medicine, Pharmacy, Vital Statistics, and General Science **1**:2.

De Mena, L., E. Coto, E. Sánchez-Ferrero, R. Ribacoba, L. M. Guisasola, C. Salvador, M. Blázquez, and V. Alvarez. 2009. Mutational screening of the mortalin gene (HSPA9) in Parkinson's disease. J Neural Transm **116**:1289-1293.

Double, K. L., D. B. Rowe, F. M. Carew-Jones, M. Hayes, D. K. Chan, J. Blackie, A. Corbett, R. Joffe, V. S. Fung, J. Morris, P. Riederer, M. Gerlach, and G. M.

Halliday. 2009. Anti-melanin antibodies are increased in sera in Parkinson's disease. Exp Neurol **217**:297-301.
Fahn, S., and R. Elton. 1987. Members of the UPDRS Development Committee. Unified Parkinson's disease rating scale. Pages 153-163.
Gibb, W. R., and A. J. Lees. 1988. The relevance of the Lewy body to the pathogenesis of idiopathic Parkinson's disease. J Neurol Neurosurg Psychiatry **51**:745-752.
Gold, M., R. Pul, J. P. Bach, M. Stangel, and R. Dodel. 2012. Pathogenic and physiological autoantibodies in the central nervous system. Immunol Rev **248**:68-86.
Grerogy R. Warnes, B. B., Lodewijk Bonebakker, Robert Gentleman, Wolfgang Huber, Andy Liaw, Thomas Lumley, Martin Maechler, Arni Magnusson, Steffen Moeller, Marc Schwartz, Bill Venables. 2014. gplots: Various R programming tools for plotting data. Page Various R programming tools for plotting data.
Han, M., E. Nagele, C. DeMarshall, N. Acharya, and R. Nagele. 2012. Diagnosis of Parkinson's disease based on disease-specific autoantibody profiles in human sera. PLoS One **7**:e32383.
Hobson, A., N. Seixas, D. Sterling, and B. A. Racette. 2011. Estimation of particulate mass and manganese exposure levels among welders. Ann Occup Hyg **55**:113-125.
Hong, Z., M. Shi, K. A. Chung, J. F. Quinn, E. R. Peskind, D. Galasko, J. Jankovic, C. P. Zabetian, J. B. Leverenz, G. Baird, T. J. Montine, A. M. Hancock, H. Hwang, C. Pan, J. Bradner, U. J. Kang, P. H. Jensen, and J. Zhang. 2010. DJ-1 and alpha-synuclein in human cerebrospinal fluid as biomarkers of Parkinson's disease. Brain **133**:713-726.
Huang da, W., B. T. Sherman, and R. A. Lempicki. 2009. Systematic and integrative analysis of large gene lists using DAVID bioinformatics resources. Nat Protoc **4**:44-57.
Jin, J., C. Hulette, Y. Wang, T. Zhang, C. Pan, R. Wadhwa, and J. Zhang. 2006. Proteomic identification of a stress protein, mortalin/mthsp70/GRP75: relevance to Parkinson disease. Mol Cell Proteomics **5**:1193-1204.
Jin, J., G. J. Li, J. Davis, D. Zhu, Y. Wang, C. Pan, and J. Zhang. 2007. Identification of novel proteins associated with both alpha-synuclein and DJ-1. Mol Cell Proteomics **6**:845-859.
Lee, M. S., and C. D. Marsden. 1994. Neurological sequelae following carbon monoxide poisoning clinical course and outcome according to the clinical types and brain computed tomography scan findings. Mov Disord **9**:550-558.
Lin, X., T. J. Cook, C. P. Zabetian, J. B. Leverenz, E. R. Peskind, S. C. Hu, K. C. Cain, C. Pan, J. S. Edgar, D. R. Goodlett, B. A. Racette, H. Checkoway, T. J. Montine, M. Shi, and J. Zhang. 2012. DJ-1 isoforms in whole blood as potential biomarkers of Parkinson disease. Sci Rep **2**:954.
Magdalinou, N., A. J. Lees, and H. Zetterberg. 2014. Cerebrospinal fluid biomarkers in parkinsonian conditions: an update and future directions. J Neurol Neurosurg Psychiatry.
McKhann, G., D. Drachman, M. Folstein, R. Katzman, D. Price, and E. M. Stadlan. 1984. Clinical diagnosis of Alzheimer's disease: report of the NINCDS-ADRDA Work

Group under the auspices of Department of Health and Human Services Task Force on Alzheimer's Disease. Neurology **34**:939-944.
Monahan, A. J., M. Warren, and P. M. Carvey. 2008. Neuroinflammation and peripheral immune infiltration in Parkinson's disease: an autoimmune hypothesis. Cell Transplant **17**:363-372.
Nagele, E., M. Han, C. Demarshall, B. Belinka, and R. Nagele. 2011. Diagnosis of Alzheimer's disease based on disease-specific autoantibody profiles in human sera. PLoS One **6**:e23112.
Neff, F., X. Wei, C. Nolker, M. Bacher, Y. Du, and R. Dodel. 2008. Immunotherapy and naturally occurring autoantibodies in neurodegenerative disorders. Autoimmun Rev **7**:501-507.
Papachroni, K. K., N. Ninkina, A. Papapanagiotou, G. M. Hadjigeorgiou, G. Xiromerisiou, A. Papadimitriou, A. Kalofoutis, and V. L. Buchman. 2007. Autoantibodies to alpha-synuclein in inherited Parkinson's disease. J Neurochem **101**:749-756.
Papuc, E., J. Kurzepa, E. Kurys-Denis, A. Grabarska, W. Krupski, and K. Rejdak. 2014. Humoral response against glial derived antigens in Parkinson's disease. Neurosci Lett **566**:77-81.
Pennington, K., J. Peng, C. C. Hung, R. E. Banks, and P. A. Robinson. 2010. Differential effects of wild-type and A53T mutant isoform of alpha-synuclein on the mitochondrial proteome of differentiated SH-SY5Y cells. J Proteome Res **9**:2390-2401.
Racette, B. A. 2013. Manganism in the 21st century: The Hanninen lecture. Neurotoxicology.
Racette, B. A., S. R. Criswell, J. I. Lundin, A. Hobson, N. Seixas, P. T. Kotzbauer, B. A. Evanoff, J. S. Perlmutter, J. Zhang, L. Sheppard, and H. Checkoway. 2012. Increased risk of parkinsonism associated with welding exposure. Neurotoxicology **33**:1356-1361.
Racette, B. A., S. D. Tabbal, D. Jennings, L. Good, J. S. Perlmutter, and B. Evanoff. 2005. Prevalence of parkinsonism and relationship to exposure in a large sample of Alabama welders. Neurology **64**:230-235.
Roels, H. A., R. M. Bowler, Y. Kim, B. Claus Henn, D. Mergler, P. Hoet, V. V. Gocheva, D. C. Bellinger, R. O. Wright, M. G. Harris, Y. Chang, M. F. Bouchard, H. Riojas-Rodriguez, J. A. Menezes-Filho, and M. M. Téllez-Rojo. 2012. Manganese exposure and cognitive deficits: a growing concern for manganese neurotoxicity. Neurotoxicology **33**:872-880.
Sato, H., T. Kato, and S. Arawaka. 2013. The role of Ser129 phosphorylation of alpha-synuclein in neurodegeneration of Parkinson's disease: a review of in vivo models. Rev Neurosci **24**:115-123.
Shi, M., J. Jin, Y. Wang, R. P. Beyer, E. Kitsou, R. L. Albin, M. Gearing, C. Pan, and J. Zhang. 2008. Mortalin: a protein associated with progression of Parkinson disease? J Neuropathol Exp Neurol **67**:117-124.
Shi, M., C. P. Zabetian, A. M. Hancock, C. Ginghina, Z. Hong, D. Yearout, K. A. Chung, J. F. Quinn, E. R. Peskind, D. Galasko, J. Jankovic, J. B. Leverenz, and J. Zhang. 2010. Significance and confounders of peripheral DJ-1 and alpha-synuclein in Parkinson's disease. Neurosci Lett **480**:78-82.

Singleton, A. B., M. Farrer, J. Johnson, A. Singleton, S. Hague, J. Kachergus, M. Hulihan, T. Peuralinna, A. Dutra, R. Nussbaum, S. Lincoln, A. Crawley, M. Hanson, D. Maraganore, C. Adler, M. R. Cookson, M. Muenter, M. Baptista, D. Miller, J. Blancato, J. Hardy, and K. Gwinn-Hardy. 2003. alpha-Synuclein locus triplication causes Parkinson's disease. Science **302**:841.

Stamelou, M., and G. U. Hoeglinger. 2013. Atypical parkinsonism: an update. Curr Opin Neurol **26**:401-405.

Team, R. C. 2014. A language environment for statistical computing. R Foundation for Statistical Computing, Vienna, Austria.

Van Laar, V. S., A. A. Dukes, M. Cascio, and T. G. Hastings. 2008. Proteomic analysis of rat brain mitochondria following exposure to dopamine quinone: implications for Parkinson disease. Neurobiol Dis **29**:477-489.

Wang, J., J. G. Hoekstra, C. Zuo, T. J. Cook, and J. Zhang. 2013. Biomarkers of Parkinson's disease: current status and future perspectives. Drug Discov Today **18**:155-162.

Wilhelm, K. R., K. Yanamandra, M. A. Gruden, V. Zamotin, M. Malisauskas, V. Casaite, A. Darinskas, L. Forsgren, and L. A. Morozova-Roche. 2007. Immune reactivity towards insulin, its amyloid and protein S100B in blood sera of Parkinson's disease patients. Eur J Neurol **14**:327-334.

Tables & Figures

Table 1: Summary of pooled samples used in the autoantibody screening assay.

Population	Pool	N	UPDRSIII mean ± SD	Age	M:F Ratio
Controls	1-1	10	n/a	65.2 ± 7.5	3:2
	1-2	10	n/a	65.3 ± 7.7	3:2
	1-3	10	n/a	63.8 ± 7.2	3:2
AD	2-1	5	n/a	71.6 ± 13.8	2:3
	2-2	5	n/a	71.3 ± 13.2	2:3
	2-3	5	n/a	71.0 ± 4.7	2:3
Early PD (UPDRSIII <15)	3-1	5	12.4 ± 2.1	63.6 ± 9.2	2:3
	3-2	5	9.6 ± 4.8	62.6 ± 11.1	2:3
	3-3	5	11.2 ± 1.3	63.2 ± 11.5	1:4
Middle PD (UPDRSIII 15-30)	4-1	10	20.5 ± 5.3	63.8 ± 7.1	3:2
	4-2	10	22.0 ± 3.2	63.8 ± 4.5	3:2
	4-3	10	20.6 ± 3.6	63.2 ± 6.4	1:4
Late PD (UPDRSIII >30)	5-1	10	47.6 ± 9.1	69.9 ± 8.6	3:2
	5-2	10	45.9 ± 8.7	70.6 ± 8.5	3:2
	5-3	10	47.5 ± 7.7	71.5 ± 8.2	3:2

Abbreviation: SD = standard deviation; UPDRSIII = Unified Parkinson Disease Rating Scale Motor Subscore III

Table 2: Subject demographic data of the clinical neurodegenerative disease sample group.

Sample	N	UPDRSIII (Mean ±SD)	Age (Mean ±SD)	% Male
Controls	138	n/a	58.9 ± 16.3	73.9%
AD	28	n/a	66.8 ± 10.5	82.1%
Early PD (UPDRSIII <15)	70	9.7 ± 3.4	62.2 ± 9.3	58.6%
Middle PD (UPDRSIII 15-30)	78	21.4 ± 4.8	64.3 ± 10.5	87.2%
Late PD (UPDRSIII >30)	63	40.4 ± 9.4	66.8 ± 9.5	82.5%

Abbreviation: AD = Alzheimer disease; PD = Parkinson disease; SD = standard deviation; UPDRSIII = Unified Parkinson Disease Rating Scale Motor Subsection Part III

Table 3: Subject demographic data of the occupational welder group.

Sample	N	UPDRSIII (Mean ± SD)	Age (Mean ±SD)	% Male
Normal (UPDRSIII <6)	95	2.9 ± 1.6	46.4 ± 12.0	93.7%
Intermediate (UPDRSIII 6 - <15)	125	9.3 ± 2.7	51.5 ± 11.2	90.4%
PS (UPDRSIII ≥15)	59	19.8 ± 3.5	55.1 ± 11.9	96.6%

Abbreviation: SD = standard deviation; UPDRSIII = Unified Parkinson Disease Rating Scale Motor Subsection Part III

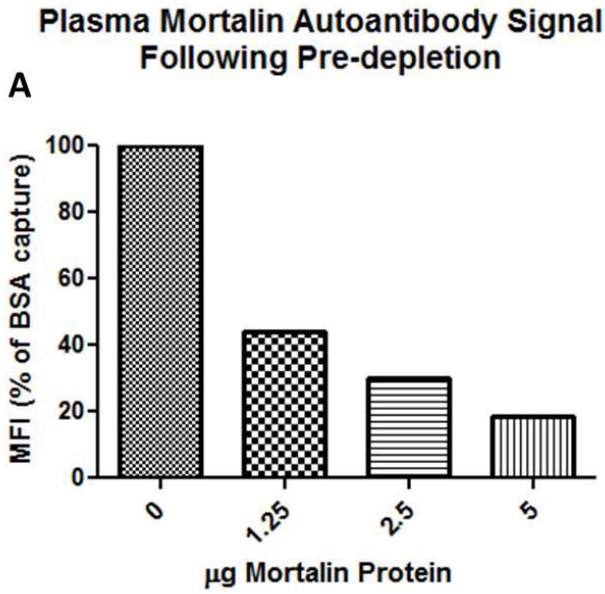

Figure 1: Pre-depleting mortalin antibodies from human plasma decreased Luminex assay signal intensity. Increasing the quantity of capture mortalin protein resulted in decreased analyte signal intensity as determined using the mean fluorescent intensity (MFI) of the sample. The graph represents the MFI ratio of the indicated sample to the non-depleted control sample (BSA capture).

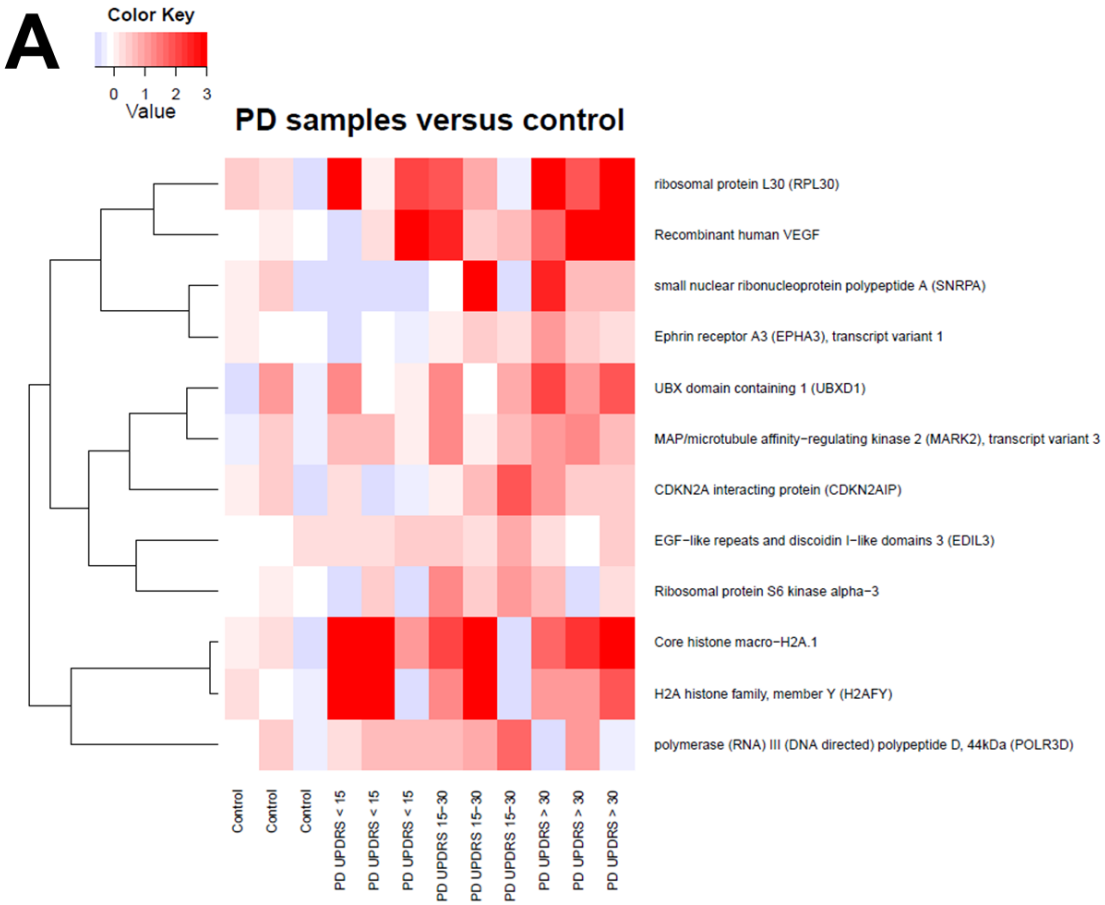
A
Color Key
0 1 2 3
Value
PD samples versus control
ribosomal protein L30 (RPL30)
Recombinant human VEGF
small nuclear ribonucleoprotein polypeptide A (SNRPA)
Ephrin receptor A3 (EPHA3), transcript variant 1
UBX domain containing 1 (UBXD1)
MAP/microtubule affinity−regulating kinase 2 (MARK2), transcript variant 3
CDKN2A interacting protein (CDKN2AIP)
EGF−like repeats and discoidin I−like domains 3 (EDIL3)
Ribosomal protein S6 kinase alpha−3
Core histone macro−H2A.1
H2A histone family, member Y (H2AFY)
polymerase (RNA) III (DNA directed) polypeptide D, 44kDa (POLR3D)
Control
Control
Control
PD UPDRS < 15
PD UPDRS < 15
PD UPDRS < 15
PD UPDRS 15−30
PD UPDRS 15−30
PD UPDRS 15−30
PD UPDRS > 30
PD UPDRS > 30
PD UPDRS > 30

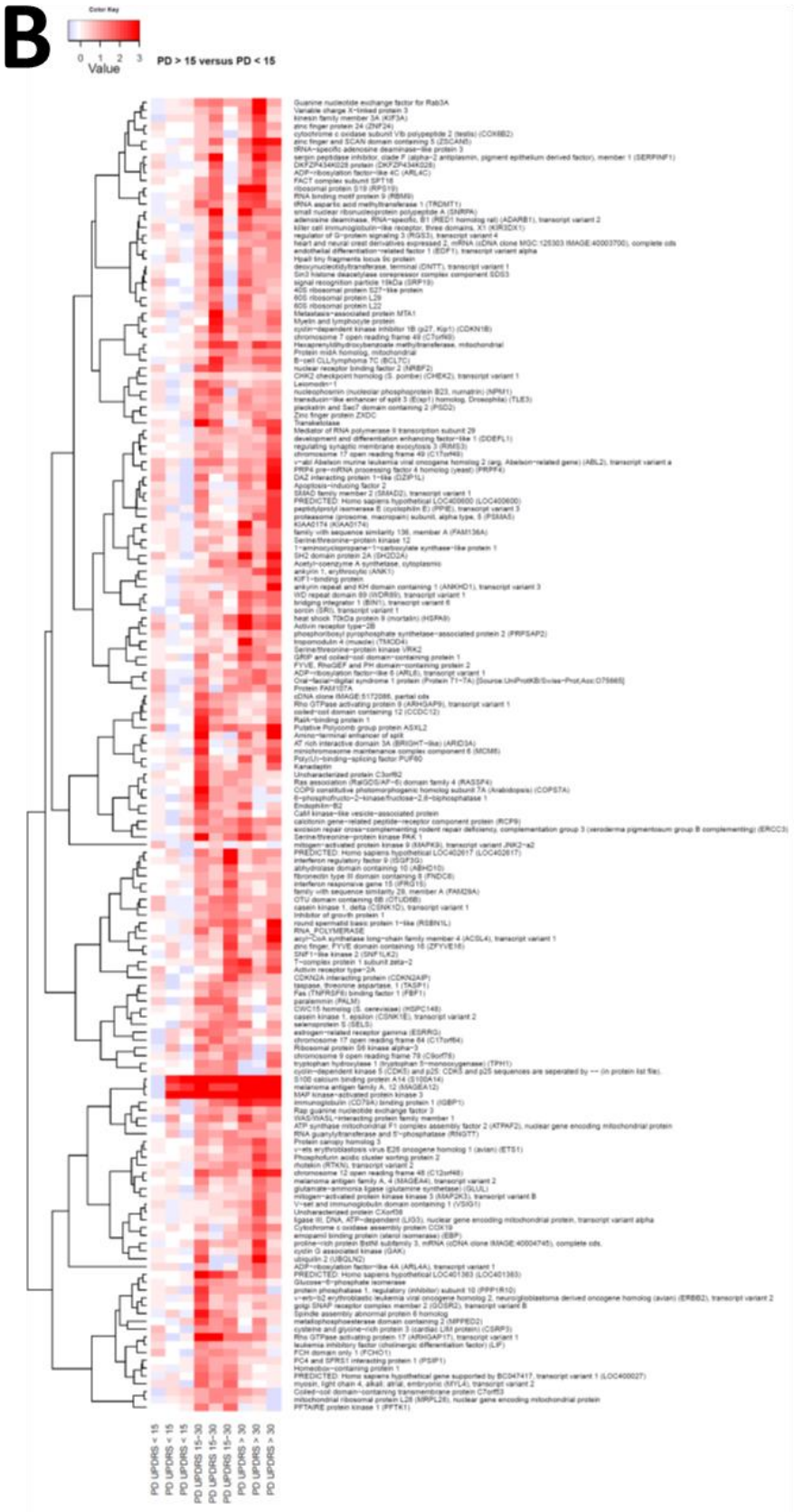
B
Color Key
0 1 2 3
Value
PD > 15 versus PD < 15
PD UPDRS < 15
PD UPDRS < 15
PD UPDRS < 15
PD UPDRS 15–30
PD UPDRS 15–30
PD UPDRS 15–30
PD UPDRS > 30
PD UPDRS > 30
PD UPDRS > 30

Figure 2: Profiling data heatmaps. (A) Heatmap displays all autoantibodies that were discovered to be significantly elevated ($p<0.05$) in late-stage iPD patients (UPDRSIII >30) as compared to healthy controls. (B) Heatmap displays all autoantibodies that were discovered to be significantly elevated in PD patients in late-stage iPD patients (UPDRSIII >30) as compared to early-stage iPD patients (UPDRSIII <15).

Table 4: Plasma autoantibodies to proteins discovered to be at least 50% elevated as compared to the reference group in the profiling study.

Gene	Protein	Uniprot #	Ratio UPDRS>30/ UPDRS<15	CNS related?	Neurodeg Disease?	Ref
UBQLN2	Ubiquilin 2	Q9UHD9	9.55	Yes	ALS	Dauod 2011
SH2D2A	SH2 domain protein 2A	Q9NP31	6.96		MS	Spurkland 2009
RPS19	Ribosomal protein S19	P39019	6.09			
HSPA9	Mortalin	P38646	5.99	Yes	PD, AD	Jin 2006; Shi 2009
DZIP1L	DAZ interacting protein 1-like	Q8IYY4	5.89	Yes	PD	Valente 2012
IST1	IST1 homolog	P53990	5.77			
ZSCAN5	Zinc finger and SCAN domain containing 5	Q7Z7L9	5.66			
RAB3IL1	Guanine nucleotide exchange factor for Rab3A	Q8TBN0	5.52	Yes	PD	Chen 2013
IGBP1	Immunoglobulin binding protein 1	P78318	5.03			
SNRPA	Small nuclear ribonucleoprotein polypeptide A	P09012	5.02			
SERPINF1	Serpin peptidase inhibitor, clade F, member 1	P36955	4.93	Yes	PD, ALS	Falk 2009; Yasuda 2007; Bilak 1999; Kuncl 2002

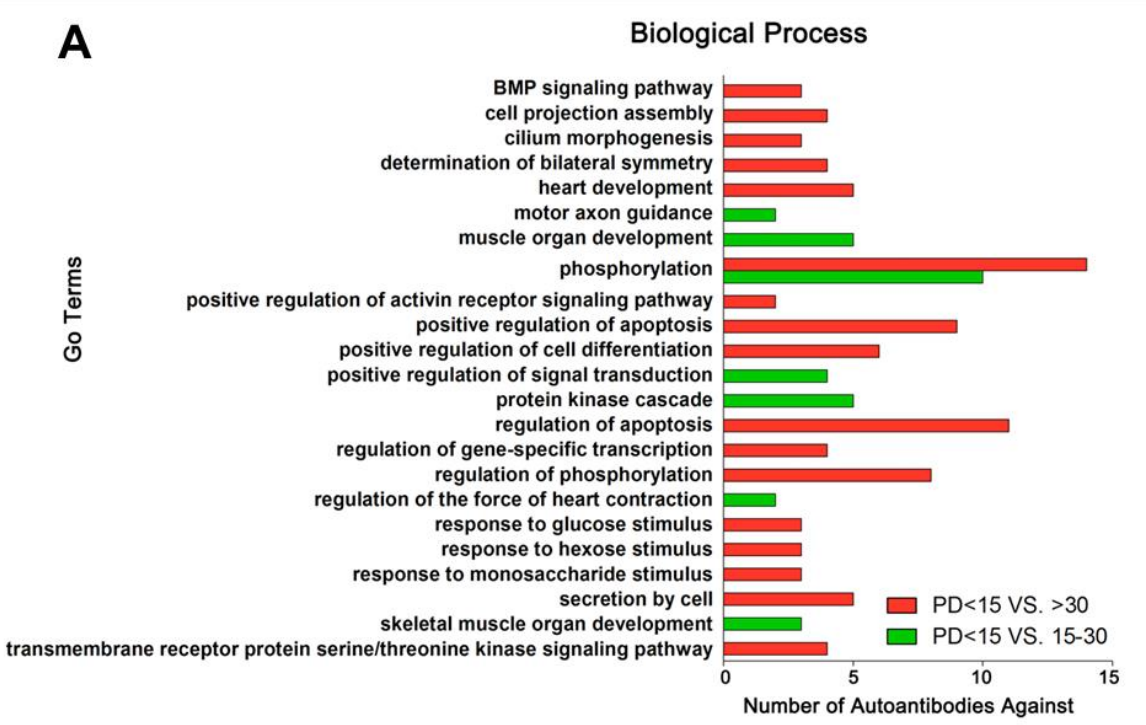
A
Biological Process
BMP signaling pathway
cell projection assembly
cilium morphogenesis
determination of bilateral symmetry
heart development
motor axon guidance
muscle organ development
phosphorylation
positive regulation of activin receptor signaling pathway
positive regulation of apoptosis
positive regulation of cell differentiation
positive regulation of signal transduction
protein kinase cascade
regulation of apoptosis
regulation of gene-specific transcription
regulation of phosphorylation
regulation of the force of heart contraction
response to glucose stimulus
response to hexose stimulus
response to monosaccharide stimulus
secretion by cell
skeletal muscle organ development
transmembrane receptor protein serine/threonine kinase signaling pathway
Go Terms
PD<15 VS. >30
PD<15 VS. 15-30
0
5
10
15
Number of Autoantibodies Against

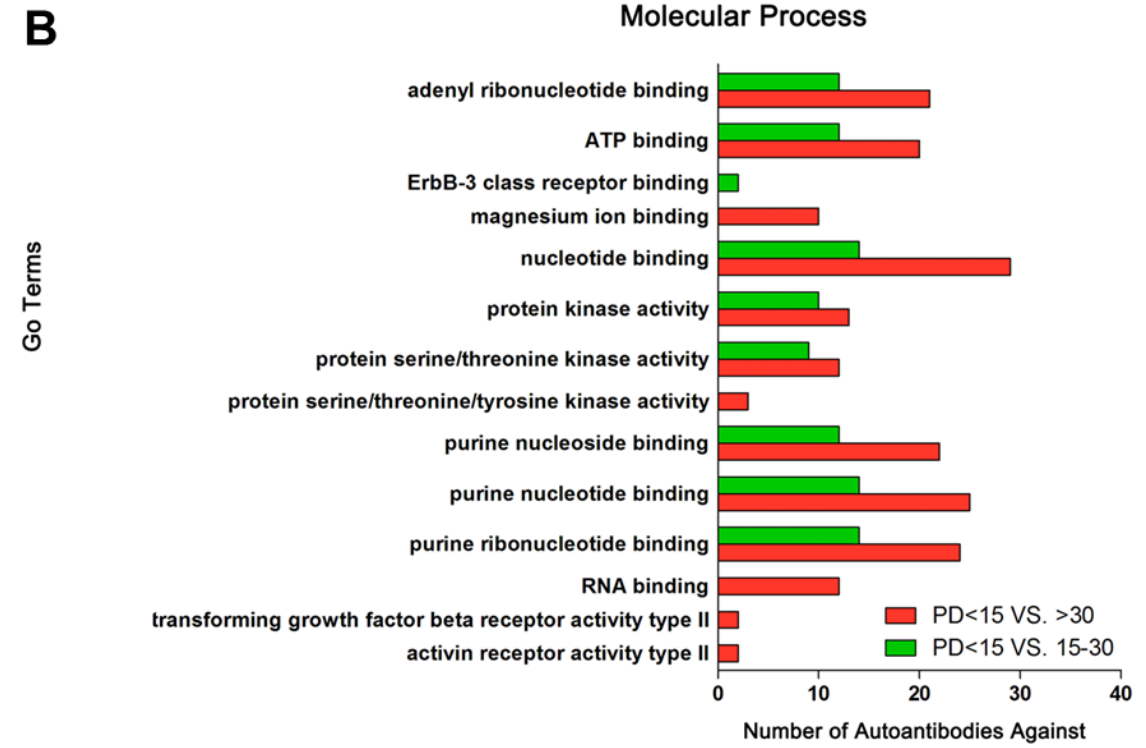
B
Molecular Process
adenyl ribonucleotide binding
ATP binding
ErbB-3 class receptor binding
magnesium ion binding
nucleotide binding
protein kinase activity
protein serine/threonine kinase activity
protein serine/threonine/tyrosine kinase activity
purine nucleoside binding
purine nucleotide binding
purine ribonucleotide binding
RNA binding
transforming growth factor beta receptor activity type II
activin receptor activity type II
Go Terms
PD<15 VS. >30
PD<15 VS. 15-30
0
10
20
30
40
Number of Autoantibodies Against

Figure 3: Gene ontology categories for differentifally expressed autoantibodies in PD patients with varying PD severity. Functional classification of proteins found to have up-regulated presence of blood plasma autoantibodies against in later-stage patients with regard to (A) biological processes and (B) molecular functions.

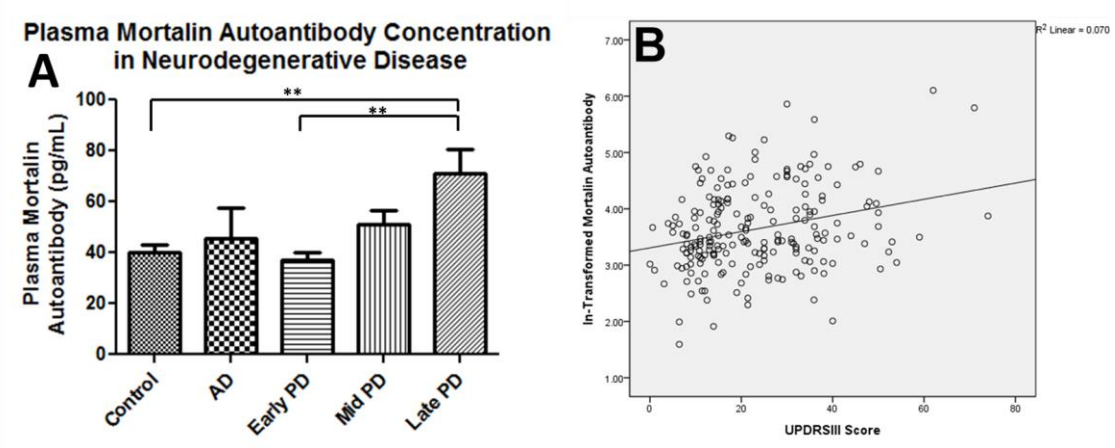

Figure 4: Plasma mortalin autoantibodies increase with iPD severity. (A) Mean plasma mortalin antibody levels were found to be significantly elevated in iPD patients with UPDRSIII scores >30 as compared to both iPD cases with UPDRSIII scores <15 and healthy controls. Data presented as mean ± standard error (**p<0.001). (B) Regression analysis with plasma mortalin autoantibody level as the dependent variable and UPDRSIII score, age, and gender as independent variables amongst subjects diagnosed with iPD. A statistically significant positive correlation was observed (r=0.011; p=0.002).

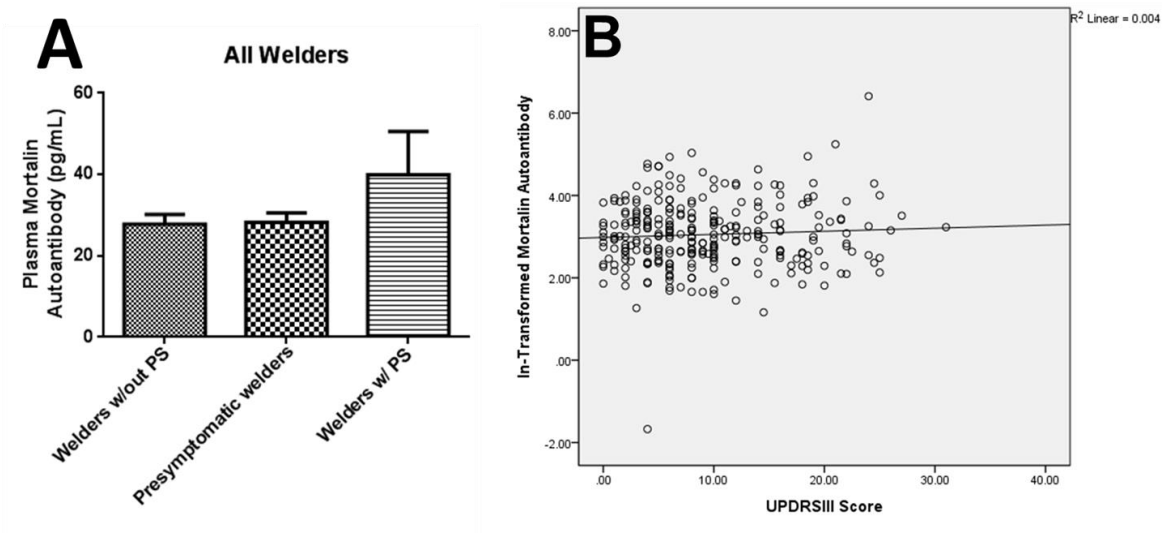

Figure 5: Association of plasma mortalin autoantibodies with manganese-induced PS. (A) Mean plasma mortalin antibody levels were found to be slightly higher in manganese-exposed welders with signs of PS as compared to those without parkinsonism. (B) Regression analysis with plasma mortalin autoantibody level as the dependent variable and UPDRSIII score, age, and gender as independent variables amongst manganese-exposed occupational welders. No association between plasma mortalin autoantibody level and UPDRSIII score was observed.

CHAPTER 4: MORTALIN IS EXPRESSED BY ASTROCYTES AND DECREASED IN THE MIDBRAIN OF PARKINSON'S DISEASE PATIENTS

Abstract

Mortalin, an essential mitochondrial chaperone protein, has previously been implicated in the pathogenesis of a wide array of diseases, including neurodegenerative conditions such as Parkinson's disease (PD) and Alzheimer's disease. Previous reports have consistently described mortalin protein levels to be lower in the brain tissue of patients with neurodegenerative disease, with expression demonstrated to be lower in neurons of post-mortem PD brain specimens. However, to date, mortalin expression has not yet been evaluated in astrocytes of post-mortem brain tissue from either normal or PD subjects. Here, we demonstrate the presence of mortalin in human astrocytes and find the protein to be significantly reduced in this cell type in the substantia nigra pars compacta, but not structures of the corpus striatum, in PD subjects as compared to age/gender-matched controls. These findings highlight the potential contribution of disrupted astroglial function in the pathogenesis of PD.

Introduction

The pathologic and clinical features defining Parkinson's disease (PD) have been established for several decades; however, the underlying mechanisms which lead to disease initiation and progression remain poorly understood. Recent advances in genetic screening technology have led to the identification of at least 18 loci for which mutation and/or aberrant expression are associated with disease incidence (Klein and Westenberger 2012). While the study of these genes and their protein products has led to considerable insight into dysfunctional processes and pathways that may contribute to disease development, the mechanistic etiology of the vast majority of idiopathic PD incidence is

incompletely understood. Additionally, to date, mechanistic investigations regarding PD pathogenesis have largely focused on neurons, whose dysfunction and eventual death are responsible for the cardinal clinical signs of the disease. Yet, a growing body of evidence implicates critical roles for astrocytes, which play vital roles in supporting the health of neurons under normal conditions (Bélanger et al. 2011) and in disease pathogenesis (Halliday and Stevens 2011).

In the current investigation, we focused on mortalin, a multi-functional chaperone protein previously implicated to play a role in PD pathology (Jin et al. 2006, Jin et al. 2007, Shi et al. 2008, De Mena et al. 2009, Burbulla et al. 2010, Chiasserini et al. 2011). Mortalin has been demonstrated to be decreased in the mitochondrial fraction of whole tissue lysates in the substantia nigra pars compacta (SNpc) of PD patients, (Jin et al. 2006) and was found to be associated with disease severity (Shi et al. 2008). *In vitro* mechanistic studies have demonstrated the direct interaction of mortalin with α-synuclein, (Jin et al. 2007) a protein intricately linked to PD pathogenesis. Further, mutated forms of mortalin (Burbulla et al. 2010) and its reduced expression (Jin et al. 2006) enhances neuronal toxicity in cell model systems.

While it has been shown that mortalin is decreased in neuronal cell bodies of PD patients, (Jin et al. 2006) mortalin expression within astrocytes has not been quantitatively evaluated to date. In this study, we first demonstrate that mortalin is expressed in brain astrocytes, and subsequently measure relative levels of mortalin protein in the SNpc and structures of the corpus striatum in post-mortem tissue of PD patients and healthy age- and gender-matched controls.

Materials & Methods

Identification of Mortalin in Astrocytes

Primary cortical glial cell cultures were generated from postnatal mouse pup brains harvested at 1-3 days following birth. Following decapitation, brains were carefully removed and transferred into ice-cold DMEM/F12 culture media (Gibco #11330-032, Life Technologies, Grand Island, NY, USA). Using a Leica L2 microscope (Leica Microsystems Inc, Buffalo Grove, IL, USA), both hemispheres of the cortex were isolated and meninges were carefully removed mechanically. Isolated cortical tissue was washed with plain DMEM/F12 media 3 times, transferred to digestion media [0.5 mM EDTA, 0.2 mg/mL L-cysteine, 150 U/mL papain, 10 mg/mL DNase in DMEM/F12], and incubated at 37°C for 30 minutes. Following digestion, the tissue was washed 3 times with culture medium [10% fetal bovine serum and 1% penicillin/streptomycin in DMEM/F12] pre-equilibrated to 37°C. After the final wash, the tissue was triturated using a flame-polished glass pipette in 10 mL culture medium, and the supernatant passed through a 100 micron nylon cell strainer into a conical tube. This process was repeated in 5 mL culture medium, and the resulting supernatant was transferred into 75 cm^2 vented tissue culture flasks (BD Falcon #35136, BD Biosciences, San Jose, CA, USA) coated with poly-D-lysine hydrobromide (BD Biosciences #354210). Following overnight incubation at 37°C with a 5% CO_2 atmosphere, the culture medium was replaced and the cultures were returned to the incubator for an additional 9-14 days before experimental use.

Following the incubation period, microglia were removed forcibly by striking the flask several times, aspirating the media, striking the flask again and washing with PBS

(pH 7.4). Trypsin (with 0.25% EDTA, Gibco #25200-056) was then added to the cellular monolayer, the flask was returned to the incubator for 5 minutes and cells were collected by washing with 10mL culture medium. The supernatant was transferred to a conical tube, centrifuged at 3,000 RPM and the pellet was resuspended to a plating density of $5x10^5$ cells/mL. This preparation resulted in a culture of primary mouse astrocytes of >95% purity (data not shown).

Transfection

Cells to be transfected were plated as described above in culture medium without antibiotics. Transfections were carried out using Lipofectamine 2000 reagent (Life Technologies #11668019) according to the manufacturer's protocol, with slight modifications. Briefly, Lipofectamine and 2X siRNA [either mortalin (Mm_Hspa9a_6 #SI02712710) or AllStars Negative Control (#1027201), Qiagen (Venlo, Limburg, Netherlands)] were incubated in Opti MEM media (Life Technologies #31985070) for 5 minutes at room temperature, combined and incubated at room temperature for an additional 20 minutes. Following the incubation period, the Lipofectamine/siRNA complex was added to the antiobiotic-free media, stored in the incubator overnight and the media changed to that containing antibiotics.

Western Blot

After allowing primary astrocytes to grow to confluency in a poly-D-lysine coated 6-well plate, the cells were washed once with ice cold PBS, collected in 100 μL lysis buffer [150 μM NaCl, 500 μM Tris-HCl, 1% (v/v) NP-40, 10% (v/v) 1X protease inhibitor cocktail, 1 μM PMSF, 10 μM NaF, 0.2 μM Na_3VO_4 in deionized water],

immediately flash frozen on dry ice and stored at -80°C. After thawing on ice, cellular lysates were sonicated, centrifuged at 15,000 RPM and supernatants were transferred to a clean 1.5 mL eppendorf tube. Following protein quantification by biochronic acid assay according to the manufacturer's protocol (Pierce #23225, Thermo Scientific, Waltham, MA, USA), equal amounts of protein were diluted into 2X Laemmli sample buffer (#61-0737, Bio-Rad Laboratories, Inc., Hercules, CA, USA) containing 5% (v/v) 2-mercaptoethanol, loaded onto a 10-20% Tris-HCl polyacrylamide gel (Bio-Rad #345-0042), and separated by electrophoresis (100V for 10 minutes; 120 V for 110 minutes). Proteins were then transferred to a PVDF membrane (Bio-Rad #162-0177) by applying a constant current of 0.36A for ~18 hours.

For protein visualization, membranes were first incubated for 1 hour at room temperature in blocking buffer [5% non-fat milk in TBS-T], followed by incubation with the primary antibody (mortalin #ADI-SPS-825, Enzo Life Sciences, Inc., Farmingdale, NY, USA; β-actin #ab8226, Abcam plc, Cambridge, MA, USA) and diluted into blocking buffer overnight at 4°C. Membranes were then washed 3 times with TBS-T, and the membrane was incubated with the secondary antibody (anti-mouse IgG, HRP-linked #50-195-914, Cell Signaling Technology, Beverly, MA, USA) for 1 hour at room temperature. After washing 3 times with TBS-T, enhanced chemilumescent reagents (Amersham ECL #RPN2209, GE Healthcare Bio-Sciences, Pittsburgh, PA, USA) were applied to the membrane for 2 minutes and the signal visualized on X-ray film.

Quantitative PCR

Primary astrocytes were plated into 6-well plates as described above. After reaching confluency, the cells were washed once with room temperature PBS, collected

in Trizol reagent (Invitrogen #15596-026, Life Technologies) and total RNA were isolated via a phenol-chloroform extraction method with slight modifications (Chomczynski and Sacchi 1987). Genomic DNA was removed using a TURBO DNA-free Kit (Life Technologies #AM1907), isolated RNA was quantified using a NanoDrop ND 1000 spectrophotometer (Thermo Scientific), and cDNA was generated using equal inputs of RNA template using a high-capacity cDNA reverse transcription kit (Life Technologies #4368814). Quantitative real-time PCR was performed using TaqMan reagents (Life Technologies) with off-the-shelf primer sets (Life Technologies #4331185; Hsap9 Mm00477716_g1 (mortalin); Gfap Mm01253033_m1 (GFAP); Rbfox3 Mm01248771_m1 (NeuN); Cd68 Mm03047340_m1 (CD68)) according to the manufacture's protocol on a ViiA7 PCR system (Life Technologies).

Human Brain Specimen Preparation

This study was approved by the University of Washington Institutional Review Board. Formalin-fixed paraffin embedded human brain specimens were provided from 6 PD patients and 6 age/gender-matched controls for this study courtesy of the University of Washington Alzheimer's Disease Research Center neuropathology core. Specimens from the midbrain and the corpus striatum were cut to a thickness of 4-5 μm and tissue sections were mounted onto glass microscope slides.

Immunofluorescent Staining

Human tissue sections were prepared as described previously,(Hoekstra et al. 2014) with slight modifications. Briefly, the tissues were deparaffinized in 100% xylenes (4 x 10 minutes), washed in a 1:1 mixture of xylenes and ethanol (2 x 5 minutes) and

rehydrated by washing in 100% (2 x 5 minutes), 95% (1 x 3 minutes), 70% (1 x 3 minutes) and 50% (1 x 3 minutes) ethanol. Tissues were then washed in deionized water (briefly) and PBS (2 x 5 minutes) and antigen retrieval was carried out by heating specimens submerged in 10mM citric acid (pH 6.0) to a boil and maintaining them at a high temperature for 15 minutes. After cooling for 30 minutes at room temperature, tissues were washed with 50mM Tris-buffered saline containing 0.05% Tween-20 (TBS-T; 3 x 10 min), and incubated with blocking buffer [5% normal goat serum, 2% bovine serum albumin, 0.1% Triton 100-X diluted in TBS-T] overnight at 4°C. The following day, the primary antibodies (rabbit anti-mortalin [Sigma SQ-15 #G4045] and chicken anti-GFAP [Millipore #AB5541]) were diluted (anti-mortalin 1:100; anti-GFAP 1:500) into blocking buffer and again incubated with tissues overnight at 4°C. Following the primary antibody incubation period, tissues were washed in TBS-T containing 5% normal goat serum and 2% bovine serum albumin (3 x 10 min), and secondary antibodies conjugated with Alexa fluorophores (568 goat anti-chicken and 488 goat anti-rabbit, Life Sciences) diluted 1:500 in washing buffer and were incubated at 4°C overnight. The following day the tissues were washed in TBS-T (3 x 10 minutes) and gently rocked in a solution of 70% ethanol containing 0.3% Sudan Black B to reduce autofluorescence. Finally, tissues were briefly rinsed with 70% ethanol, washed in TBS-T (3 x 10 minutes), covered with Vectashield mounting medium with DAPI (Vector Laboratories, Inc., Burlingame, CA, USA), affixed with a cover glass and sealed with nail polish.

Confocal Microscopy

Images of human astrocytes labeled for GFAP and mortalin as described above were acquired using an Olympus Fluoview-1000 (version 3.1b) scanning confocal

microscope (488 nm argon ion laser (green) and 561 nm DPSS laser (red)) at the Center on Human Development and Disability at the University of Washington. 60X (numerical aperture 1.35) and 100X (numerical aperture 1.40) PlanSApo oil immersion objectives were used to acquire 1024 x 1024 pixel images with a 2X zoom. Channel images were obtained sequentially by frame, using Kalman averaging. A step size of 0.2 μm was used to obtain a Z-series of 26 - 38 image planes per channel. Single-plane TIFF images were deconvolved using NIS-Elements Software (Nikon Elements Inc., Melville, NY, USA).

Quantitative Fluorescence Microscopy

Relative quantification of astroglial mortalin signal intensity within the SNpc was performed as described previously,(Hoekstra et al. 2014) with slight modifications. Imaging was carried out using a Nikon Eclipse Ti (Nikon Instruments Inc., Melville, NY, USA) instrument under 60X magnification, and exposure times for each channel were determined by randomly using the auto-exposure feature over several random fields across several unique subjects. The chosen exposure times were 250 ms for the 568 nm signal (GFAP) and 450 ms for the 488 nm signal (mortalin). Z-series images were acquired from 15 randomly selected astroglial-containing fields based on GFAP-positive signals. Following deconvolution, regions of interest were defined by their GFAP signal and mortalin fluorescence intensity was quantified within the astrocytes using NIS-Elements software (Nikon).

Relative quantification of astroglial mortalin signal intensity within structures of the corpus striatum (caudate, putamen, globus pallidus internal and external segments) was performed as above, but using a DeltaVision Elite imaging system (GE Healthcare, Issaquah, WA, USA) which offers the advantage of extremely short exposure times and

very fast data acquisition. Using the auto-exposure feature in 8 randomly selected fields for 3 unique subjects, the exposure times were chosen to be 18.0ms for the 568nm signal and 18.2ms for the 488nm signal. Data were processed and analyzed as described above, but using softWoRx software (GE Healthcare).

Results

Identification of Mortalin in Astrocytes

As mentioned earlier, mortalin has not previously been identified in astrocytes of healthy individuals and its involvement in neurodegenerative diseases has only been described in neurons. Given that mortalin antibody could, at least in theory, cross-interact with other proteins, we first sought to show that mortalin is definitively expressed in astrocytes. We first utilized mouse primary astrocytes to accomplish this. The presence of mortalin within purified mouse primary astrocytes was identified by both Western blot and quantitative PCR (**Figure 6**). The positive identification of the protein as mortalin was further confirmed by knocking down the *HSPA9* gene with siRNA (**Figure 6A**). Furthermore, the purity of the mouse primary astrocyte cultures was confirmed by high gene expression of GFAP (astroglial marker) and very low expression ($C_t > 35$) of NeuN (neuronal marker) and CD68 (microglial marker; **Figure 6B**).

Human Subject Overview

Human brain tissue specimens from the SNpc and the corpus striatum were obtained from 6 PD subjects and 6 age/gender-matched controls (**Table 5**). On average, controls were slightly older (73.7 years of age) upon autopsy as compared to PD subjects (71.8 years of age), but differences were not statistically significant. Each group was comprised of 4 males and 2 females, reflecting the relative predisposition of PD in males

as compared to females. The post-mortem interval was slightly higher in PD patients (11.6 hours) compared to controls (6.2 hours) but again was not statistically significant. PD disease duration ranged from 2 to 43 years.

Differential Mortalin Protein Expression Human Astrocytes

Building upon our findings in mouse astrocytes, we found that the mortalin protein resides within human astrocytes in both control and PD subjects utilizing confocal microscopy techniques (**Figure 7**). To the best of our knowledge, these data represent the first report of the presence of native mortalin protein within human astrocytes that are not tumorigenic.

To characterize potential differences in astroglial mortalin protein levels between PD subjects and controls, a quantitative fluorescence microscopy approach was employed. A significant decrease of mortalin protein fluorescent signal was observed in the SNpc of PD subjects as compared to controls. Conversely, no significant change in mortalin protein was found in structures of the corpus striatum of PD subjects as compared to controls (**Figure 8**).

Discussion

In this study, we provide evidence of the presence of mortalin in both primary mouse astrocyte cultures and post-mortem human brain tissue. To date, mortalin has been studied largely in the context of neurons, with only a few reports describing enhanced mortalin expression in gliomas (Takano et al. 1997, Baudet et al. 1998, Mishra and Kaur 2013) and not detected in normal astrocytes by immunohistochemistry (Takano et al. 1997). Here we used immunofluorescence, as it is typically significantly more sensitive than standard immunohistochemistry techniques. Further, we applied primary and

secondary antibodies for an extended amount of time as compared to that reported previously (Takano et al. 1997). Taken together, these differences may explain why we were able to detect mortalin within astrocytes in this study. Increased mortalin expression in tumor-derived astrocytes is consistent with the general observation that the protein becomes overexpressed in tumorigenic cells (Wadhwa et al. 2006). On the other hand, a role for mortalin in healthy astrocytes or its dysfunction in the astrocytes of neurodegenerative patients has not yet been described. Given that mortalin is known to be decreased in the brain tissue of not only PD patients, but also AD patients, (Park et al. 2014) the demonstration of the presence of mortalin within astrocytes is significant in that it opens the possibility that the protein is modulated in neurodegenerative disease in cell types other than neurons.

To address the question of whether or not mortalin is altered in astrocytes under disease conditions, we utilized a quantitative immunofluorescent staining approach to investigate astroglial mortalin levels in PD patients as compared to age and gender-matched controls. Interestingly, we found a statistically significant 35% decrease in mortalin protein within astrocytes of the SNpc in PD patients, despite the fact that neurodegeneration is usually associated with increased astrogliosis. This result is consistent with a previous report on decreased mortalin in the mitochondrial fraction of whole tissue SNpc lysates in PD patients (Jin et al. 2006). Conversely, we found no significant difference within structures of the corpus striatum. These results reflect the pathology typically observed in PD, with severe neuronal loss and the presence of Lewy bodies in the SNpc while neurons of both the striatum and globus pallidus do not

typically develop Lewy bodies and are far less affected in PD cases without accompanying dementia (Tsuboi et al. 2007).

Whether a reduction of mortalin has an impact on astroglial function, and what effect this may have on neuronal health, is currently unclear. Mortalin is typically described as an important mitochondrial protein, playing an active role in the mitochondrial import of nuclear encoded proteins, bioenergetics and protein integrity maintenance (Deocaris et al. 2008). It is widely understood that astrocytes play a role in nurturing neuronal health by providing energy via glycogenesis, metabolic support and antioxidants, as well as regulating ions, neurotransmitters and synaptic transmission. Thus it is plausible that impairment of mortalin expression in astrocytes could lead to altered mitochondrial function, which in turn could impair astrocyte function and have an ultimate adverse effect on proximal neurons. Further mechanistic studies are needed to address this possibility.

In conclusion, we demonstrate here for the first time the expression of the gene and presence of mortalin protein within the astrocytes of both healthy subjects and PD patients. Furthermore, we found astroglial mortalin to be significantly reduced in the SNpc of PD patients as compared to controls. Further studies are needed to elucidate the potential mechanistic implications of reduced astroglial mortalin in PD pathology.

References

Baudet, C., E. Perret, B. Delpech, M. Kaghad, P. Brachet, D. Wion, and D. Caput. 1998. Differentially expressed genes in C6.9 glioma cells during vitamin D-induced cell death program. Cell Death Differ **5**:116-125.

Burbulla, L. F., C. Schelling, H. Kato, D. Rapaport, D. Woitalla, C. Schiesling, C. Schulte, M. Sharma, T. Illig, P. Bauer, S. Jung, A. Nordheim, L. Schöls, O. Riess, and R. Krüger. 2010. Dissecting the role of the mitochondrial chaperone mortalin in Parkinson's disease: functional impact of disease-related variants on mitochondrial homeostasis. Hum Mol Genet **19**:4437-4452.

Bélanger, M., I. Allaman, and P. J. Magistretti. 2011. Brain energy metabolism: focus on astrocyte-neuron metabolic cooperation. Cell Metab **14**:724-738.

Chiasserini, D., A. Tozzi, A. de Iure, M. Tantucci, F. Susta, P. L. Orvietani, K. Koya, L. Binaglia, and P. Calabresi. 2011. Mortalin inhibition in experimental Parkinson's disease. Mov Disord **26**:1639-1647.

Chomczynski, P., and N. Sacchi. 1987. Single-step method of RNA isolation by acid guanidinium thiocyanate-phenol-chloroform extraction. Anal Biochem **162**:156-159.

De Mena, L., E. Coto, E. Sánchez-Ferrero, R. Ribacoba, L. M. Guisasola, C. Salvador, M. Blázquez, and V. Alvarez. 2009. Mutational screening of the mortalin gene (HSPA9) in Parkinson's disease. J Neural Transm **116**:1289-1293.

Deocaris, C. C., S. C. Kaul, and R. Wadhwa. 2008. From proliferative to neurological role of an hsp70 stress chaperone, mortalin. Biogerontology **9**:391-403.

Halliday, G. M., and C. H. Stevens. 2011. Glia: initiators and progressors of pathology in Parkinson's disease. Mov Disord **26**:6-17.

Hoekstra, J. G., T. J. Cook, T. Stewart, H. A. Mattison, M. T. Dreisbach, Z. S. Hoffer, and J. Zhang. 2014. Astrocytic dynamin-like protein 1 regulates neuronal protection against excitotoxicity in Parkinson's disease. American Journal of Pathology **in press**.

Jin, J., C. Hulette, Y. Wang, T. Zhang, C. Pan, R. Wadhwa, and J. Zhang. 2006. Proteomic identification of a stress protein, mortalin/mthsp70/GRP75: relevance to Parkinson disease. Mol Cell Proteomics **5**:1193-1204.

Jin, J., G. J. Li, J. Davis, D. Zhu, Y. Wang, C. Pan, and J. Zhang. 2007. Identification of novel proteins associated with both alpha-synuclein and DJ-1. Mol Cell Proteomics **6**:845-859.

Klein, C., and A. Westenberger. 2012. Genetics of Parkinson's disease. Cold Spring Harb Perspect Med **2**:a008888.

Mishra, R., and G. Kaur. 2013. Aqueous ethanolic extract of Tinospora cordifolia as a potential candidate for differentiation based therapy of glioblastomas. PLoS One **8**:e78764.

Park, S. J., J. H. Shin, J. I. Jeong, J. H. Song, Y. K. Jo, E. S. Kim, E. H. Lee, J. J. Hwang, E. K. Lee, S. J. Chung, J. Y. Koh, D. G. Jo, and D. H. Cho. 2014. Down-regulation of mortalin exacerbates Aβ-mediated mitochondrial fragmentation and dysfunction. J Biol Chem **289**:2195-2204.

Shi, M., J. Jin, Y. Wang, R. P. Beyer, E. Kitsou, R. L. Albin, M. Gearing, C. Pan, and J. Zhang. 2008. Mortalin: a protein associated with progression of Parkinson disease? J Neuropathol Exp Neurol **67**:117-124.

Takano, S., R. Wadhwa, Y. Yoshii, T. Nose, S. C. Kaul, and Y. Mitsui. 1997. Elevated levels of mortalin expression in human brain tumors. Exp Cell Res **237**:38-45.

Tsuboi, Y., H. Uchikado, and D. W. Dickson. 2007. Neuropathology of Parkinson's disease dementia and dementia with Lewy bodies with reference to striatal pathology. Parkinsonism Relat Disord **13 Suppl 3**:S221-224.

Wadhwa, R., S. Takano, K. Kaur, C. C. Deocaris, O. M. Pereira-Smith, R. R. Reddel, and S. C. Kaul. 2006. Upregulation of mortalin/mthsp70/Grp75 contributes to human carcinogenesis. Int J Cancer **118**:2973-2980.

Tables & Figures

Table 5: Human subjects in PD post-mortem brain tissue study. HC, healthy controls; PD, Parkinson's disease; PMI, post-mortem interval. Subjects were matched on age and gender.

	HC (n = 6)	PD (n = 6)
Age (yrs)	73.67 ± 9.91	71.86 ± 11.55
Sex (female/male)	4/2	4/2
PMI (hrs)	6.22 ± 2.60	11.60 ± 7.80
Age at onset (yrs)		48.00 ± 14.34
Disease duration (yrs)		22.40 ± 16.13

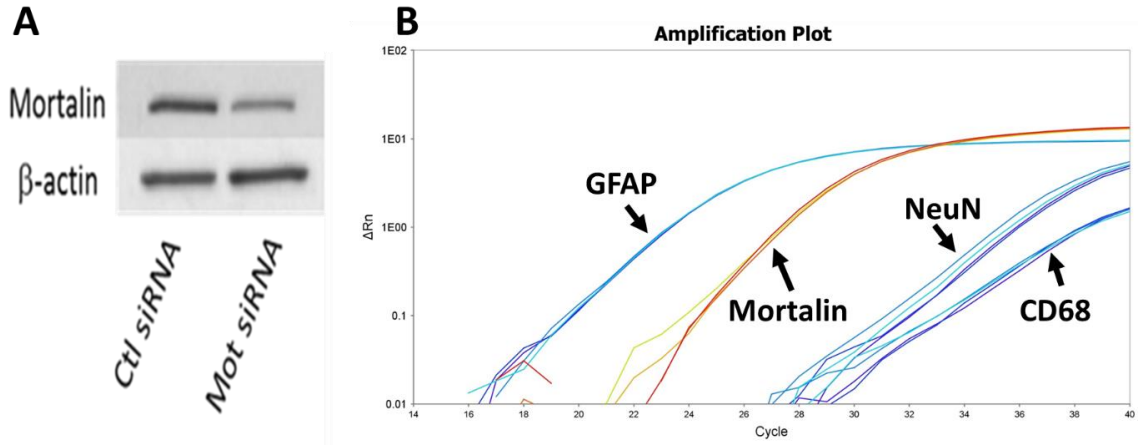

Figure 6: Identification of mortalin protein in mouse primary astrocytes. Astroglial expression of native mortalin was demonstrated by Western blot and qPCR. (A) Detection of mortalin by Western blot along with confirmation following *HSPA9* siRNA transfection. (B) Mortalin gene expression was detected by qPCR along with high expression of GFAP and low expression of NeuN and CD68, demonstrating purity of the culture and therefore high probability of the presence of mortalin in astrocytes.

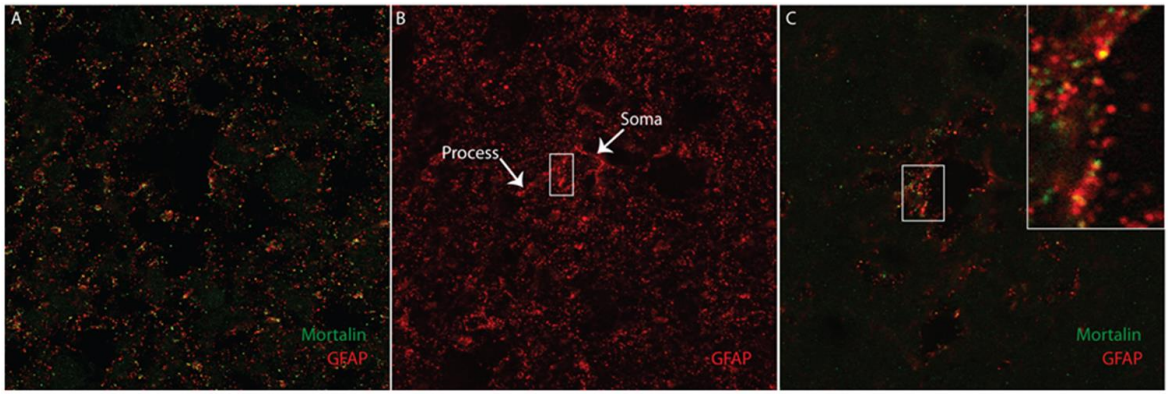

Figure 7: Identification of mortalin in human astroctyes. Human brain tissue was stained for GFAP (red) and mortalin (green). Co-localization was observed by fluorescent confocal microscopy, represented by distinct yellow puncta. (A) Representative full field image at 60X magnification. (B) Representative stack projection of a 60X field stained for GFAP demonstrating the appearance of an astrocyte. White arrowheads indicate the astroglial soma and associated process. (C) Representative single plane image at 100X magnification, with 3X zoom inset in the area indicated by the white box.

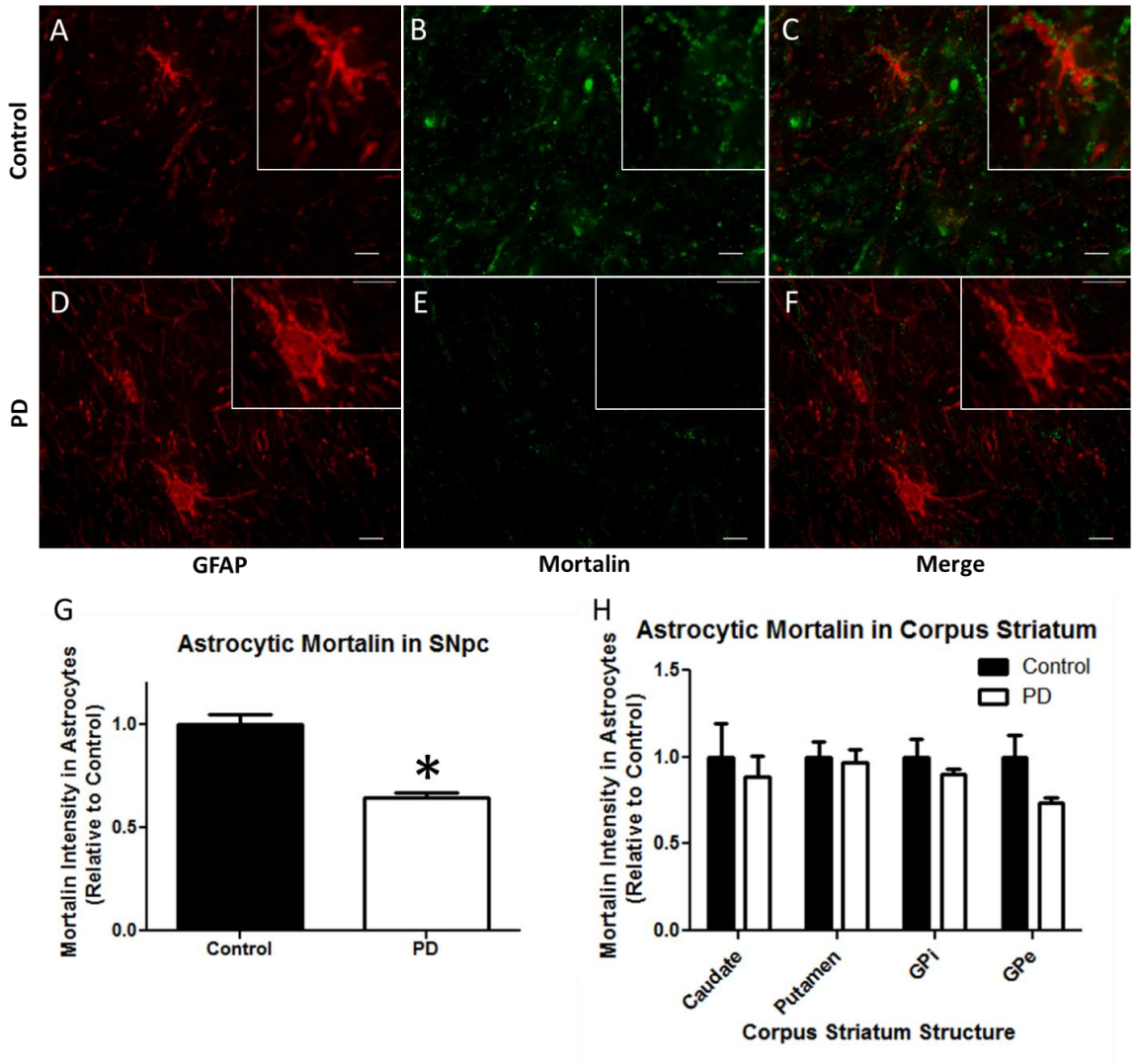

Figure 8: Astroglial mortalin is decreased in the SNpc of PD patients. Human brain tissue from PD patients (N = 6) and age/gender-matched controls (N = 6) was stained for GFAP (red) and mortalin (green), and the mortalin fluorescent signal within GFAP marked astrocytes quantified. (A-C) Representative images from the SNpc of a control specimen and (D-F) for a PD specimen. (G) Mortalin was found to be significantly lower in the astrocytes of the SNpc of PD subjects as compared to controls whereas (H) no significant differences were observed in structures of the corpus striatum.

CHAPTER 5: ASTROGLIAL MORTALIN IS DECREASED IN THE STRIATUM OF MANGANESE-EXPOSED MINE WORKERS

Abstract

Parkinsonism (PS) refers to a collection of signs and symptoms that indicate a movement disorder characterized by abnormal motor function, which presents clinically in the form of bradykinesia, postural instability, muscle rigidity and tremor. Although the most common cause of PS is Parkinson's disease (PD), associated with the dysfunction and death of dopaminergic neurons in the brainstem (particularly within the substantia nigra pars compacta (SNpc)) as well as dopaminergic depletion in the corpus striatum nuclei, a number of atypical parkinsonian disorders present similarly. While the underlying pathologic mechanisms that lead to parkinsonian syndromes are incompletely understood, there is a growing consensus among investigators that both genetic susceptibility and environmental exposures play critical roles in disease development. Previously, we identified the essential mitochondrial protein mortalin to be decreased in human astrocytes of the SNpc in PD patients as compared to age/gender-matched healthy controls, but not in the gray matter nuclei of the corpus striatum. In this study, we identified a decrease of astroglial mortalin in the corpus striatum of manganese-exposed mine workers, but in contrast to PD patients, no difference was observed in the SNpc. Manganese is an essential micronutrient but is also known as a neurotoxicant with excessive acute exposures associated with a parkinsonian disorder known as manganism. These results indicate a potential shared mechanism of neurodegeneration amongst PD patients and manganese-exposed individuals on opposing ends of the nigrostriatal pathway.

Introduction

Parkinsonism (PS) refers to a collection of neurological syndromes whose clinical symptoms include bradykinesia, muscle rigidity, postural instability, and resting tremor (Galvan and Wichmann 2008). There are many causes associated with symptoms of PS, the most common being Parkinson disease (PD), with its motor symptoms largely attributable to the death of dopaminergic neurons in the substantia nigra pars compacta (SNpc) and resultant depletion of striatal dopamine (Vingerhoets et al. 1997). Various specific environmental factors and occupational exposures, including pesticides and heavy metals, have been suggested to play a role in the development of PS, with possible overlapping mechanisms resulting in the manifestation of idiopathic PD (iPD) (Racette 2013).

A particular environmental agent of interest is manganese (Mn), an essential dietary nutrient for which historically acute and excessive occupational exposures have been long known to cause symptoms of PS commonly referred to as manganism (Couper 1837). While the associations between both acute high-level and chronic low-level Mn exposure and PS are well established, it is quite clear that pathologically, manganism and iPD differ substantially, given the fact that the histopathological changes associated with high-level Mn exposure are not consistently seen in the SNpc, as in PD, but rather tend to occur in the gray matter nuclei of the corpus striatum, particularly the globus pallidus (Perl and Olanow 2007). However a potential role of lower-level chronic exposure in the development of iPD remains to be established, and indeed more recent investigations have shown evidence demonstrating that PS affecting welders who are exposed to modestly increased levels of Mn may indeed have overlapping pathologies with iPD

(Racette et al. 2012). Oxidative stress, mitochondrial dysfunction, and neuroinflammation have been reported upon exposure both *in vitro* and *in vivo*, suggesting possible underlying mechanisms of Mn-induced neurotoxicity (Milatovic et al. 2009).

Mn uptake by astrocytes may occur via divalent metal transporter 1 (DMT1) and by neurons via transferrin and other specific transporter systems, such as the dopamine transporter (DAT) (Chen et al. 2006, Erikson and Aschner 2006, Anderson et al. 2007). Astrocytes sequester inorganic Mn to concentrations 50 to 60-fold greater than similarly exposed neurons (Aschner et al. 1992, Aschner et al. 1999). Initial experimental evidence suggested that intracellular Mn largely accumulates within the mitochondria (Gavin et al. 1999, Morello et al. 2008). Recent studies have challenged this notion by demonstrating preferential accumulation within the nucleus (Kalia et al. 2008) and Golgi apparatus (Carmona et al. 2010). The critical role of glial cells in Mn-induced neurotoxicity was demonstrated recently by Zhang et al, who showed that astrocytes were required for Mn to elicit toxic effects on dopaminergic neurons at low concentrations *in vitro* (1-30 μM) (Zhang et al. 2010).

In a previous study, we observed a decrease of astroglial mortalin, a multi-functional protein implicated in a variety of neurological diseases (Flachbartová and Kovacech 2013), in the SNpc of PD patients as compared to age/gender-matched controls, but found no difference in astrocytic mortalin in the corpus striatum (Cook et al., manuscript under review). Considering the potential pathologic overlap between iPD and Mn-induced PS, and the preferential accumulation of Mn within astrocytes, we hypothesized that Mn exposure may contribute to the reduced astroglial mortalin seen in this cohort. To test this hypothesis, we evaluated astroglial mortalin in human brain

specimens originating from a unique cohort of Mn and non-Mn mine workers within the same geographical region of South Africa.

Materials & Methods

Human Brain Specimen Preparation

Human brain tissue specimens were acquired and prepared as described previously (Gonzalez-Cuyar et al. 2013). Formalin-fixed paraffin embedded human brain specimens were provided for 16 brain specimens from workers with an occupational history of mining-related jobs in the Northern Cape Province of South Africa. Eight of these subjects had documented occupational exposure to Mn, and the other 8 served as controls and were age/gender-matched but were not exposed to Mn (i.e., worked in mines other than Mn mines). Formalin fixed paraffin embedded (FFPE) tissues from the midbrain and the corpus striatum were sectioned onto glass slides at a thickness of 4-5 μm.

Immunofluorescent Staining

Human tissue sections were prepared as described previously (Cook et al., manuscript under review; Hoekstra et al., in press), with slight modifications. Briefly, following deparaffinization and antigen retrieval, tissues were incubated with blocking buffer [5% normal goat serum, 2% bovine serum albumin, 0.1% Triton 100-X diluted in TBS-T] overnight at 4°C and then primary antibodies (rabbit anti-mortalin [Sigma SQ-15 #G4045] and chicken anti-GFAP [Millipore #AB5541]) diluted into blocking buffer (anti-mortalin 1:100; anti-GFAP 1:500) were applied to tissues overnight at 4°C. After washing in TBS-T containing 5% normal goat serum and 2% bovine serum albumin, secondary antibodies conjugated with Alexa fluorophores (568 goat anti-chicken and 488

goat anti-rabbit; Life Technologies, Grand Island, NY, USA) diluted 1:500 in the washing buffer were applied to tissues at 4°C overnight. The following day the tissues were again washed in TBS-T and gently rocked in a solution of 70% ethanol containing 0.3% Sudan Black B to reduce autofluorescence. Finally, tissues were briefly rinsed with 70% ethanol, washed in TBS-T, covered with Vectashield mounting medium with DAPI (Vector Laboratories, Inc., Burlingame, CA, USA), affixed with a cover glass and sealed with nail polish.

Quantitative Fluorescence Microscopy

Quantitative fluorescence microscopy was carried out as described previously (Cook et al., manuscript under review), with slight modifications. Imaging of the SNpc was performed on a Nikon Eclipse Ti (Nikon Instruments Inc., Melville, NY, USA) instrument under 60X magnification, and exposure times for each channel were determined by randomly using the auto-exposure feature over several random fields, and across several unique subjects. The chosen exposure times were 250 ms for the 568 nm signal (GFAP) and 450 ms for the 488 nm signal (mortalin). Z-series images were acquired from 15 randomly selected astroglial-containing fields based on GFAP-positive signals. Following deconvolution, regions of interest were defined by their GFAP signal and mortalin fluorescence intensity was quantified within the astrocytes using NIS-Elements software (Nikon).

Relative quantification of astroglial mortalin signal intensity within structures of the corpus striatum (caudate, putamen, globus pallidus internal and external segments) was performed as above, but using a DeltaVision Elite imaging system (GE Healthcare, Issaquah, WA, USA) which offers the advantage of extremely short exposure times and

very fast data acquisition. Using the auto-exposure feature in 8 randomly selected fields for 3 unique subjects, the exposure times were chosen to be 18.0 ms for the 568 nm signal and 18.2 ms for the 488 nm signal. Data were processed and analyzed as described above, but using softWoRx software (GE Healthcare).

Results

Subject Overview

Human brain tissue specimens from the SNpc and the corpus striatum were obtained from 8 Mn and 8 non-Mn age/gender-matched miner workers (acting as controls) with a history of employment within the same geographic region of South Africa (**Table 6**). All subjects included were male and of similar race/ethnicity, of similar age (median age of was 60 and 57 for controls and Mn-exposed miners, respectively). Although all subjects worked in mining for at least 2 years, the average years in mining differed somewhat between the 8 controls (11.5 yrs) and Mn-exposed (18.4 yrs). However, this difference was not statistically different because of the wide range in years spent in mining for both control (2.2 – 18.8 yrs) and Mn-exposed (2.1 – 31.4 yrs) workers.

Mortalin Protein Expression in Human Astrocytes of Miners

To characterize potential differences in astroglial mortalin protein levels between Mn and non-Mn mine workers, a quantitative fluorescence microscopy approach was employed. Mortalin protein fluorescent signal was observed to be decreased in all structures of the corpus striatum (**Figures 9, 10**) of Mn mine workers as compared to

non-Mn mine workers, with a statistically significant decrease in the caudate. Conversely, no significant change in mortalin protein was found in the SNpc (**Figure 10**).

Discussion

In this study, we tested the hypothesis that occupational exposure to Mn is associated with a decrease in astrocytic mortalin protein levels in humans. Previously, we observed a decrease of astroglial mortalin within the SNpc of PD patients as compared to age/gender-matched controls (Cook et al., manuscript under review). This observation was consistent with reports of a general decrease of mortalin within this structure in homogenized whole brain lysates (Jin et al. 2006). Subsequent *in vitro* analyses have demonstrated that experimental model toxicants of PD, including rotenone exposure (Jin et al. 2006) and α-synuclein overexpression (Pennington et al. 2010) in neuronal cell lines, as well as *in vivo* administration of 6-hydroxydopamine (Chiasserini et al. 2011) and dopamine quinone (Van Laar et al. 2008), are capable of causing a decrease in mortalin. However, the potential for neurotoxic agents to have a similar effect on astrocytes has not yet been evaluated, particularly in human brain specimens.

To address this question, we focused this investigation on Mn-exposed individuals, as Mn is not only a known neurotoxicant (Guilarte 2013), but also preferentially accumulates within astrocytes (Aschner et al. 1992, Aschner et al. 1999). Our observations provide evidence that neurodegenerative toxicants are capable of eliciting pathologic effects on not only neurons, but astrocytes as well. This observation contributes to a growing body of evidence suggesting that astroglial dysfunction contributes to the etiology of neurodegenerative conditions (Halliday and Stevens 2011).

Even further, it may suggest that the initial insult in Mn-induced degeneration occurs in astrocytes prior to neuronal death (Gonzalez-Cuyar et al. 2013).

In a sample population of Mn mine workers, we observed a statistically significant decrease of astroglial mortalin in the caudate nucleus of the corpus striatum and a consistent, but non-statistically significant, trend towards decrease in other regions of the corpus striatum (putamen, and the internal and external segments of the globus pallidus) as compared to age and gender-matched non-Mn mine workers with an occupational history in the same geographic region of South Africa. Conversely, no difference was observed in the SNpc of these subjects. Interestingly, these results further characterize the findings by Gonzalez-Cuyar et al of decrease of astrocytes in the caudate nucleus and putamen in this same cohort of Mn-exposed individuals as compared to age/gender-matched controls in cell density analyses (Gonzalez-Cuyar et al. 2013). These results differ from what we previously reported in a similar human tissue study comparing PD patients to age/gender-matched healthy controls, where a significant decrease of astroglial mortalin was observed in the SNpc of PD patients and no difference in the structures of the corpus striatum (Cook et al., manuscript under review). These observations are also consistent with the histopathologic changes observed in both conditions. More specifically, extensive neuronal damage in the SNpc of PD patients with relative sparing of the corpus striatum, while high-level Mn exposures have been historically characterized by neuronal loss and gliosis of the corpus striatum with sparing of neurons in the SNpc (Lucchini et al. 2009, Gonzalez-Cuyar et al. 2013).

Nonetheless, the finding of reduced astroglial mortalin in both PD patients and Mn exposed individuals represents a potential shared mechanism of action on either side

of the nigrostriatal pathway, whose projections link neuronal efferent axons from the SNpc to the corpus striatum. The major neurotransmitter exchanged along this pathway is dopamine, whose depletion is largely responsible for the signs and symptoms of parkinsonism. Dysfunction of dopamine transmission may occur on either end of this pathway, i.e. by either the dopamine producing neurons of the SNpc or neurons of the striatum which receive dopamine. In either case, the disrupted transmission of dopamine may present clinically in the form of a movement disorder, be it PD with associated pathology in the SNpc, or Mn-induced parkinsonism in the form of pathology in the corpus striatum. In this regard, our observations of reduced mortalin in astrocytes of the SNpc in PD patients and in astrocytes of the striatum in Mn-exposed individuals indicate a potential shared mechanism within distinct anatomical brain regions that ultimately contribute toward neuronal dysfunction along the nigrostriatal pathway and result in clinically similar signs and symptoms, yet are pathologically distinct. On one hand dopamine production is disrupted, and on the other the reception of dopamine is impaired. In either case, impairment of astroglial function may be a precursor to eventual neuronal dysfunction.

In this study, we consider depletion of astroglial mortalin to be an indicator of cellular dysfunction. However, the functional consequence of reduced astroglial mortalin has not yet been described; furthermore, the consequential effect of astroglial dysfunction on neuronal health has not been established. Future mechanistic studies are necessary to elucidate this potential effect.

In conclusion, we have observed reduced astroglial mortalin in the corpus striatum of a sample population of Mn-exposed individuals, similar to what was

previously described in the SNpc of PD patients (Cook et al, manuscript under review). Taken together, these observations represent a potential shared mechanism of action which manifest in pathologically distinct movement disorders with similar overlapping signs and symptoms. Mechanistic investigations are needed to define the role of reduced mortalin with regard to astroglial function and its consequence in neurodegenerative conditions.

References

Anderson, J. G., P. T. Cooney, and K. M. Erikson. 2007. Inhibition of DAT function attenuates manganese accumulation in the globus pallidus. Environ Toxicol Pharmacol **23**:179-184.

Aschner, M., M. Gannon, and H. K. Kimelberg. 1992. Manganese uptake and efflux in cultured rat astrocytes. J Neurochem **58**:730-735.

Aschner, M., K. E. Vrana, and W. Zheng. 1999. Manganese uptake and distribution in the central nervous system (CNS). Neurotoxicology **20**:173-180.

Carmona, A., G. Devès, S. Roudeau, P. Cloetens, S. Bohic, and R. Ortega. 2010. Manganese accumulates within golgi apparatus in dopaminergic cells as revealed by synchrotron X-ray fluorescence nanoimaging. ACS Chem Neurosci **1**:194-203.

Chen, M. K., J. S. Lee, J. L. McGlothan, E. Furukawa, R. J. Adams, M. Alexander, D. F. Wong, and T. R. Guilarte. 2006. Acute manganese administration alters dopamine transporter levels in the non-human primate striatum. Neurotoxicology **27**:229-236.

Chiasserini, D., A. Tozzi, A. de Iure, M. Tantucci, F. Susta, P. L. Orvietani, K. Koya, L. Binaglia, and P. Calabresi. 2011. Mortalin inhibition in experimental Parkinson's disease. Mov Disord **26**:1639-1647.

Couper, J. 1837. On the effects of black oxide of manganese when inhaled into the lungs. British Annals of Medicine, Pharmacy, Vital Statistics, and General Science **1**:2.

Erikson, K. M., and M. Aschner. 2006. Increased manganese uptake by primary astrocyte cultures with altered iron status is mediated primarily by divalent metal transporter. Neurotoxicology **27**:125-130.

Flachbartová, Z., and B. Kovacech. 2013. Mortalin - a multipotent chaperone regulating cellular processes ranging from viral infection to neurodegeneration. Acta Virol **57**:3-15.

Galvan, A., and T. Wichmann. 2008. Pathophysiology of parkinsonism. Clin Neurophysiol **119**:1459-1474.

Gavin, C. E., K. K. Gunter, and T. E. Gunter. 1999. Manganese and calcium transport in mitochondria: implications for manganese toxicity. Neurotoxicology **20**:445-453.

Gonzalez-Cuyar, L. F., G. Nelson, S. R. Criswell, P. Ho, J. A. Lonzanida, H. Checkoway, N. Seixas, B. B. Gelman, B. A. Evanoff, J. Murray, J. Zhang, and B. A. Racette. 2013. Quantitative neuropathology associated with chronic manganese exposure in South African mine workers. Neurotoxicology.

Guilarte, T. R. 2013. Manganese neurotoxicity: new perspectives from behavioral, neuroimaging, and neuropathological studies in humans and non-human primates. Front Aging Neurosci **5**:23.

Halliday, G. M., and C. H. Stevens. 2011. Glia: initiators and progressors of pathology in Parkinson's disease. Mov Disord **26**:6-17.

Jin, J., C. Hulette, Y. Wang, T. Zhang, C. Pan, R. Wadhwa, and J. Zhang. 2006. Proteomic identification of a stress protein, mortalin/mthsp70/GRP75: relevance to Parkinson disease. Mol Cell Proteomics **5**:1193-1204.

Kalia, K., W. Jiang, and W. Zheng. 2008. Manganese accumulates primarily in nuclei of cultured brain cells. Neurotoxicology **29**:466-470.

Lucchini, R. G., C. J. Martin, and B. C. Doney. 2009. From manganism to manganese-induced parkinsonism: a conceptual model based on the evolution of exposure. Neuromolecular Med **11**:311-321.

Milatovic, D., S. Zaja-Milatovic, R. C. Gupta, Y. Yu, and M. Aschner. 2009. Oxidative damage and neurodegeneration in manganese-induced neurotoxicity. Toxicol Appl Pharmacol **240**:219-225.

Morello, M., A. Canini, P. Mattioli, R. P. Sorge, A. Alimonti, B. Bocca, G. Forte, A. Martorana, G. Bernardi, and G. Sancesario. 2008. Sub-cellular localization of manganese in the basal ganglia of normal and manganese-treated rats An electron spectroscopy imaging and electron energy-loss spectroscopy study. Neurotoxicology **29**:60-72.

Pennington, K., J. Peng, C. C. Hung, R. E. Banks, and P. A. Robinson. 2010. Differential effects of wild-type and A53T mutant isoform of alpha-synuclein on the mitochondrial proteome of differentiated SH-SY5Y cells. J Proteome Res **9**:2390-2401.

Perl, D. P., and C. W. Olanow. 2007. The neuropathology of manganese-induced Parkinsonism. J Neuropathol Exp Neurol **66**:675-682.

Racette, B. A. 2013. Manganism in the 21st century: The Hanninen lecture. Neurotoxicology.

Racette, B. A., S. R. Criswell, J. I. Lundin, A. Hobson, N. Seixas, P. T. Kotzbauer, B. A. Evanoff, J. S. Perlmutter, J. Zhang, L. Sheppard, and H. Checkoway. 2012. Increased risk of parkinsonism associated with welding exposure. Neurotoxicology **33**:1356-1361.

Van Laar, V. S., A. A. Dukes, M. Cascio, and T. G. Hastings. 2008. Proteomic analysis of rat brain mitochondria following exposure to dopamine quinone: implications for Parkinson disease. Neurobiol Dis **29**:477-489.

Vingerhoets, F. J., M. Schulzer, D. B. Calne, and B. J. Snow. 1997. Which clinical sign of Parkinson's disease best reflects the nigrostriatal lesion? Ann Neurol **41**:58-64.

Zhang, P., K. M. Lokuta, D. E. Turner, and B. Liu. 2010. Synergistic dopaminergic neurotoxicity of manganese and lipopolysaccharide: differential involvement of microglia and astroglia. J Neurochem **112**:434-443.

Tables & Figures

Table 6: Human subjects in the mine worker brain tissue study. Data represented as mean (min, max). PMI, post-mortem interval.

	Non-Mn Mine Workers (n = 8)	Mn Mine Workers (n = 8)
Age (yrs)	60.13 (44.21, 79.53)	57.28 (46.43, 70.59)
Sex (male/female)	8/0	8/0
PMI (days)	4.63 (2.00, 9.00)	5.13 (2.00, 9.00)
Yrs in Mn mines	0	11.91 (1.20, 31.41)
Total yrs in mines	11.50 (2.15, 18.78)	18.39 (2.15, 31.41)

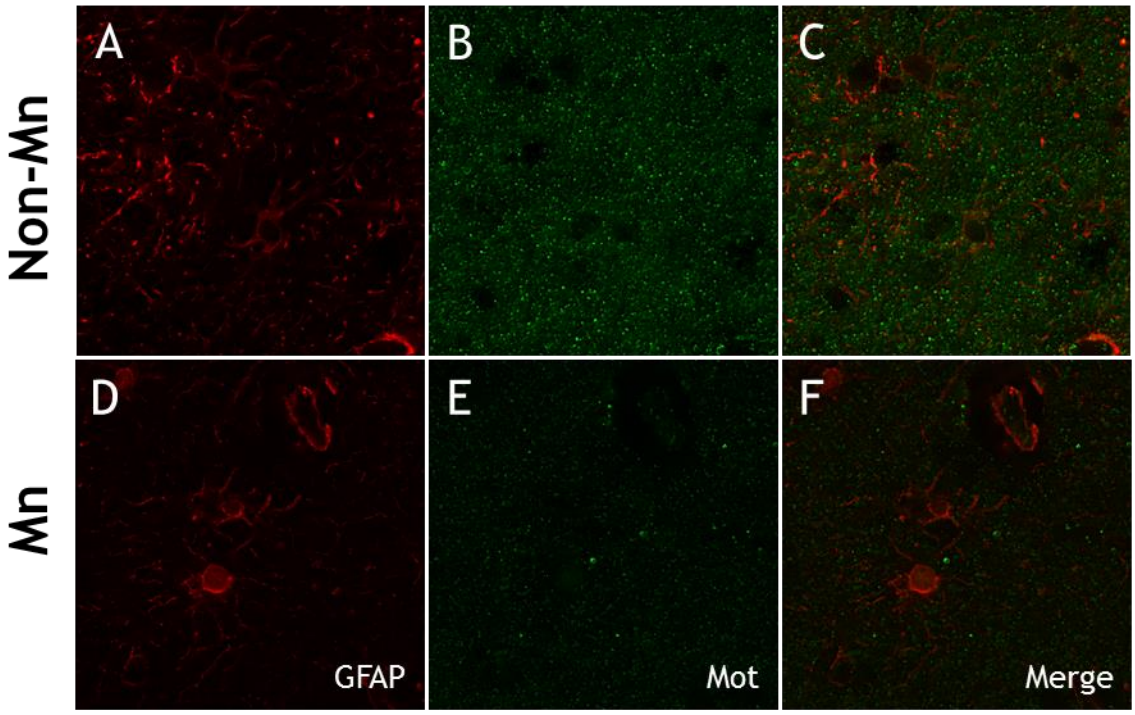

Figure 9: Astroglial mortalin fluorescent imaging in Mn and non-Mn exposed mine workers. Human brain tissue from non-Mn mine workers (N = 8) and age/gender-matched Mn-mine workers (N = 8) was stained for GFAP (red) and mortalin (green), and the mortalin flourescent signal was quantified within the GFAP signal. (A-C) Representative images from the caudate of non-Mn mine worker (control) and (D-F)

from the caudate of a Mn mine worker. White arrowheads indicate mortalin localized within the astrocyte.

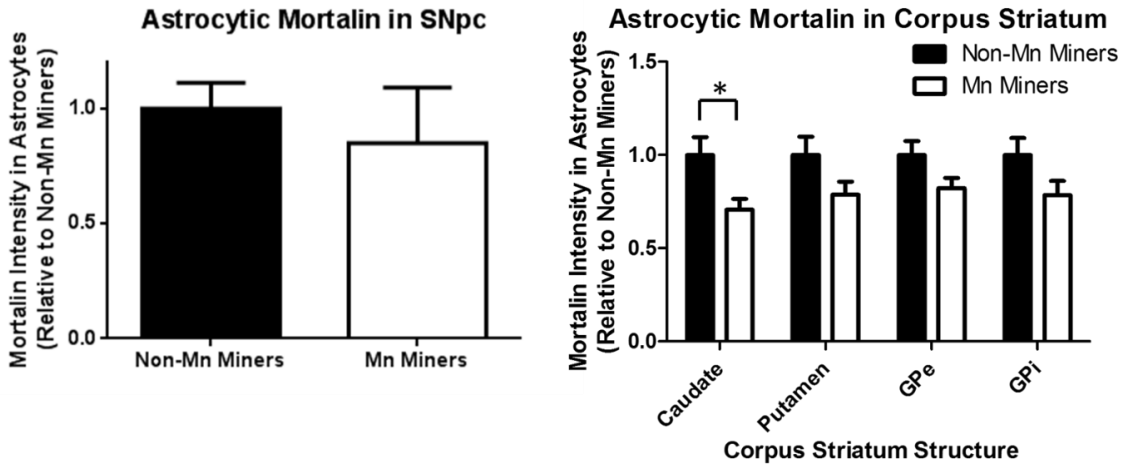

Figure 10: Astroglial mortalin in SNpc and corpus striatum of Mn-exposed and un-exposed mine workers. (A) Mortalin was found to be similar in human astrocytes of the SNpc. (B) Mortalin was found to be decreased in structures of the corpus striatum of Mn mine workers as compared to non-Mn mine workers, with statistical significance achieved in the caudate nucleus; *$p < 0.05$.

CHAPTER 6: REDUCED ASTROGLIAL MORTALIN ENHANCES NEURONAL SUSCEPTIBILITY TO MANGANESE TOXICITY

Abstract

Manganese is an essential nutrient for which exposure has long been known to be causative of neurotoxicity most frequently observed clinically in the form parkinsonism, a collection of signs and symptoms of impaired motor function. Within the brain, manganese preferentially accumulates within astrocytes, which play key roles in supporting neuronal health and regulating neural transmission at synapses. Recently, it was found that the mitochondrial chaperone protein mortalin is reduced in astrocytes of the caudate of manganese exposed individuals. In the present study, we utilized a primary cell co-culture system to evaluate the potential consequence of reduced astroglial mortalin in the context of Mn exposure on neuronal health. It was found that neurons cultured in the presence of astrocytes expressing reduced levels of mortalin were more sensitive than those expressing endogenous levels to Mn treatment, observed as a decrease in the number of presynaptic terminals. Subsequent functional assessments of astrocytes revealed impaired intracellular calcium signaling and an increased presence of aggregated proteins in Mn treated astrocytes with mortalin knocked down, and these effects were mitigated in astrocytes lacking expression of α-synuclein. Furthermore, mortalin knockdown was found to be causative of endoplasmic reticulum stress, while 10 mM Mn treatment resulted in elevated production of reactive oxygen species. To conclude, a ‘two-hit’ model involving ER and oxidative stress, of which α-synuclein may be a key mediator, is proposed as an underlying mechanism leading to astroglial dysfunction stemming from dysregulation of interacellular calcium signaling and an

accumulation of aggregated proteins, which ultimately have adverse consequences on synaptic health.

Introduction

Mortalin is a multi-functional protein most commonly described as a mitochondrial chaperone involved in stress response, mitochondrial biogenesis, import of nuclear-proteins into the mitochondria and maintenance of protein integrity (Deocaris et al. 2008). However, several additional functions have been described, including acting as part of the ER-mitochondria tethering machinery via its interaction with VDAC1 (Schwarzer et al. 2002). Dysfunction of mortalin has been associated with a number of disease processes (Deocaris et al. 2007), including neurodegenerative disorders such as Alzheimer's disease (AD) and Parkinson's disease (PD) (Jin et al. 2012). More recently, mortalin has been found to be decreased in the astrocytes of PD patients (Cook et al., manuscript under review) and also manganese (Mn)-exposed mine workers (Cook et al., manuscript in preparation).

Mn is an essential dietary nutrient whose over-exposure has long been recognized as being neurotoxic (Couper 1837). Acute, high-level exposures cause a parkinsonian syndrome referred to as manganism (Huang et al. 2007) and chronic, low-level exposures have been hypothesized as a risk factor contributing to PD development and/or progression (Racette et al. 2001, Park et al. 2005, Finkelstein and Jerrett 2007, Willis et al. 2010, Wright Willis et al. 2010, Willis et al. 2012), although this proposition is controversial (Mortimer et al. 2012). Previous studies have shown that Mn in the brain preferentially accumulates within astrocytes (Aschner et al. 1992, Aschner et al. 1999) and studies in nonhuman primates and rodents associated with high-level exposures

demonstrate that Mn tends to preferentially deposit within the globus pallius and the striatum (Suzuki et al. 1975, Roels et al. 1997). Proposed mechanisms of Mn neurotoxicity include oxidative stress, disruption of mitochondrial respiration, and damage to the dopaminergic, glutamatergic and GABAergic synapses (Tuschl et al. 2013), and astrocytes have been demonstrated to play essential roles in mediating its toxic effects on neurons (Zhang et al. 2010).

Astrocytes are the most abundant cell type in the brain, and their major function is to support and protect neuronal health, which they do at the synapse by providing energy in the form of ATP, clearance of neurotransmitters and signaling ions, and supplying antioxidant molecules such as GSH (Perea et al. 2014). On the other hand, astrocytes may release soluble toxic molecules, thereby adversely affecting neuronal health (Rappold and Tieu 2010). Astrocytes can therefore play important roles in toxic and pathologic actions eliciting harmful effects on neurons. For these reasons, in this investigation we sought mechanisms of Mn-neurotoxicity by focusing on astroglial mortalin using *in vitro* primary culture model systems. We describe increased neuronal susceptibility to Mn toxicity when cultured with astrocytes expressing reduced levels of mortalin and report potential mechanisms related to astrocyte function that may explain these results.

Materials & Methods

Cell Culture

Primary astrocyte cultures were prepared from the cortex of 1-3 day old mouse pups (WT C57/BL6J (#000664) or SNCA KO B6; 129X1-*Snca*^{tm1Rosl}/J (#003692), both from The Jackson Laboratory, Bar Harbor, ME, USA). Following decapitation, brains were transferred to ice-cold DMEM/F12 (Gibco #11330-032, Life Technologies, Grand

Island, NY, USA), cortices were dissected under a Leica L2 dissection microscope (Leica Microsystems Inc, Buffalo Grove, IL, USA) and meninges were carefully removed mechanically. After dissections were complete, the isolated tissue was transferred to a sterile-filtered, pre-warmed digestion medium [0.5 mM EDTA, 0.2 mg/mL L-cysteine, 150 U/mL papain, 10 mg/mL DNase in DMEM/F12] and incubated at 37°C for 30 minutes. The digestion medium was then aspirated and the tissue washed 3 times with pre-warmed culture medium [DMEM/F12 containing 10% fetal bovine serum (Thermo Fisher Scientific Inc. #MT35010CV, Waltham, MA, USA) and 1% penicillin/streptomycin (Corning Inc. #30-002-CI, Corning, NY, USA)]. Tissue was then triturated, once in 10 mL and once in 5 mL of culture medium, with a flame-polished glass Pasteur pipette and the supernatant was transferred to a 50 mL conical tube through a 100 μm cell strainer (Corning Inc. #352360). The cell suspension was diluted to a final volume of 10 mL culture medium per 3 mouse cortices, transferred to culture flasks pre-coated with poly-D-lysine hydrobromide (BD Biosciences #354210, San Jose, CA, USA) at an approximate density of 3 brains per flask and placed in a 37°C incubator with a 5% CO_2 supplemented atmosphere. The medium was freshly replaced the following day and the glial cells were allowed to mature in the incubator for 10 - 15 days prior to experimental use.

After reaching maturity and prior to experimental use, to remove microglia, cultures were enhanced for primary astrocytes by physically striking the flask 8 times on each side, aspirating the medium and striking the flask 8 times on each side once again. Approximately 10 mL of PBS was added to the remaining cellular monolayer and the flask was struck again as described above. After aspirating the PBS, adhered cells were

lifted from the flask bottom by incubating with approximately 4 mL trypsin-EDTA (0.25%; Life Technologies #25200-056) in a 37°C incubator for 5 minutes. The dissociated cells were washed from the flask bottom in culture medium, transferred to a 50 mL conical tube and centrifuged at 3500 RPM for 10 minutes. Following centrifugation, the resulting supernatant was aspirated and the pellet resuspended to a single-cell solution using a serological pipette. The number of cells in solution was then quantified using a hemocytometer, diluted in culture medium to a plating density of 5 x 10^5 cells/mL and transferred to experimental plates or dishes pre-coated with poly-D-lysine. This preparation yielded a primary astroglial culture of >95% (data not shown).

siRNA Transfection

Cell cultures in antibiotic-free culture medium were transfected with either control (Qiagen #1027201, Venlo, Limburg, Netherlands) or mortalin (Mm_Hspa9a_6; Qiagen #SI02712710) siRNA using Lipofectamine 2000 reagent (Life Technologies #11668019) according to the manufacturer's protocol, with slight modifications. Lipofectamine 2000 reagent was aliquoted into Opti MEM medium (Life Technologies #31985070) at the volume specified by the manufacturer and siRNA quantities were doubled to increase knockdown efficiency. After gentle mixing, Lipofectamine 2000 and siRNA were incubated separately at room temperature in Opti MEM for 5 minutes, then combined and incubated for additional 20 minutes. Following the incubation periods, the Lipofectamine/siRNA complex was added to the culture medium at the volume specified by the manufacturer's protocol and returned to the incubator overnight. The media was changed to one containing antibiotics the following day.

Western Blot

Primary astrocytes were allowed to grow to confluency in a 6-well plate (~3 days), after which time culture medium was changed to that with or without $MnCl_2$ (Sigma-Aldrich Corporation #M3634, St. Louis, MO, USA). Following a 72-hour incubation period, cells were washed once with ice-cold PBS (pH 7.4), collected by physically scraping in a lysis buffer [150 μM NaCl, 500 μM Tris-HCl, 1% (v/v) NP-40, 10% (v/v) 1X protease inhibitor cocktail (Sigma-Aldrich #P2714), 1μM PMSF, 10 μM NaF, 0.2 μM Na_3VO_4 in deionized water], flash-frozen on dry ice and stored at -80°C for further processing. Samples were subsequently thawed on ice, sonicated quickly 40 times on ice at a setting of 1 using a Branson Sonifier 150 (Branson Ultrasonics, Danbury, CT, USA) and centrifuged at 15000 RPM for 10 minutes at 4°C. Supernatants were then transferred to clean tubes, and a bicinchoninic acid protein assay was performed according to the manufacturer's protocol (Thermo Scientific Inc. #23225, Rockford, IL, USA) at a dilution of 1:50. Approximately 30 μg of protein were loaded onto a precast 10-20% Tris-HCl gel (Bio-Rad #345-0042, Hercules, CA, USA) and separated by electrophoresis (100V for 10 minutes; 160V for 70 minutes). Proteins were then transferred overnight at 4°C to a PVDF membrane at a constant current of 0.36 A. The membrane was then incubated for 1 hour at room temperature in blocking buffer (5% non-fat milk powder dissolved into TBS-T), after which time the primary antibody (mortalin #ADI-SPS-825, Enzo Life Sciences, Inc., Farmindale, NY, USA; β-actin #ab8226, Abcam plc, Cambridge, MA, USA) was added at a dilution of 1:3000 and incubated at 4°C overnight. After washing in TBS-T (2 x 5 minutes and 2 x 10 minutes), the membrane was incubated at room temperature for 1 hour with the horseradish

peroxidase conjugated secondary antibody diluted 1:20000 (anti-mouse IgG, HRP-linked; Cell Signaling Technology #50-195-914, Beverly, MA, USA) in TBS-T containing 3% bovine serum albumin (Sigma-Aldrich #A9647). Following another series of washes in TBS-T (2 x 5 minutes and 2 x 10 minutes), enhanced chemilumescent reagents (Amersham ECL; GE Healthcare Bio-Sciences Corp. #RPN2209, Picastaway, NJ, USA) was applied to the membrane for 2 minutes, the membrane was exposed to X-ray film (BioExpress #F-9029, Kaysville, UT, USA) and the protein signal visualized by passing the film through a developer machine.

Quantitative PCR

For qPCR analysis, primary astrocytes were grown to confluency in 6-well plates and then treated with $MnCl_2$. Following the treatment period, astroglial monolayers were washed once with room temperature PBS, collected in 1 mL of TRIzol reagent (Life Technologies #15596-018, Carlsbad, CA, USA) and stored at -80°C for further processing. Frozen samples were thawed on ice and RNA isolation was performed following a well-established phenol-chloroform extraction method (Chomczynski and Sacchi 1987) with slight modifications. After thawing, 200 μL chloroform were added to each 1 mL sample, the mixture was shaken well by hand for 15 seconds and the samples were allowed to rest at room temperature for 5 minutes. Samples were then centrifuged at 12000 RPM in a centrifuge cooled to 4°C. Following centrifugation, the aqueous phase of each sample was carefully transferred, so as not to include the interphase, to a new tube. Nucleic acids were then precipitated using isopropanol and pelleted by centrifuging at 15000 RPM. The resulting pellet was washed 3 times with 70% ethanol made using DEPC water, with a 10 minute 15000 RPM centrifugation following each wash. The

purified pellet was air dried for approximately 15 minutes and then dissolved in 30 μL of RNase free water.

To remove genomic DNA, the isolated nucleic acids were treated with DNase (Life Technologies #AM1907) according to the manufacturer's protocol. The remaining RNA was then cleaned using a kit (Qiagen) following the manufacturer's instructions. RNA was eluted from the clean-up column in 30 mL of RNase-free water and the RNA content quantified using a NanoDrop 2000 instrument (Thermo Scientific). Equal amounts of RNA template inputs were used to generate cDNA following the manufacturer's protocol for a reverse transcription kit (Life Technologies #4368814). Gene expression was then quantified with a TaqMan Gene Expression Assay according to the manufacturer's protocol. Each reaction contained 10 ng of cDNA, a TaqMan probe set (Life Technologies #4331182; *Hspa9*: Mm00477716_g1; *Ddit3*: Mm01135937_g1; *Ubc*: Mm01198158_m1; *Psmc4*: Mm00457191_m1) and TaqMan Universal PCR Master Mix (Life Technologies #4369016). Reaction solutions were loaded in quadruplicate to a 384-well plate and analyzed with a Viia7 Real-Time PCR System (Life Technologies) using the manufacturer's recommended thermal cycling conditions (hold at 50°C for 2 minutes, hold at 95°C for 10 minutes, cycle 40 times between 95°C for 15 seconds and 60°C for 1 minute). Relative quantification of gene expression was determined by calculating ΔΔCt values for each sample.

DCF Assay

To evaluate production of reactive oxygen species, the 2', 7' – dichlorofluorescein (DCF) assay was used. Primary astrocytes were plated into 96-well plates and transfected as described above then allowed to grow to confluency. To perform

the assay, cells were washing once with pre-warmed Hank's balanced salt solution (HBSS; Thermo Fisher Scientific #SH3026801) and then incubated with DCF reagent (EMD Millipore #287810, Billerica, MA, USA) dissolved in DMSO and diluted to a concentration of 1 μM in HBSS (0.01% DMSO following dilution) for 15 minutes at 37°C in the dark. Cells were then washed again once with HBSS after which the medium was replaced with either 0 or 10 μM Mn dissolved in HBSS and the plate returned to a 37°C incubator for 1 hour. Following the incubation period, the fluorescent signal was read using a SpectraMax plate reader (Molecular Devices, LLC, Sunnyvale, CA, USA) with excitation/emission set to 488/520 nm.

Immunofluorescence Microscopy of Primary Neurons

To study neuronal endpoints, an *in vitro* direct-contact co-culture model system between mouse primary astrocytes and rat primary neurons was used. Cortical primary mouse astrocytes were dissected, cultured and plated at a density of 2.5×10^4 cells/well as described above onto 12 mm glass coverslips (Glaswarenfabrik Karl Hecht GmbH & Co. KG #0110529, Sondenheim, Germany) pre-coated with poly-D-lysine in a 24-well plate. Transfections were carried out the following day as described above. Primary rat neuronal cultures isolated from the striatum of 1-3 day old pups were prepared 5 days after plating primary mouse astrocytes. Brains were dissected in an ice-cold neuronal dissection medium [2% B27 supplement (Life Technologies #17504-044) and 0.25% L-glutamine (200 mM; Life Technologies #25030164) in Neurobasal A medium (Life Technologies #10888-022)], the striatum was isolated, meninges were carefully removed mechanically and the tissue transferred to a 50 mL conical tube containing neuronal dissection medium and kept on ice. After completing dissections, tissue was transferred

to an enzyme solution [0.25% L-glutamine, 20 μg/mL DNase I (Worthington Biochemical #LS002138, Lakewood, NJ, USA) and 15 U/mL papain (Worthington Biochemical #LS003127) in Hibernate A (BrainBits, LLC, Springfield, IL, USA)] and incubated at 30°C for 15 minutes. Tissue was then washed 3 times in pre-warmed culture medium [10% FBS and 1% penicillin/streptomycin in DMEM/F12], triturated 3 times with a flame-polished glass Pasteur pipette and transferred following each trituration to a 50 mL conical tube through a 100 μm cell strainer. The cell suspension was centrifuged at 1100 RPM for 5 minutes, the resulting pellet was resuspended in culture medium and cells counted using a hemocytometer. The suspended cells were then seeded directly on the aforementioned monolayer of astroglial cells at a density of 4.5×10^4 cells/coverslip. Two days following primary rat brain cell seeding, arabinofuranosyl cytidine (Ara-C; Sigma-Aldrich #C1768) was added at a concentration of 5 μM to prevent proliferation of rat glial cells.

Manganese chloride ($MnCl_2$; Sigma-Aldrich #M8054) was dissolved in culture medium and added to the co-cultures at the indicated concentrations 9 days after adding neuronal cells to the co-culture model system. The treatment duration was 5 days, after which time cells were washed once with room temperature PBS (pH 7.4) and fixed in 4% paraformaldehyde (Wako Chemicals USA, Inc. #163-20145, Richmond, VA, USA). For immunofluorescent staining, coverslips were washed in PBS (pH 7.4; 2 x 5 minutes) while gently rocking at room temperature. The fixed cells were then incubated with a blocking solution [4% normal goat serum (Vector Laboratories #S-1000, Peterborough, UK), 1% bovine serum albumin (Sigma-Aldrich #A-9647) and 0.4% Triton X-100 (Sigma-Aldrich #X100)] for 1 hour at room temperature. Following blocking, primary

antibodies (mouse anti-MAP2 (Abcam plc #ab11267, Cambridge, UK); rabbit anti-synaptophysin (Abcam #ab23754)) were diluted 1:100 in blocking buffer and incubated with the samples overnight at 4°C on an orbital shaker. The next day, coverslips were washed (3 x 5 minutes) with PBS containing 0.1% Tween-20 (Sigma-Aldrich #P5927), incubated with a secondary antibody solution (AlexaFluor 488 goat anti-rabbit (Life Technologies #A11034) and AlexaFluor 568 goat anti-mouse (Life Technologies #A11031) diluted 1:500 in PBS containing 0.3% Triton X-100) for 1 hour at room temperature with gentle rocking and washed (3 x 5 minutes) once again with PBS containing 0.1% Tween-20. Following the final wash, coverslips were mounted onto glass microscope slides (VWR International, LLC #48311-600, Radnor, PA, USA) using Vectashield Mounting Medium with DAPI (Vector Laboratories #H-1200), sealed with nail polish and stored at 4°C.

Imaging was carried out on a Nikon Eclipse Ti Imaging System (Nikon Instruments Inc., Melville, NY, USA) under 20X magnification, and exposure times for each channel were determined by using the auto-exposure feature over several random fields for several unique specimens. The chosen exposure times were 12 ms for the 568 nm signal (MAP2) and 384 ms for the 488 nm signal (synaptophysin). Images were acquired for a random selection of 20 neuron-containing fields for each specimen. Experiments were performed on 3 biologically independent sample preparations. The acquired images were analyzed by a blinded operator using Neurolucida software (v11.03, MBF Bioscience, Williston, VT, USA). Neuronal processes were assessed by tracing neurites based on their MAP2 signal. Pre-synaptic terminals were assessed counting all synaptophysin puncta that were localized along the MAP2 signal.

Intracellular Calcium Signaling

Astroglial intracellular calcium was assessed using Fluo-4-AM dye (Life Technologies #F14201). Primary astrocytes were plated as described above onto 35 mm imaging dishes with a 14 mm glass cover slip embedded in the center (MatTek Corporation #P35G-1.5-14-C, Ashland, MA, USA) pre-coated with poly-D-lysine. Transfections were carried out the following day as described above. Four days after plating, cells were treated with fresh media or that containing 10 μM $MnCl_2$ for a period of 24 hours. Following the treatment period, Fluo-4-AM dye was prepared by dissolving a lyophilized 50 μg aliquot in 10 μL DMSO containing 4% Pluronic F-127 (Life Technologies #P3000MP) and shaking for 30 minutes at room temperature while protected from light, then 90 μL of pre-warmed artificial cerebrospinal fluid (ACSF; 125 μM NaCl, 2.5 μM KCl, 1 μM $MgCl_2$, 2 μM $CaCl_2$, 1.25 μM NaH_2PO_4, 10 mM glucose, 10 mM HEPES) was added to create the working solution. Imaging dishes were washed once with ACSF, loaded with Fluo-4-AM dye at a concentration of 5 μg/mL ACSF and placed in a 37°C incubator for 30 minutes. The loading solution was then replaced with fresh ACSF and returned to the incubator for 10 minutes. This process was repeated twice for a total of 3 washes of 10 minutes each, and after the final wash 2 mL of ACSF was added to the dish. Live cell imaging was carried out using a Nikon Eclipse Ti instrument (Nikon Instruments Inc.) with a 37°C atmosphere under 60X magnification. Light source power was set to 33% and a ND-4 neutral density filter was used to minimize photobleaching. Exposure time was constant at 200 ms. After selecting a field of astrocytes to image, baseline fluorescent intensities were collected on the GFP channel with 2x2 binning every second for approximately 2 minutes. Calcium responses were

then stimulated by adding 100 μM adenosine 5'-triphosphate (ATP; Sigma-Aldrich #A9187) and data continued to be recorded for a total of 10 minutes. Data were analyzed by determining the ratio of the maximum calcium response to ATP (defined as F) to an averaged 5-second representative baseline measurement (defined as F_0) as calculated by $(F - F_0)/F$ (defined as $\Delta F/F_0$). Experiments were repeated at least 6 times using biologically independent samples. The resulting data for all replicates were represented as a continuous probability plot for each experimental condition and analyzed statistically using a two-sample Kolmogorov-Smirnov test to determine if responses between two groups were equal.

Protein Aggregation

Primary astrocytes were plated onto 12 mm glass coverslips and transfected the following day as described above and allowed to grow to confluency (approximately 4 days). Cells were treated with 0 or 10 μM $MnCl_2$ for 24 hours, washed once with PBS and fixed with 4% paraformaldehyde. Aggregated proteins were detected using ProteoStat reagent (Enzo Life Sciences, Inc. #ENZ-51035) according to the manufacture's protocol. The coverslips were washed twice with PBS and incubated with a permeabilizing solution (manufacturer's assay buffer containing 0.5% Triton X-100 and 3 mM EDTA, pH 8) on ice for 30 minutes. The coverslips were again washed twice with PBS and incubated with Proteostat Aggresome Detection Reagent diluted 1:2,000 in the manufacturer's assay buffer for 30 minutes at room temperature. After a final PBS wash, coverslips were mounted onto glass microscope slides using Vectashield with DAPI and sealed with nail polish. Imaging was carried out using the aforementioned Nikon Eclipse Ti instrument under 60X magnification. Z-series stacks (0.2 μm step size) were acquired

on the red channel for 10 randomly selected fields. Exposure times were kept constant and determined for each experiment using the auto-exposure feature. After deconvolving the images, quantitative fluorescent intensity data were acquired for the astrocytes by defining regions of interest inclusive of the cells within the field of view. Data are represented as total fluorescence intensity per unit area as defined by the selected regions of interest.

Results

Effect of Manganese on Astroglial Mortalin Expression

We first studied the effect Mn treatment has on mortalin protein and gene expression using Western blot and qPCR. Primary mouse astrocytes were treated with concentrations of Mn ranging from 0 to 500 μM. Mortalin protein expression was found to decrease in a dose-dependent manner, while mRNA expression was conversely found to increase in a dose-dependent manner (**Figure 11**).

Reduced Astroglial Mortalin Enhances Neuronal Susceptibility to Mn Toxicity

Given the finding that Mn treatment may decrease astroglial mortalin protein levels and considering our previous finding that astrolial mortalin is decreased in the caudate of Mn-exposed humans (Chapter 6), we next evaluated neuronal susceptibility to Mn toxicity in the presence of astrocytes carrying either endogenous or reduced levels of mortalin. To accomplish this, we utilized an astrocyte-neuron co-culture model system and took an immunofluorescent staining approach to evaluate neuronal health. Neurite outgrowth as assessed by MAP2 staining was found to be unchanged regardless of mortalin expression or Mn treatment condition (**Figure 12C**). However, the number of presynaptic terminals, as indicated by synaptophysin staining, were found to be decreased

in cultures treated with 10 μM Mn in which mortalin had been knocked-down (**Figure 12D**).

Intracellular Calcium Signaling

We next searched for a mechanistic link between reduced astroglial mortalin and fewer neuronal synapses in the presence of Mn, with the hypothesis that astroglial intracellular calcium is altered in cells exposed to Mn and/or with reduced mortalin expression. To test this hypothesis, primary mouse astrocytes expressing endogenous or reduced levels of mortalin were pre-treated with Mn and intracellular calcium responses to ATP measured using Fluo-4-AM calcium indicator dye. Treatment with 10 μM Mn significantly reduced astroglial calcium response to ATP (**Figure 13A**), confirming a previous report (Tjalkens et al. 2006). Mortalin knockdown had no effect on calcium response to ATP under the control condition, but further reduced intracellular calcium in cells treated with 10 μM Mn, consistent with the aforementioned synaptophysin data. Interestingly, when repeating these studies in astrocytes cultured from SNCA KO mice, although Mn treatment still suppressed calcium responses, the effect of mortalin knockdown was mitigated (**Figure 13B**).

Stress of Organelles Involved in Intracellular Calcium Signaling

As mitochondria and the endoplasmic reticulum (ER) represent the major cellular location for regulation of intracellular calcium dynamics, we next searched for signs of stress within these organelles. While mitochondrial calcium imaging yielded no differences among the experimental conditions (data not shown), a significant elevation in the production of reactive oxygen species (ROS) was observed in astrocytes treated

with 10 μM Mn (**Figure 14A**). However, mortalin expression level did not alter ROS generation in Mn-treated cells. On the other hand, mortalin knockdown was found to increase expression of the *Ddit3* gene, which encodes the C/EBP homologous protein (CHOP) and is indicative of ER stress (**Figure 14B**). However, Mn treatment alone did not induce ER stress and did not potentiate the stress observed in cells expressing reduced levels of mortalin.

Intracellular Protein Aggregation

ER stress may be caused by depleted calcium levels within its lumen resulting in the misfolding of proteins and subsequently evoke the unfolded protein response (UPR). An inability of the UPR to restore proper ER function, and repair and/or degrade misfolded proteins may lead to protein aggregation. The data indicating decreased intracellular calcium response to ATP and indications of both ER stress upon knocking down mortalin and production of ROS with 10 μM Mn treatment led us to evaluate levels of aggregated proteins in these astrocytes. Using Proteostat, a fluorescent dye which binds aggregated proteins, we observed no significant differences dependent on mortalin knockdown or Mn treatment alone, but cells both transfected with mortalin siRNA and treated with 10 μM Mn were found to have an elevated abundance of aggregated proteins (**Figure 15A**). On the other hand, no differences were noted when these experiments were repeated using SNCA KO astrocytes (**Figure 15B**).

Discussion

In this study, we tested the hypothesis that reduced expression of astroglial mortalin modulates neuronal sensitivity to Mn toxicity. This study builds upon our previous human observational study that found reduced astroglial mortalin levels in the caudate of Mn exposed individuals as compared to those not exposed to Mn (Chapter 6). To evaluate the direct effect Mn has on astroglial mortalin, we first measured protein and mRNA expression in mouse primary astrocytes treated with Mn. Interestingly, we found Mn treatment decreased astroglial protein levels of mortalin in a dose-dependent manner. Conversely, mortalin mRNA expression increased with Mn treatment concentration, which may be indicative of a compensatory mechanism in response to the loss of mortalin protein. These results demonstrate that Mn alone is capable of modulating astroglial mortalin.

While the initial results show a direct effect of short-term Mn exposure on astroglial mortalin, clear differences in expression were not observed until the treatment concentration reached at least 125 μM Mn. Although it has been demonstrated that this Mn concentration is achievable in the brain tissue of experimentally exposed primates (Suzuki et al. 1975), it is likely that these instances are rare in humans and represent an event of extreme exposure which would not reflect the chronic, low-level exposures more commonly experienced in present day occupational and non-occupational settings (Lucchini et al. 2009). At the same time, it is neither practical nor possible to determine the effect of low-level Mn expression over an extended period of time *in vitro*. Therefore, in order to model the effect of reduced astroglial mortalin as observed in Mn exposed

humans, we knocked down its expression using siRNA and explored the interaction between suppressed mortalin and low-level Mn treatment.

As Mn is an established neurotoxicant, we asked whether reduced astroglial mortalin expression can affect neuronal susceptibility to Mn toxicity using a direct-contact co-culture system. While no effect was observed using measures of neurite outgrowth (such as length of dendrites and extent of branching), the number of presynaptic terminals along the neurites was found to be significantly decreased after treatment with 10 μM Mn in neurons cultured with astrocytes expressing reduced levels of mortalin. These results demonstrate that reduced astroglial mortalin combined with low-level exposure to Mn may adversely affect neuronal health.

Next, we studied the effect of reduced mortalin and/or Mn treatment on astroglial function to explore potential mechanisms contributing to the observed synaptic sensitivity to Mn. A major function of astrocytes involves support of neuronal health and regulation of synaptic transmitters, and in this regard they respond to neuronal activity by increasing intracellular calcium which in turn leads to astroglial release of transmitters which regulate synaptic communication (Stephen et al. 2014). Therefore, we evaluated intracellular calcium signaling in our model system, observing a decreased response to ATP stimulus after treating with Mn that has also been described previously (Tjalkens et al. 2006). Furthermore, we found that the effect of Mn on calcium response was potentiated in astrocytes with reduced mortalin expression, while the knockdown had no effect on untreated cells. Additionally, carrying out the same set of experiments in astrocytes cultured from SNCA KO mice, which lack expression of α-synuclein,

mitigated the combined effect of reduced mortalin and Mn treatment observed in the WT cells.

Since the ER and mitochondria are primarily responsible for intracellular calcium signaling (Verkhratsky et al. 2012), indicators of stress related to these organelles was evaluated in our model system. It was found that mortalin knockdown, but not Mn treatment, increased ER stress while Mn treatment, but not mortalin knockdown, increased the production of ROS. In this regard, the only condition in which both ER stress and ROS production are elevated is Mn treatment combined with reduced mortalin expression. It also followed that this was the only condition that was observed to have an increased presence of aggregated proteins. It is thus proposed that underlying mechanism of action responsible for the observed decrease in neuronal presynaptic terminals involves a 'two-hit' process, with one hit being increased oxidative stress resulting from Mn treatment and the other being increased ER stress caused by calcium dysregulation resulting from decreased mortalin expression. The combined effect of these processes results in an accumulation of aggregated proteins. As mentioned above, intracellular calcium is involved in neoron-glia communication in that increases of its concentration are associated with the release of neuroreactive substances, including trophic factors and growth factors that are essential for proper neuronal development and function (Parpura et al. 1994, Pasti et al. 1997, Carmignoto 2000, Haydon 2001, Di Castro et al. 2011).

Intriguingly, astrocytes lacking the α-synuclein protein were resistant to the effects described above, suggesting that the protein plays an important role in the observed processes. α-Synuclein is a unique protein that has an unusually high propensity to aggregate (Cho et al. 2009, Trexler and Rhoades 2010), a phenomenon of critical

importance in the pathology of PD (Braak et al. 2003). While α-synuclein aggregation is generally described in the context of neurons in this regard, it has also been shown to similarly aggregate in astrocytes as a function of disease severity (Braak et al. 2007). Decreased mortalin expression has been demonstrated in the brain tissue of PD patients (Jin et al. 2006), and α-synuclein has been shown to interact directly with mortalin (Jin et al. 2007). As ER stress has also been implicated in PD (Mercado et al. 2013), the results presented here linking suppressed mortalin expression with increased ER stress suggest a mechanistic relationship to PD pathogenesis. On the other hand, Mn exposure is a known risk factor for parkinsonism (Racette 2013) and it has been shown that Mn treatment can induce α-synuclein aggregation *in vitro* (Uversky et al. 2001) and in both neurons and glial cells of Mn exposed non-human primates (Verina et al. 2013). In considering these previously reported findings and taken together with the results presented in the current study, it is speculated that α-synuclein may play an important mediating role in the 'two-hit' model of action proposed here.

In conclusion, we found that decreased astroglial expression of mortalin increases neuronal susceptibility to Mn toxicity. It is proposed that the underlying mechanism of action involves a 'two-hit' gene-environment interaction including both ER and oxidative stress, which may be linked by α-synuclein.

References

Aschner, M., M. Gannon, and H. K. Kimelberg. 1992. Manganese uptake and efflux in cultured rat astrocytes. J Neurochem **58**:730-735.

Aschner, M., K. E. Vrana, and W. Zheng. 1999. Manganese uptake and distribution in the central nervous system (CNS). Neurotoxicology **20**:173-180.

Braak, H., U. Rüb, W. P. Gai, and K. Del Tredici. 2003. Idiopathic Parkinson's disease: possible routes by which vulnerable neuronal types may be subject to neuroinvasion by an unknown pathogen. J Neural Transm **110**:517-536.

Braak, H., M. Sastre, and K. Del Tredici. 2007. Development of alpha-synuclein immunoreactive astrocytes in the forebrain parallels stages of intraneuronal pathology in sporadic Parkinson's disease. Acta Neuropathol **114**:231-241.

Carmignoto, G. 2000. Reciprocal communication systems between astrocytes and neurones. Prog Neurobiol **62**:561-581.

Cho, M. K., G. Nodet, H. Y. Kim, M. R. Jensen, P. Bernado, C. O. Fernandez, S. Becker, M. Blackledge, and M. Zweckstetter. 2009. Structural characterization of alpha-synuclein in an aggregation prone state. Protein Sci **18**:1840-1846.

Chomczynski, P., and N. Sacchi. 1987. Single-step method of RNA isolation by acid guanidinium thiocyanate-phenol-chloroform extraction. Anal Biochem **162**:156-159.

Couper, J. 1837. On the effects of black oxide of manganese when inhaled into the lungs. British Annals of Medicine, Pharmacy, Vital Statistics, and General Science **1**:2.

Deocaris, C. C., S. C. Kaul, and R. Wadhwa. 2008. From proliferative to neurological role of an hsp70 stress chaperone, mortalin. Biogerontology **9**:391-403.

Deocaris, C. C., N. Widodo, T. Ishii, S. C. Kaul, and R. Wadhwa. 2007. Functional significance of minor structural and expression changes in stress chaperone mortalin. Ann N Y Acad Sci **1119**:165-175.

Di Castro, M. A., J. Chuquet, N. Liaudet, K. Bhaukaurally, M. Santello, D. Bouvier, P. Tiret, and A. Volterra. 2011. Local Ca2+ detection and modulation of synaptic release by astrocytes. Nat Neurosci **14**:1276-1284.

Finkelstein, M. M., and M. Jerrett. 2007. A study of the relationships between Parkinson's disease and markers of traffic-derived and environmental manganese air pollution in two Canadian cities. Environ Res **104**:420-432.

Haydon, P. G. 2001. GLIA: listening and talking to the synapse. Nat Rev Neurosci **2**:185-193.

Huang, C. C., N. S. Chu, C. S. Lu, R. S. Chen, M. Schulzer, and D. B. Calne. 2007. The natural history of neurological manganism over 18 years. Parkinsonism Relat Disord **13**:143-145.

Jin, J., T. J. Cook, J. G. Hoekstra, and J. Zhang. 2012. Mortalin in Neurological Diseases.*in* S. C. Kaul and R. Wadhwa, editors. Mortalin Biology: Life, Stress and Death. Springer Science+Business Media B.V., Springer Dordrecht Heidelberg London New York.

Jin, J., C. Hulette, Y. Wang, T. Zhang, C. Pan, R. Wadhwa, and J. Zhang. 2006. Proteomic identification of a stress protein, mortalin/mthsp70/GRP75: relevance to Parkinson disease. Mol Cell Proteomics **5**:1193-1204.

Jin, J., G. J. Li, J. Davis, D. Zhu, Y. Wang, C. Pan, and J. Zhang. 2007. Identification of novel proteins associated with both alpha-synuclein and DJ-1. Mol Cell Proteomics **6**:845-859.

Lucchini, R. G., C. J. Martin, and B. C. Doney. 2009. From manganism to manganese-induced parkinsonism: a conceptual model based on the evolution of exposure. Neuromolecular Med **11**:311-321.

Mercado, G., P. Valdés, and C. Hetz. 2013. An ERcentric view of Parkinson's disease. Trends Mol Med **19**:165-175.

Mortimer, J. A., A. R. Borenstein, and L. M. Nelson. 2012. Associations of welding and manganese exposure with Parkinson disease: review and meta-analysis. Neurology **79**:1174-1180.

Park, R. M., P. A. Schulte, J. D. Bowman, J. T. Walker, S. C. Bondy, M. G. Yost, J. A. Touchstone, and M. Dosemeci. 2005. Potential occupational risks for neurodegenerative diseases. Am J Ind Med **48**:63-77.

Parpura, V., T. A. Basarsky, F. Liu, K. Jeftinija, S. Jeftinija, and P. G. Haydon. 1994. Glutamate-mediated astrocyte-neuron signalling. Nature **369**:744-747.

Pasti, L., A. Volterra, T. Pozzan, and G. Carmignoto. 1997. Intracellular calcium oscillations in astrocytes: a highly plastic, bidirectional form of communication between neurons and astrocytes in situ. J Neurosci **17**:7817-7830.

Perea, G., M. Sur, and A. Araque. 2014. Neuron-glia networks: integral gear of brain function. Front Cell Neurosci **8**:378.

Racette, B. A. 2013. Manganism in the 21st century: The Hanninen lecture. Neurotoxicology.

Racette, B. A., L. McGee-Minnich, S. M. Moerlein, J. W. Mink, T. O. Videen, and J. S. Perlmutter. 2001. Welding-related parkinsonism: clinical features, treatment, and pathophysiology. Neurology **56**:8-13.

Rappold, P. M., and K. Tieu. 2010. Astrocytes and therapeutics for Parkinson's disease. Neurotherapeutics **7**:413-423.

Roels, H., G. Meiers, M. Delos, I. Ortega, R. Lauwerys, J. P. Buchet, and D. Lison. 1997. Influence of the route of administration and the chemical form (MnCl2, MnO2) on the absorption and cerebral distribution of manganese in rats. Arch Toxicol **71**:223-230.

Schwarzer, C., S. Barnikol-Watanabe, F. P. Thinnes, and N. Hilschmann. 2002. Voltage-dependent anion-selective channel (VDAC) interacts with the dynein light chain Tctex1 and the heat-shock protein PBP74. Int J Biochem Cell Biol **34**:1059-1070.

Stephen, T. L., S. Gupta-Agarwal, and J. T. Kittler. 2014. Mitochondrial dynamics in astrocytes. Biochem Soc Trans **42**:1302-1310.

Suzuki, Y., T. Mouri, K. Nishiyama, and N. Fujii. 1975. Study of subacute toxicity of manganese dioxide in monkeys. Tokushima J Exp Med **22**:5-10.

Tjalkens, R. B., M. J. Zoran, B. Mohl, and R. Barhoumi. 2006. Manganese suppresses ATP-dependent intercellular calcium waves in astrocyte networks through alteration of mitochondrial and endoplasmic reticulum calcium dynamics. Brain Res **1113**:210-219.

Trexler, A. J., and E. Rhoades. 2010. Single molecule characterization of α-synuclein in aggregation-prone states. Biophys J **99**:3048-3055.

Tuschl, K., P. B. Mills, and P. T. Clayton. 2013. Manganese and the brain. Int Rev Neurobiol **110**:277-312.

Uversky, V. N., J. Li, and A. L. Fink. 2001. Metal-triggered structural transformations, aggregation, and fibrillation of human alpha-synuclein. A possible molecular NK between Parkinson's disease and heavy metal exposure. J Biol Chem **276**:44284-44296.

Verina, T., J. S. Schneider, and T. R. Guilarte. 2013. Manganese exposure induces α-synuclein aggregation in the frontal cortex of non-human primates. Toxicol Lett **217**:177-183.

Verkhratsky, A., J. J. Rodríguez, and V. Parpura. 2012. Calcium signalling in astroglia. Mol Cell Endocrinol **353**:45-56.

Willis, A. W., B. A. Evanoff, M. Lian, A. Galarza, A. Wegrzyn, M. Schootman, and B. A. Racette. 2010. Metal emissions and urban incident Parkinson disease: a community health study of Medicare beneficiaries by using geographic information systems. Am J Epidemiol **172**:1357-1363.

Willis, A. W., M. Schootman, N. Kung, B. A. Evanoff, J. S. Perlmutter, and B. A. Racette. 2012. Predictors of survival in patients with Parkinson disease. Arch Neurol **69**:601-607.

Wright Willis, A., B. A. Evanoff, M. Lian, S. R. Criswell, and B. A. Racette. 2010. Geographic and ethnic variation in Parkinson disease: a population-based study of US Medicare beneficiaries. Neuroepidemiology **34**:143-151.

Zhang, P., K. M. Lokuta, D. E. Turner, and B. Liu. 2010. Synergistic dopaminergic neurotoxicity of manganese and lipopolysaccharide: differential involvement of microglia and astroglia. J Neurochem **112**:434-443.

Figures

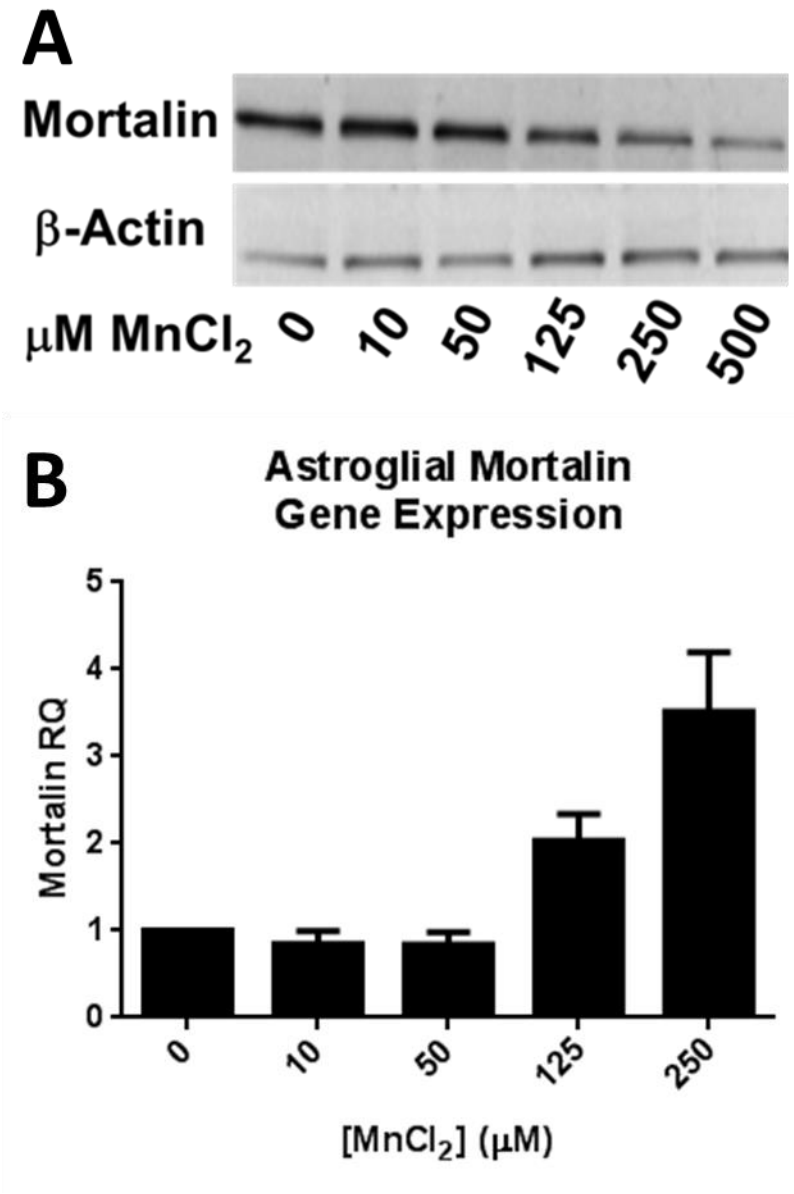

Figure 11: Effect of Mn treatment on astroglial mortalin expression. Astroglial mortalin expression was quantified following Mn treatment by Western blot and qPCR. (A) Mortalin protein levels are decreased as Mn concentration is increased in a dose-dependent manner. (B) Mortalin mRNA levels are increased as Mn concentration is increased in a dose-dependent manner.

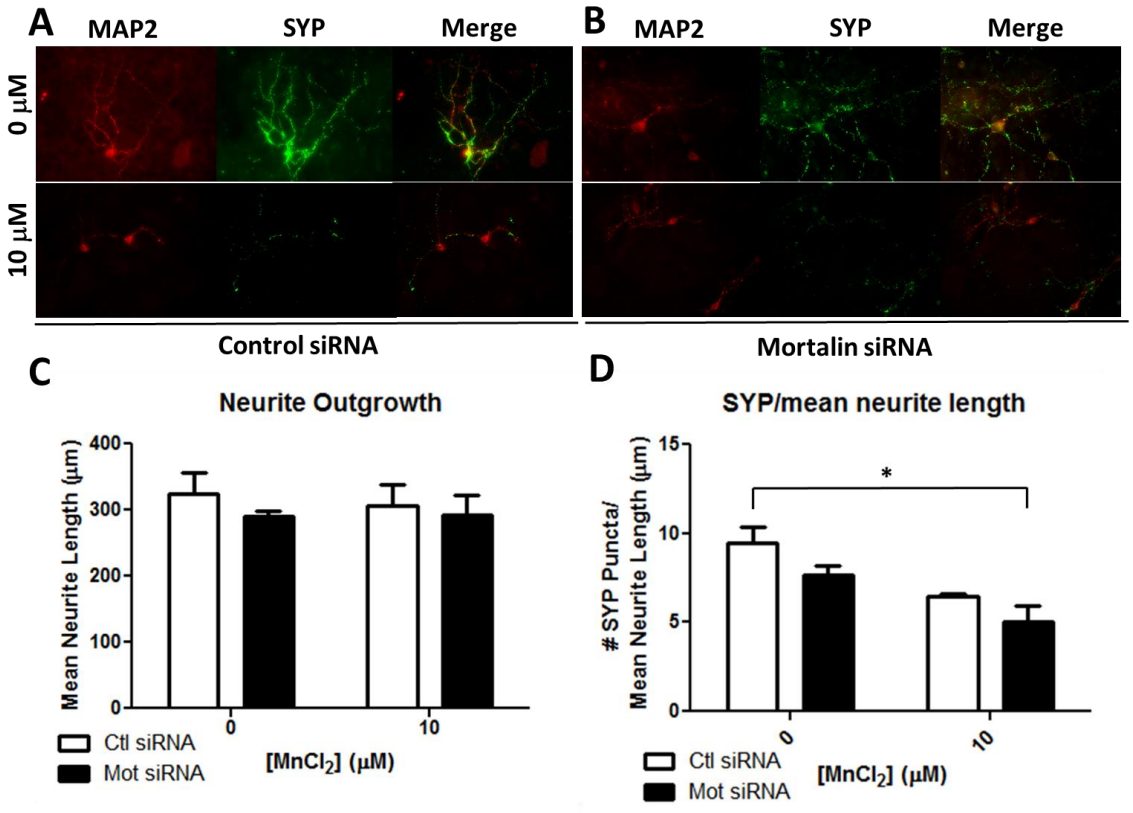

Figure 12: Reduced astroglial mortalin increases neuronal susceptibility to Mn toxicity. Primary striatal neurons were plated directly on top of primary astrocytes expressing either (A) endogenous or (B) reduced levels of mortalin. Co-cultures were then treated with 0 or 10 μM Mn and stained for MAP2 (red) and synaptophysin (green). (C) No difference of neurite outgrowth was observed among the experimental groups. (D) Astrocytes with mortalin expression knocked down and treated with 10 mM Mn were found to have a significantly reduced number of synaptophysin puncta per unit of neurite length. *$p < 0.05$.

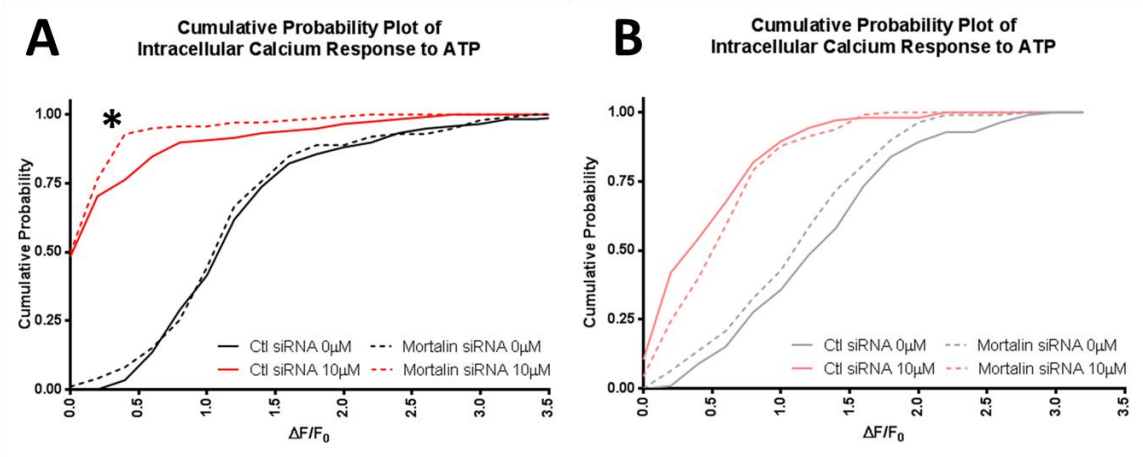

Figure 13: Intracellular calcium signaling. Intracellular calcium response to ATP stimulus was evaluated in primary astrocytes expressing either endogenous or reduced levels of mortalin and treated with 0 or 10 μM Mn. (A) Wild type astrocytes were found to have a suppressed calcium response when treated with Mn, and this effect was potentiated when mortalin expression was knocked down. (B) SNCA KO astrocytes were found to have a suppressed calcium response when treated with Mn, but mortalin knockdown did not affect the results.

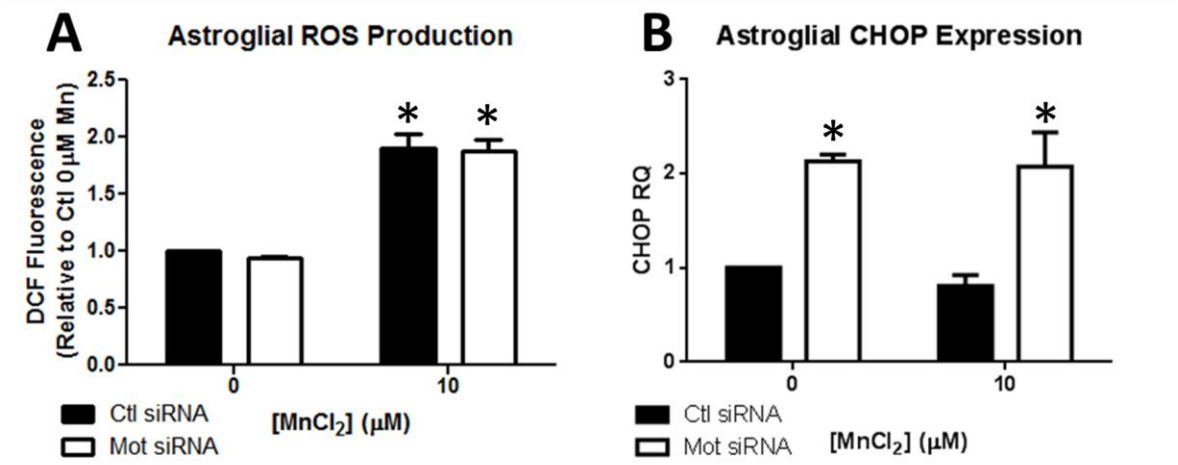

Figure 14: Indicators of oxidative and ER stress. (A) Reactive oxygen species were found to be increased in astrocytes treated with 10 mM Mn, but mortalin knockdown had no effect. (B) ER stress as indicated by CHOP expression was found to be increased when mortalin expression was knocked down, but Mn treatment had no effect. *$p < 0.05$.

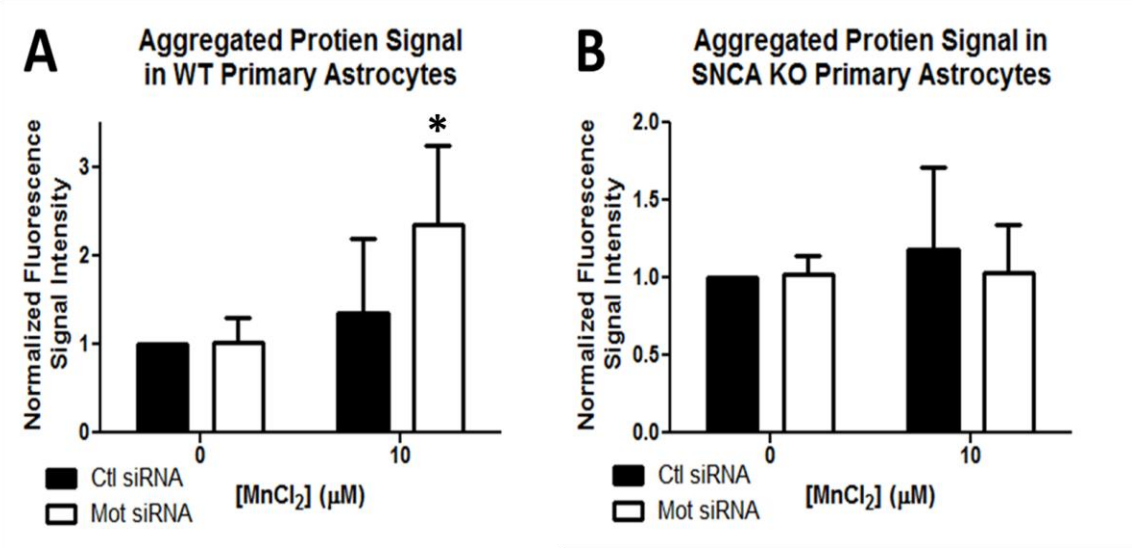

Figure 15: Intracellular protein aggregation. Protein aggregation was evaluated using Proteostat reagent in astrocytes expressing endogenous or reduced levels of mortalin and treated with 0 or 10 μM Mn. (A) Wild type astrocytes with mortalin knocked down were found to contain increased amounts of aggregated proteins after treatment with 10 mM Mn. (B) No difference in aggregated protein signal was observed in SNCA KO astrocytes in any of the experimental conditions. *$p < 0.05$.

CHAPTER 7: CONCLUSIONS

Human exposure to manganese (Mn) represents a classic example of a U-shaped dose-response in that while a minimal dietary amount is required for optimal health, excessive exposure has been definitively demonstrated to carry adverse outcomes. The harmful effects of Mn exposure were first described by James Couper nearly two centuries ago in response to a case cluster of parkinsonism symptoms experienced by employees of an industrial process involving the grinding of Mn oxide (Couper 1837). The condition described by Couper became known as manganism, and a number of similar clusters among individuals experiencing high-level Mn exposures as part of their occupation emerged in the following decades (Mena et al. 1967, Cook et al. 1974, Huang et al. 2007). It is thus clear that Mn has a historical significance in terms of discernable neurotoxicity. The extreme high-level exposures that caused acute-onset manganism in years past are no longer a significant public health threat – the risk has been characterized and exposures have accordingly been controlled in occupational settings such that classical episodes of manganism are rarely observed today. However, Mn exposure still occurs regularly not only in a number of occupations, but also in the greater community, albeit at concentrations much too low to be causative of acute-onset manganism.

A shift in the Mn exposure paradigm from acute, high-level exposure toward chronic, low-level exposure raises important public health questions, which are the basis for this dissertation. In this regard, a number of studies have described either a significantly elevated prevalence of parkinsonism (PS) among workers occupationally exposed to Mn (Racette et al. 2001, Racette et al. 2005, Racette et al. 2012) or an increased incidence and/or earlier age of onset of Parkinson's disease (PD) associated

with populations experiencing elevated Mn exposures in their environment (Park et al. 2005, Finkelstein and Jerrett 2007, Willis et al. 2010, Wright Willis et al. 2010, Willis et al. 2012). Therefore, the objective of the studies described here was to characterize quantifiable biological alterations in Mn exposed populations and to identify novel mechanisms of neurotoxicity reflective of modern day low-level exposures.

Chapter 2 describes a biomarker study that involved the profiling of plasma autoantibodies in PD patients which identified antibodies against mortalin as being increased in the PD group as compared to controls. This study was then extended to specifically evaluate mortalin autoantibody levels in individual plasma samples from PD patients and controls, and also included plasma collected from a cohort of welders, an occupation recognized as experiencing modest exposures to Mn, described to have an elevated prevalence of PS as compared to non-welding controls (Racette et al. 2012). It was found that PD patients had elevated mortalin autoantibody levels as compared to controls, while welders exhibiting symptoms of PS trended toward higher mortalin autoantibody levels as compared to welders without PS. It is important to note that there are some significant differences between these two populations, namely that the PD patients are much older and generally presented clinically with much more severe signs and symptoms of PS as compared the welders. Nonetheless, the finding of elevated mortalin autoantibody levels among the subjects with the most severe motor dysfunction within each group is indicative of an encouraging PS biomarker.

Chapters 3 and 4 are related studies carried out in two separate populations. In Chapter 3, astroglial mortalin levels were quantified in the post-mortem brain tissue of PD patients and age/gender-matched controls. As mortalin levels have already been

shown to be decreased in brain tissue homogenates and neurons specifically (Jin et al. 2006), it was hypothesized that they would also be decreased in PD astrocytes. After definitively showing the presence of mortalin in non-tumorigenic human astrocytes for the first time, it was found that the protein is indeed decreased in the astrocytes of the substantia nigra pars compacta (SNpc) of PD patients, but not in structures of the corpus striatum (caudate, putamen, globus pallidus internal and external segments). With these findings in mind, unique access to post-mortem brain tissue of Mn and non-Mn mine workers, and considering Mn preferentially accumulates within astrocytes (Aschner et al. 1992), it was next hypothesized that Mn exposure alters astroglial mortalin levels. In the study of mine workers, it was found that astroglial mortalin is decreased in structures of the corpus striatum, particularly the caudate, but not the SNpc. These results were in contrast to the PD findings, but were not surprising because Mn preferentially deposits in these structures (Perl and Olanow 2007) and in fact support the hypothesis that Mn can influence mortalin expression. Although mortalin was found to be decreased in distinct brain regions for PD patients and Mn mine workers, together the results of Chapters 3 and 4 suggest a potential shared pathologic pathway between the two groups.

Chapter 5 follows-up on the results of Chapter 4 by exploring potential mechanisms of neurotoxicity related to decreased astroglial mortalin expression and Mn exposure. It was found that neurons cultured *in vitro* with astrocytes expressing decreased levels of mortalin were more sensitive to Mn toxicity than those cultured with astrocytes expressing endogenous levels of mortalin, demonstrated by a decreased number of presynaptic terminals. Subsequent *in vitro* studies assessing astroglial function under these conditions revealed altered intracellular calcium signaling and an increased

presence of aggregated proteins in Mn treated astrocytes with suppressed mortalin expression. Interestingly, these effects were mitigated in experiments using astrocytes lacking α-synuclein, a protein critical to PD pathogensis. Further, it was found that knocking down mortalin induced endoplasmic reticulum stress, while 10 μM Mn treatment increased the production of reactive oxygen species. These data led to the proposition of a 'two-hit' model to explain the observations, in which an adverse genetic occurrence (reduced mortalin) combined with an environmental exposure (Mn) to ultimately produce a toxic effect (reduction of presynaptic terminals).

Taken together, the results of these studies indicate that Mn exposures experienced by modern day populations, despite being orders of magnitude lower than th causative of acute onset manganism, are sufficient to cause discernable biological alterations in humans. The focus of these investigations was on mortalin, a protein implicated in a wide array of diseases including PD, the most common cause of PS. Although PD and Mn-induced PS are increasingly being recognized as distinct conditions, evidence presented here indicates potential overlapping pathological processes.

BIBLIOGRAPHY

Allen, M. T., and L. S. Levy. 2013. Parkinson's disease and pesticide exposure--a new assessment. Crit Rev Toxicol **43**:515-534.

Anderson, J. G., P. T. Cooney, and K. M. Erikson. 2007. Inhibition of DAT function attenuates manganese accumulation in the globus pallidus. Environ Toxicol Pharmacol **23**:179-184.

Archelos, J. J., and H. P. Hartung. 2000. Pathogenetic role of autoantibodies in neurological diseases. Trends Neurosci **23**:317-327.

Archibald, F. S., and C. Tyree. 1987. Manganese poisoning and the attack of trivalent manganese upon catecholamines. Arch Biochem Biophys **256**:638-650.

Aschner, M., and M. Gannon. 1994. Manganese (Mn) transport across the rat blood-brain barrier: saturable and transferrin-dependent transport mechanisms. Brain Res Bull **33**:345-349.

Aschner, M., M. Gannon, and H. K. Kimelberg. 1992. Manganese uptake and efflux in cultured rat astrocytes. J Neurochem **58**:730-735.

Aschner, M., K. E. Vrana, and W. Zheng. 1999. Manganese uptake and distribution in the central nervous system (CNS). Neurotoxicology **20**:173-180.

Au, C., A. Benedetto, and M. Aschner. 2008. Manganese transport in eukaryotes: the role of DMT1. Neurotoxicology **29**:569-576.

Avila, D. S., P. Gubert, R. Fachinetto, C. Wagner, M. Aschner, J. B. Rocha, and F. A. Soares. 2008. Involvement of striatal lipid peroxidation and inhibition of calcium influx into brain slices in neurobehavioral alterations in a rat model of short-term oral exposure to manganese. Neurotoxicology **29**:1062-1068.

Baek, S. Y., J. H. Cho, E. S. Kim, H. J. Kim, S. Yoon, B. S. Kim, J. B. Kim, C. R. Lee, C. Yoo, J. H. Lee, H. Lee, J. Park, J. W. Kim, and Y. Kim. 2004. CDNA array analysis of gene expression profiles in brain of mice exposed to manganese. Ind Health **42**:315-320.

Baek, S. Y., M. J. Lee, H. S. Jung, H. J. Kim, C. R. Lee, C. Yoo, J. H. Lee, H. Lee, C. S. Yoon, Y. H. Kim, J. Park, J. W. Kim, B. S. Jeon, and Y. Kim. 2003. Effect of manganese exposure on MPTP neurotoxicities. Neurotoxicology **24**:657-665.

Barhoumi, R., J. Faske, X. Liu, and R. B. Tjalkens. 2004. Manganese potentiates lipopolysaccharide-induced expression of NOS2 in C6 glioma cells through mitochondrial-dependent activation of nuclear factor kappaB. Brain Res Mol Brain Res **122**:167-179.

Baselar, W., T. Croston, and J. Hollander. 2012. Functional characteristics of mortalin. Pages 55-80 *in* S. C. Kaul and R. Wadwha, editors. Mortalin Biology: Life, Stress and Death. Springer Science+Business Media B.V., Springer Dordrecht Heidelberg London New York.

Baudet, C., E. Perret, B. Delpech, M. Kaghad, P. Brachet, D. Wion, and D. Caput. 1998. Differentially expressed genes in C6.9 glioma cells during vitamin D-induced cell death program. Cell Death Differ **5**:116-125.

Benkler, M., N. Agmon-Levin, S. Hassin-Baer, O. S. Cohen, O. D. Ortega-Hernandez, A. Levy, S. D. Moscavitch, M. Szyper-Kravitz, M. Damianovich, M. Blank, J. Chapman, and Y. Shoenfeld. 2012. Immunology, autoimmunity, and autoantibodies in Parkinson's disease. Clin Rev Allergy Immunol **42**:164-171.

Bennett, D. A., L. A. Beckett, A. M. Murray, K. M. Shannon, C. G. Goetz, D. M. Pilgrim, and D. A. Evans. 1996. Prevalence of parkinsonian signs and associated mortality in a community population of older people. N Engl J Med **334**:71-76.

Besong-Agbo, D., E. Wolf, F. Jessen, M. Oechsner, E. Hametner, W. Poewe, M. Reindl, W. H. Oertel, C. Noelker, M. Bacher, and R. Dodel. 2013. Naturally occurring α-synuclein autoantibody levels are lower in patients with Parkinson disease. Neurology **80**:169-175.

Braak, H., U. Rüb, W. P. Gai, and K. Del Tredici. 2003. Idiopathic Parkinson's disease: possible routes by which vulnerable neuronal types may be subject to neuroinvasion by an unknown pathogen. J Neural Transm **110**:517-536.

Braak, H., M. Sastre, and K. Del Tredici. 2007. Development of alpha-synuclein immunoreactive astrocytes in the forebrain parallels stages of intraneuronal pathology in sporadic Parkinson's disease. Acta Neuropathol **114**:231-241.

Burbulla, L. F., C. Schelling, H. Kato, D. Rapaport, D. Woitalla, C. Schiesling, C. Schulte, M. Sharma, T. Illig, P. Bauer, S. Jung, A. Nordheim, L. Schöls, O. Riess, and R. Krüger. 2010. Dissecting the role of the mitochondrial chaperone mortalin in Parkinson's disease: functional impact of disease-related variants on mitochondrial homeostasis. Hum Mol Genet **19**:4437-4452.

Burton, N. C., and T. R. Guilarte. 2009. Manganese neurotoxicity: lessons learned from longitudinal studies in nonhuman primates. Environ Health Perspect **117**:325-332.

Bélanger, M., I. Allaman, and P. J. Magistretti. 2011. Brain energy metabolism: focus on astrocyte-neuron metabolic cooperation. Cell Metab **14**:724-738.

Carmignoto, G. 2000. Reciprocal communication systems between astrocytes and neurones. Prog Neurobiol **62**:561-581.

Carmona, A., G. Devès, S. Roudeau, P. Cloetens, S. Bohic, and R. Ortega. 2010. Manganese accumulates within golgi apparatus in dopaminergic cells as revealed by synchrotron X-ray fluorescence nanoimaging. ACS Chem Neurosci **1**:194-203.

Caudle, W. M., T. S. Guillot, C. R. Lazo, and G. W. Miller. 2012. Industrial toxicants and Parkinson's disease. Neurotoxicology **33**:178-188.

Chahine, L. M., M. B. Stern, and A. Chen-Plotkin. 2014. Blood-based biomarkers for Parkinson's disease. Parkinsonism Relat Disord **20 Suppl 1**:S99-103.

Chang, Y., S. U. Jin, Y. Kim, K. M. Shin, H. J. Lee, S. H. Kim, J. H. Ahn, S. J. Park, K. S. Jeong, Y. C. Weon, and H. Lee. 2013. Decreased brain volumes in manganese-exposed welders. Neurotoxicology **37**:182-189.

Chen, C. J., and S. L. Liao. 2002. Oxidative stress involves in astrocytic alterations induced by manganese. Exp Neurol **175**:216-225.

Chen, J. Y., G. C. Tsao, Q. Zhao, and W. Zheng. 2001. Differential cytotoxicity of Mn(II) and Mn(III): special reference to mitochondrial [Fe-S] containing enzymes. Toxicol Appl Pharmacol **175**:160-168.

Chen, M. K., J. S. Lee, J. L. McGlothan, E. Furukawa, R. J. Adams, M. Alexander, D. F. Wong, and T. R. Guilarte. 2006. Acute manganese administration alters dopamine transporter levels in the non-human primate striatum. Neurotoxicology **27**:229-236.

Chiasserini, D., A. Tozzi, A. de Iure, M. Tantucci, F. Susta, P. L. Orvietani, K. Koya, L. Binaglia, and P. Calabresi. 2011. Mortalin inhibition in experimental Parkinson's disease. Mov Disord **26**:1639-1647.

Cho, M. K., G. Nodet, H. Y. Kim, M. R. Jensen, P. Bernado, C. O. Fernandez, S. Becker, M. Blackledge, and M. Zweckstetter. 2009. Structural characterization of alpha-synuclein in an aggregation prone state. Protein Sci **18**:1840-1846.

Chomczynski, P., and N. Sacchi. 1987. Single-step method of RNA isolation by acid guanidinium thiocyanate-phenol-chloroform extraction. Anal Biochem **162**:156-159.

Cook, D. G., S. Fahn, and K. A. Brait. 1974. Chronic manganese intoxication. Arch Neurol **30**:59-64.

Couper, J. 1837. On the effects of black oxide of manganese when inhaled into the lungs. British Annals of Medicine, Pharmacy, Vital Statistics, and General Science **1**:2.

De Mena, L., E. Coto, E. Sánchez-Ferrero, R. Ribacoba, L. M. Guisasola, C. Salvador, M. Blázquez, and V. Alvarez. 2009. Mutational screening of the mortalin gene (HSPA9) in Parkinson's disease. J Neural Transm **116**:1289-1293.

Deocaris, C. C., S. C. Kaul, and R. Wadhwa. 2008. From proliferative to neurological role of an hsp70 stress chaperone, mortalin. Biogerontology **9**:391-403.

Deocaris, C. C., N. Widodo, T. Ishii, S. C. Kaul, and R. Wadhwa. 2007. Functional significance of minor structural and expression changes in stress chaperone mortalin. Ann N Y Acad Sci **1119**:165-175.

Dexter, D. T., A. Carayon, F. Javoy-Agid, Y. Agid, F. R. Wells, S. E. Daniel, A. J. Lees, P. Jenner, and C. D. Marsden. 1991. Alterations in the levels of iron, ferritin and other trace metals in Parkinson's disease and other neurodegenerative diseases affecting the basal ganglia. Brain **114 (Pt 4)**:1953-1975.

Di Castro, M. A., J. Chuquet, N. Liaudet, K. Bhaukaurally, M. Santello, D. Bouvier, P. Tiret, and A. Volterra. 2011. Local Ca2+ detection and modulation of synaptic release by astrocytes. Nat Neurosci **14**:1276-1284.

Dobson, A. W., S. Weber, D. C. Dorman, L. K. Lash, K. M. Erikson, and M. Aschner. 2003. Oxidative stress is induced in the rat brain following repeated inhalation exposure to manganese sulfate. Biol Trace Elem Res **93**:113-126.

Dodd, C. A., D. L. Ward, and B. G. Klein. 2005. Basal Ganglia accumulation and motor assessment following manganese chloride exposure in the C57BL/6 mouse. Int J Toxicol **24**:389-397.

Dorman, D. C., M. F. Struve, B. A. Wong, J. A. Dye, and I. D. Robertson. 2006. Correlation of brain magnetic resonance imaging changes with pallidal manganese concentrations in rhesus monkeys following subchronic manganese inhalation. Toxicol Sci **92**:219-227.

Double, K. L., D. B. Rowe, F. M. Carew-Jones, M. Hayes, D. K. Chan, J. Blackie, A. Corbett, R. Joffe, V. S. Fung, J. Morris, P. Riederer, M. Gerlach, and G. M. Halliday. 2009. Anti-melanin antibodies are increased in sera in Parkinson's disease. Exp Neurol **217**:297-301.

Erikson, K., and M. Aschner. 2002. Manganese causes differential regulation of glutamate transporter (GLAST) taurine transporter and metallothionein in cultured rat astrocytes. Neurotoxicology **23**:595-602.

Erikson, K. M., and M. Aschner. 2006. Increased manganese uptake by primary astrocyte cultures with altered iron status is mediated primarily by divalent metal transporter. Neurotoxicology **27**:125-130.
Erikson, K. M., A. W. Dobson, D. C. Dorman, and M. Aschner. 2004. Manganese exposure and induced oxidative stress in the rat brain. Sci Total Environ **334-335**:409-416.
Erikson, K. M., D. C. Dorman, L. H. Lash, and M. Aschner. 2007. Manganese inhalation by rhesus monkeys is associated with brain regional changes in biomarkers of neurotoxicity. Toxicol Sci **97**:459-466.
Fahn, S., and R. Elton. 1987. Members of the UPDRS Development Committee. Unified Parkinson's disease rating scale. Pages 153-163.
Finkelstein, M. M., and M. Jerrett. 2007. A study of the relationships between Parkinson's disease and markers of traffic-derived and environmental manganese air pollution in two Canadian cities. Environ Res **104**:420-432.
Flachbartová, Z., and B. Kovacech. 2013. Mortalin - a multipotent chaperone regulating cellular processes ranging from viral infection to neurodegeneration. Acta Virol **57**:3-15.
Galvan, A., and T. Wichmann. 2008. Pathophysiology of parkinsonism. Clin Neurophysiol **119**:1459-1474.
Gavin, C. E., K. K. Gunter, and T. E. Gunter. 1992. Mn2+ sequestration by mitochondria and inhibition of oxidative phosphorylation. Toxicol Appl Pharmacol **115**:1-5.
Gavin, C. E., K. K. Gunter, and T. E. Gunter. 1999. Manganese and calcium transport in mitochondria: implications for manganese toxicity. Neurotoxicology **20**:445-453.
Gianutsos, G., M. D. Seltzer, R. Saymeh, M. L. Wu, and R. G. Michel. 1985. Brain manganese accumulation following systemic administration of different forms. Arch Toxicol **57**:272-275.
Gibb, W. R., and A. J. Lees. 1988. The relevance of the Lewy body to the pathogenesis of idiopathic Parkinson's disease. J Neurol Neurosurg Psychiatry **51**:745-752.
Giordano, G., D. Pizzurro, K. VanDeMark, M. Guizzetti, and L. G. Costa. 2009. Manganese inhibits the ability of astrocytes to promote neuronal differentiation. Toxicol Appl Pharmacol **240**:226-235.
Gold, M., R. Pul, J. P. Bach, M. Stangel, and R. Dodel. 2012. Pathogenic and physiological autoantibodies in the central nervous system. Immunol Rev **248**:68-86.
Gonzalez-Cuyar, L. F., G. Nelson, S. R. Criswell, P. Ho, J. A. Lonzanida, H. Checkoway, N. Seixas, B. B. Gelman, B. A. Evanoff, J. Murray, J. Zhang, and B. A. Racette. 2013. Quantitative neuropathology associated with chronic manganese exposure in South African mine workers. Neurotoxicology.
Grerogy R. Warnes, B. B., Lodewijk Bonebakker, Robert Gentleman, Wolfgang Huber, Andy Liaw, Thomas Lumley, Martin Maechler, Arni Magnusson, Steffen Moeller, Marc Schwartz, Bill Venables. 2014. gplots: Various R programming tools for plotting data. Page Various R programming tools for plotting data.

Guilarte, T. R. 2013. Manganese neurotoxicity: new perspectives from behavioral, neuroimaging, and neuropathological studies in humans and non-human primates. Front Aging Neurosci **5**:23.
Guilarte, T. R., J. L. McGlothan, M. Degaonkar, M. K. Chen, P. B. Barker, T. Syversen, and J. S. Schneider. 2006. Evidence for cortical dysfunction and widespread manganese accumulation in the nonhuman primate brain following chronic manganese exposure: a 1H-MRS and MRI study. Toxicol Sci **94**:351-358.
Gunter, T. E., C. E. Gavin, M. Aschner, and K. K. Gunter. 2006. Speciation of manganese in cells and mitochondria: a search for the proximal cause of manganese neurotoxicity. Neurotoxicology **27**:765-776.
Gwiazda, R. H., D. Lee, J. Sheridan, and D. R. Smith. 2002. Low cumulative manganese exposure affects striatal GABA but not dopamine. Neurotoxicology **23**:69-76.
Halliday, G. M., and C. H. Stevens. 2011. Glia: initiators and progressors of pathology in Parkinson's disease. Mov Disord **26**:6-17.
Han, M., E. Nagele, C. DeMarshall, N. Acharya, and R. Nagele. 2012. Diagnosis of Parkinson's disease based on disease-specific autoantibody profiles in human sera. PLoS One **7**:e32383.
Haydon, P. G. 2001. GLIA: listening and talking to the synapse. Nat Rev Neurosci **2**:185-193.
Hazell, A. S., and M. D. Norenberg. 1997. Manganese decreases glutamate uptake in cultured astrocytes. Neurochem Res **22**:1443-1447.
Hobson, A., N. Seixas, D. Sterling, and B. A. Racette. 2011. Estimation of particulate mass and manganese exposure levels among welders. Ann Occup Hyg **55**:113-125.
Hoekstra, J. G., T. J. Cook, T. Stewart, H. A. Mattison, M. T. Dreisbach, Z. S. Hoffer, and J. Zhang. 2014. Astrocytic dynamin-like protein 1 regulates neuronal protection against excitotoxicity in Parkinson's disease. American Journal of Pathology **in press**.
Hong, Z., M. Shi, K. A. Chung, J. F. Quinn, E. R. Peskind, D. Galasko, J. Jankovic, C. P. Zabetian, J. B. Leverenz, G. Baird, T. J. Montine, A. M. Hancock, H. Hwang, C. Pan, J. Bradner, U. J. Kang, P. H. Jensen, and J. Zhang. 2010. DJ-1 and alpha-synuclein in human cerebrospinal fluid as biomarkers of Parkinson's disease. Brain **133**:713-726.
Huang, C. C., N. S. Chu, C. S. Lu, R. S. Chen, M. Schulzer, and D. B. Calne. 2007. The natural history of neurological manganism over 18 years. Parkinsonism Relat Disord **13**:143-145.
Huang da, W., B. T. Sherman, and R. A. Lempicki. 2009. Systematic and integrative analysis of large gene lists using DAVID bioinformatics resources. Nat Protoc **4**:44-57.
Ingersoll, R. T., E. B. Montgomery, and H. V. Aposhian. 1999. Central nervous system toxicity of manganese. II: Cocaine or reserpine inhibit manganese concentration in the rat brain. Neurotoxicology **20**:467-476.
Itoh, K., M. Sakata, M. Watanabe, Y. Aikawa, and H. Fujii. 2008. The entry of manganese ions into the brain is accelerated by the activation of N-methyl-D-aspartate receptors. Neuroscience **154**:732-740.

Jin, J., T. J. Cook, J. G. Hoekstra, and J. Zhang. 2012. Mortalin in Neurological Diseases.*in* S. C. Kaul and R. Wadhwa, editors. Mortalin Biology: Life, Stress and Death. Springer Science+Business Media B.V., Springer Dordrecht Heidelberg London New York.

Jin, J., C. Hulette, Y. Wang, T. Zhang, C. Pan, R. Wadhwa, and J. Zhang. 2006. Proteomic identification of a stress protein, mortalin/mthsp70/GRP75: relevance to Parkinson disease. Mol Cell Proteomics **5**:1193-1204.

Jin, J., G. J. Li, J. Davis, D. Zhu, Y. Wang, C. Pan, and J. Zhang. 2007. Identification of novel proteins associated with both alpha-synuclein and DJ-1. Mol Cell Proteomics **6**:845-859.

Kalia, K., W. Jiang, and W. Zheng. 2008. Manganese accumulates primarily in nuclei of cultured brain cells. Neurotoxicology **29**:466-470.

Klein, C., and A. Westenberger. 2012. Genetics of Parkinson's disease. Cold Spring Harb Perspect Med **2**:a008888.

Langston, J. W., P. Ballard, J. W. Tetrud, and I. Irwin. 1983. Chronic Parkinsonism in humans due to a product of meperidine-analog synthesis. Science **219**:979-980.

Lee, M. S., and C. D. Marsden. 1994. Neurological sequelae following carbon monoxide poisoning clinical course and outcome according to the clinical types and brain computed tomography scan findings. Mov Disord **9**:550-558.

Li, H. M., T. Niki, T. Taira, S. M. Iguchi-Ariga, and H. Ariga. 2005. Association of DJ-1 with chaperones and enhanced association and colocalization with mitochondrial Hsp70 by oxidative stress. Free Radic Res **39**:1091-1099.

Liccione, J. J., and M. D. Maines. 1988. Selective vulnerability of glutathione metabolism and cellular defense mechanisms in rat striatum to manganese. J Pharmacol Exp Ther **247**:156-161.

Lin, X., T. J. Cook, C. P. Zabetian, J. B. Leverenz, E. R. Peskind, S. C. Hu, K. C. Cain, C. Pan, J. S. Edgar, D. R. Goodlett, B. A. Racette, H. Checkoway, T. J. Montine, M. Shi, and J. Zhang. 2012. DJ-1 isoforms in whole blood as potential biomarkers of Parkinson disease. Sci Rep **2**:954.

Lipe, G. W., H. Duhart, G. D. Newport, W. Slikker, and S. F. Ali. 1999. Effect of manganese on the concentration of amino acids in different regions of the rat brain. J Environ Sci Health B **34**:119-132.

Lucchini, R. G., C. J. Martin, and B. C. Doney. 2009. From manganism to manganese-induced parkinsonism: a conceptual model based on the evolution of exposure. Neuromolecular Med **11**:311-321.

Ma, Z., H. Izumi, M. Kanai, Y. Kabuyama, N. G. Ahn, and K. Fukasawa. 2006. Mortalin controls centrosome duplication via modulating centrosomal localization of p53. Oncogene **25**:5377-5390.

Magdalinou, N., A. J. Lees, and H. Zetterberg. 2014. Cerebrospinal fluid biomarkers in parkinsonian conditions: an update and future directions. J Neurol Neurosurg Psychiatry.

McKhann, G., D. Drachman, M. Folstein, R. Katzman, D. Price, and E. M. Stadlan. 1984. Clinical diagnosis of Alzheimer's disease: report of the NINCDS-ADRDA Work Group under the auspices of Department of Health and Human Services Task Force on Alzheimer's Disease. Neurology **34**:939-944.

Mena, I., O. Marin, S. Fuenzalida, and G. C. Cotzias. 1967. Chronic manganese poisoning. Clinical picture and manganese turnover. Neurology **17**:128-136.
Mercado, G., P. Valdés, and C. Hetz. 2013. An ERcentric view of Parkinson's disease. Trends Mol Med **19**:165-175.
Milatovic, D., Z. Yin, R. C. Gupta, M. Sidoryk, J. Albrecht, J. L. Aschner, and M. Aschner. 2007. Manganese induces oxidative impairment in cultured rat astrocytes. Toxicol Sci **98**:198-205.
Milatovic, D., S. Zaja-Milatovic, R. C. Gupta, Y. Yu, and M. Aschner. 2009. Oxidative damage and neurodegeneration in manganese-induced neurotoxicity. Toxicol Appl Pharmacol **240**:219-225.
Mishra, R., and G. Kaur. 2013. Aqueous ethanolic extract of Tinospora cordifolia as a potential candidate for differentiation based therapy of glioblastomas. PLoS One **8**:e78764.
Monahan, A. J., M. Warren, and P. M. Carvey. 2008. Neuroinflammation and peripheral immune infiltration in Parkinson's disease: an autoimmune hypothesis. Cell Transplant **17**:363-372.
Morello, M., A. Canini, P. Mattioli, R. P. Sorge, A. Alimonti, B. Bocca, G. Forte, A. Martorana, G. Bernardi, and G. Sancesario. 2008. Sub-cellular localization of manganese in the basal ganglia of normal and manganese-treated rats An electron spectroscopy imaging and electron energy-loss spectroscopy study. Neurotoxicology **29**:60-72.
Mortimer, J. A., A. R. Borenstein, and L. M. Nelson. 2012. Associations of welding and manganese exposure with Parkinson disease: review and meta-analysis. Neurology **79**:1174-1180.
Nagele, E., M. Han, C. Demarshall, B. Belinka, and R. Nagele. 2011. Diagnosis of Alzheimer's disease based on disease-specific autoantibody profiles in human sera. PLoS One **6**:e23112.
Neff, F., X. Wei, C. Nolker, M. Bacher, Y. Du, and R. Dodel. 2008. Immunotherapy and naturally occurring autoantibodies in neurodegenerative disorders. Autoimmun Rev **7**:501-507.
Ordoñez-Librado, J. L., A. L. Gutierrez-Valdez, L. Colín-Barenque, V. Anaya-Martínez, P. Díaz-Bech, and M. R. Avila-Costa. 2008. Inhalation of divalent and trivalent manganese mixture induces a Parkinson's disease model: immunocytochemical and behavioral evidences. Neuroscience **155**:7-16.
Orr, C. F., D. B. Rowe, and G. M. Halliday. 2002. An inflammatory review of Parkinson's disease. Prog Neurobiol **68**:325-340.
Papachroni, K. K., N. Ninkina, A. Papapanagiotou, G. M. Hadjigeorgiou, G. Xiromerisiou, A. Papadimitriou, A. Kalofoutis, and V. L. Buchman. 2007. Autoantibodies to alpha-synuclein in inherited Parkinson's disease. J Neurochem **101**:749-756.
Papuc, E., J. Kurzepa, E. Kurys-Denis, A. Grabarska, W. Krupski, and K. Rejdak. 2014. Humoral response against glial derived antigens in Parkinson's disease. Neurosci Lett **566**:77-81.
Park, R. M., P. A. Schulte, J. D. Bowman, J. T. Walker, S. C. Bondy, M. G. Yost, J. A. Touchstone, and M. Dosemeci. 2005. Potential occupational risks for neurodegenerative diseases. Am J Ind Med **48**:63-77.

Park, S. J., J. H. Shin, J. I. Jeong, J. H. Song, Y. K. Jo, E. S. Kim, E. H. Lee, J. J. Hwang, E. K. Lee, S. J. Chung, J. Y. Koh, D. G. Jo, and D. H. Cho. 2014. Down-regulation of mortalin exacerbates Aβ-mediated mitochondrial fragmentation and dysfunction. J Biol Chem **289**:2195-2204.

Parpura, V., T. A. Basarsky, F. Liu, K. Jeftinija, S. Jeftinija, and P. G. Haydon. 1994. Glutamate-mediated astrocyte-neuron signalling. Nature **369**:744-747.

Pasti, L., A. Volterra, T. Pozzan, and G. Carmignoto. 1997. Intracellular calcium oscillations in astrocytes: a highly plastic, bidirectional form of communication between neurons and astrocytes in situ. J Neurosci **17**:7817-7830.

Pennington, K., J. Peng, C. C. Hung, R. E. Banks, and P. A. Robinson. 2010. Differential effects of wild-type and A53T mutant isoform of alpha-synuclein on the mitochondrial proteome of differentiated SH-SY5Y cells. J Proteome Res **9**:2390-2401.

Perea, G., M. Sur, and A. Araque. 2014. Neuron-glia networks: integral gear of brain function. Front Cell Neurosci **8**:378.

Perl, D. P., and C. W. Olanow. 2007. The neuropathology of manganese-induced Parkinsonism. J Neuropathol Exp Neurol **66**:675-682.

Rabin, O., L. Hegedus, J. M. Bourre, and Q. R. Smith. 1993. Rapid brain uptake of manganese(II) across the blood-brain barrier. J Neurochem **61**:509-517.

Racette, B. A. 2013. Manganism in the 21st century: The Hanninen lecture. Neurotoxicology.

Racette, B. A., S. R. Criswell, J. I. Lundin, A. Hobson, N. Seixas, P. T. Kotzbauer, B. A. Evanoff, J. S. Perlmutter, J. Zhang, L. Sheppard, and H. Checkoway. 2012. Increased risk of parkinsonism associated with welding exposure. Neurotoxicology **33**:1356-1361.

Racette, B. A., L. McGee-Minnich, S. M. Moerlein, J. W. Mink, T. O. Videen, and J. S. Perlmutter. 2001. Welding-related parkinsonism: clinical features, treatment, and pathophysiology. Neurology **56**:8-13.

Racette, B. A., S. D. Tabbal, D. Jennings, L. Good, J. S. Perlmutter, and B. Evanoff. 2005. Prevalence of parkinsonism and relationship to exposure in a large sample of Alabama welders. Neurology **64**:230-235.

Ran, Q., R. Wadhwa, R. Kawai, S. C. Kaul, R. N. Sifers, R. J. Bick, J. R. Smith, and O. M. Pereira-Smith. 2000. Extramitochondrial localization of mortalin/mthsp70/PBP74/GRP75. Biochem Biophys Res Commun **275**:174-179.

Rappold, P. M., and K. Tieu. 2010. Astrocytes and therapeutics for Parkinson's disease. Neurotherapeutics **7**:413-423.

Reaney, S. H., G. Bench, and D. R. Smith. 2006. Brain accumulation and toxicity of Mn(II) and Mn(III) exposures. Toxicol Sci **93**:114-124.

Roels, H., G. Meiers, M. Delos, I. Ortega, R. Lauwerys, J. P. Buchet, and D. Lison. 1997. Influence of the route of administration and the chemical form (MnCl2, MnO2) on the absorption and cerebral distribution of manganese in rats. Arch Toxicol **71**:223-230.

Roels, H. A., R. M. Bowler, Y. Kim, B. Claus Henn, D. Mergler, P. Hoet, V. V. Gocheva, D. C. Bellinger, R. O. Wright, M. G. Harris, Y. Chang, M. F. Bouchard, H. Riojas-

Rodriguez, J. A. Menezes-Filho, and M. M. Téllez-Rojo. 2012. Manganese exposure and cognitive deficits: a growing concern for manganese neurotoxicity. Neurotoxicology **33**:872-880.

Saito, A., C. M. Maier, P. Narasimhan, T. Nishi, Y. S. Song, F. Yu, J. Liu, Y. S. Lee, C. Nito, H. Kamada, R. L. Dodd, L. B. Hsieh, B. Hassid, E. E. Kim, M. González, and P. H. Chan. 2005. Oxidative stress and neuronal death/survival signaling in cerebral ischemia. Mol Neurobiol **31**:105-116.

Sato, H., T. Kato, and S. Arawaka. 2013. The role of Ser129 phosphorylation of alpha-synuclein in neurodegeneration of Parkinson's disease: a review of in vivo models. Rev Neurosci **24**:115-123.

Schwarzer, C., S. Barnikol-Watanabe, F. P. Thinnes, and N. Hilschmann. 2002. Voltage-dependent anion-selective channel (VDAC) interacts with the dynein light chain Tctex1 and the heat-shock protein PBP74. Int J Biochem Cell Biol **34**:1059-1070.

Shi, M., J. Jin, Y. Wang, R. P. Beyer, E. Kitsou, R. L. Albin, M. Gearing, C. Pan, and J. Zhang. 2008. Mortalin: a protein associated with progression of Parkinson disease? J Neuropathol Exp Neurol **67**:117-124.

Shi, M., C. P. Zabetian, A. M. Hancock, C. Ginghina, Z. Hong, D. Yearout, K. A. Chung, J. F. Quinn, E. R. Peskind, D. Galasko, J. Jankovic, J. B. Leverenz, and J. Zhang. 2010. Significance and confounders of peripheral DJ-1 and alpha-synuclein in Parkinson's disease. Neurosci Lett **480**:78-82.

Singleton, A. B., M. Farrer, J. Johnson, A. Singleton, S. Hague, J. Kachergus, M. Hulihan, T. Peuralinna, A. Dutra, R. Nussbaum, S. Lincoln, A. Crawley, M. Hanson, D. Maraganore, C. Adler, M. R. Cookson, M. Muenter, M. Baptista, D. Miller, J. Blancato, J. Hardy, and K. Gwinn-Hardy. 2003. alpha-Synuclein locus triplication causes Parkinson's disease. Science **302**:841.

Singleton, A. B., M. J. Farrer, and V. Bonifati. 2013. The genetics of Parkinson's disease: progress and therapeutic implications. Mov Disord **28**:14-23.

Stamelou, M., and G. U. Hoeglinger. 2013. Atypical parkinsonism: an update. Curr Opin Neurol **26**:401-405.

Stanwood, G. D., D. B. Leitch, V. Savchenko, J. Wu, V. A. Fitsanakis, D. J. Anderson, J. N. Stankowski, M. Aschner, and B. McLaughlin. 2009. Manganese exposure is cytotoxic and alters dopaminergic and GABAergic neurons within the basal ganglia. J Neurochem **110**:378-389.

Stephen, T. L., S. Gupta-Agarwal, and J. T. Kittler. 2014. Mitochondrial dynamics in astrocytes. Biochem Soc Trans **42**:1302-1310.

Suzuki, Y., T. Mouri, K. Nishiyama, and N. Fujii. 1975. Study of subacute toxicity of manganese dioxide in monkeys. Tokushima J Exp Med **22**:5-10.

Takano, S., R. Wadhwa, Y. Yoshii, T. Nose, S. C. Kaul, and Y. Mitsui. 1997. Elevated levels of mortalin expression in human brain tumors. Exp Cell Res **237**:38-45.

Team, R. C. 2014. A language environment for statistical computing. R Foundation for Statistical Computing, Vienna, Austria.

Tjalkens, R. B., M. J. Zoran, B. Mohl, and R. Barhoumi. 2006. Manganese suppresses ATP-dependent intercellular calcium waves in astrocyte networks through

alteration of mitochondrial and endoplasmic reticulum calcium dynamics. Brain Res **1113**:210-219.
Trexler, A. J., and E. Rhoades. 2010. Single molecule characterization of α-synuclein in aggregation-prone states. Biophys J **99**:3048-3055.
Tsuboi, Y., H. Uchikado, and D. W. Dickson. 2007. Neuropathology of Parkinson's disease dementia and dementia with Lewy bodies with reference to striatal pathology. Parkinsonism Relat Disord **13 Suppl 3**:S221-224.
Tuschl, K., P. B. Mills, and P. T. Clayton. 2013. Manganese and the brain. Int Rev Neurobiol **110**:277-312.
Uversky, V. N., J. Li, and A. L. Fink. 2001. Metal-triggered structural transformations, aggregation, and fibrillation of human alpha-synuclein. A possible molecular NK between Parkinson's disease and heavy metal exposure. J Biol Chem **276**:44284-44296.
Van Laar, V. S., A. A. Dukes, M. Cascio, and T. G. Hastings. 2008. Proteomic analysis of rat brain mitochondria following exposure to dopamine quinone: implications for Parkinson disease. Neurobiol Dis **29**:477-489.
Verina, T., J. S. Schneider, and T. R. Guilarte. 2013. Manganese exposure induces α-synuclein aggregation in the frontal cortex of non-human primates. Toxicol Lett **217**:177-183.
Verkhratsky, A., J. J. Rodríguez, and V. Parpura. 2012. Calcium signalling in astroglia. Mol Cell Endocrinol **353**:45-56.
Vingerhoets, F. J., M. Schulzer, D. B. Calne, and B. J. Snow. 1997. Which clinical sign of Parkinson's disease best reflects the nigrostriatal lesion? Ann Neurol **41**:58-64.
Wadhwa, R., S. C. Kaul, Y. Ikawa, and Y. Sugimoto. 1993. Identification of a novel member of mouse hsp70 family. Its association with cellular mortal phenotype. J Biol Chem **268**:6615-6621.
Wadhwa, R., S. Takano, K. Kaur, C. C. Deocaris, O. M. Pereira-Smith, R. R. Reddel, and S. C. Kaul. 2006. Upregulation of mortalin/mthsp70/Grp75 contributes to human carcinogenesis. Int J Cancer **118**:2973-2980.
Wang, J., J. G. Hoekstra, C. Zuo, T. J. Cook, and J. Zhang. 2013. Biomarkers of Parkinson's disease: current status and future perspectives. Drug Discov Today **18**:155-162.
Wilhelm, K. R., K. Yanamandra, M. A. Gruden, V. Zamotin, M. Malisauskas, V. Casaite, A. Darinskas, L. Forsgren, and L. A. Morozova-Roche. 2007. Immune reactivity towards insulin, its amyloid and protein S100B in blood sera of Parkinson's disease patients. Eur J Neurol **14**:327-334.
Willis, A. W., B. A. Evanoff, M. Lian, A. Galarza, A. Wegrzyn, M. Schootman, and B. A. Racette. 2010. Metal emissions and urban incident Parkinson disease: a community health study of Medicare beneficiaries by using geographic information systems. Am J Epidemiol **172**:1357-1363.
Willis, A. W., M. Schootman, N. Kung, B. A. Evanoff, J. S. Perlmutter, and B. A. Racette. 2012. Predictors of survival in patients with Parkinson disease. Arch Neurol **69**:601-607.

Wright Willis, A., B. A. Evanoff, M. Lian, S. R. Criswell, and B. A. Racette. 2010. Geographic and ethnic variation in Parkinson disease: a population-based study of US Medicare beneficiaries. Neuroepidemiology **34**:143-151.

Yang, H., X. Zhou, X. Liu, L. Yang, Q. Chen, D. Zhao, J. Zuo, and W. Liu. 2011. Mitochondrial dysfunction induced by knockdown of mortalin is rescued by Parkin. Biochem Biophys Res Commun **410**:114-120.

Yin, Z., J. Aschner, A. dos Santos, and M. Aschner. 2008. Mitochondrial-dependent manganese neurotoxicity in rat primary astrocyte cultures. Brain Res **1203**:1-11.

Yong, V. W., T. L. Perry, W. J. Godolphin, K. A. Jones, R. M. Clavier, M. Ito, and J. G. Foulks. 1986. Chronic organic manganese administration in the rat does not damage dopaminergic nigrostriatal neurons. Neurotoxicology **7**:19-24.

Zhang, P., K. M. Lokuta, D. E. Turner, and B. Liu. 2010. Synergistic dopaminergic neurotoxicity of manganese and lipopolysaccharide: differential involvement of microglia and astroglia. J Neurochem **112**:434-443.

Zhang, S., Z. Zhou, and J. Fu. 2003. Effect of manganese chloride exposure on liver and brain mitochondria function in rats. Environ Res **93**:149-157.

Zwingmann, C., D. Leibfritz, and A. S. Hazell. 2003. Energy metabolism in astrocytes and neurons treated with manganese: relation among cell-specific energy failure, glucose metabolism, and intercellular trafficking using multinuclear NMR-spectroscopic analysis. J Cereb Blood Flow Metab **23**:756-771.

Zwingmann, C., D. Leibfritz, and A. S. Hazell. 2007. Nmr spectroscopic analysis of regional brain energy metabolism in manganese neurotoxicity. Glia **55**:1610-1617.